Development of a new approach (“Myc-PDI”) for the treatment of onychomycosis

Dissertation
zur Erlangung des akademischen Grades
doctor rerum naturalium
(Dr. rer. nat.)

Im Fach Physik
Spezialisierung: Experimentalphysik

eingereicht an der
Mathematisch-Naturwissenschaftlichen Fakultät
der Humboldt-Universität zu Berlin

Von
M. Sc. Nedaa M. M. Shamali

Präsidentin der Humboldt-Universität zu Berlin
Prof. Dr.-Ing. Dr. Sabine Kunst

Dekan der Mathematisch-Naturwissenschaftlichen Fakultät
Prof. Dr. Elmar Kulke

Gutachter/in: 1. Prof. Dr. Beate Röder

2. Prof. Dr. Axel karmer

3. Prof. Dr. Oliver Benson

Datum der Promotion: 05.09.2019

Zusammenfassung

Die Onychomykose ist eine sehr häufige Erkrankung, deren Auftreten weltweit zunimmt und mit einer Pilzinfektion der Nägel einhergeht. Derzeit werden oral oder topisch verabreichte Antimykotika zur Behandlung der Onychomykose eingesetzt. Diese derzeitigen Behandlungen sind jedoch hinsichtlich Effizienz, Sicherheit und Kosten nicht zufriedenstellend. Dies motiviert Bemühungen, nach alternativen Behandlungsmethoden zu suchen. Diese Dissertation untersucht die Auswirkungen der photodynamischen Inaktivierung (PDI) auf Dermatophyten und Schimmelpilze. Als Modellorganismen werden drei der Onychomykose auslösenden Pathogene untersucht: *Trichophyton rubrum*, *Trichophyton interdigitale* und der Schimmelpilz *Scopulariopsis brevicaulis*.

Um das Potenzial der PDI gegen Onychomykose verursachende Pathogene, abzuschätzen, wurden Phototoxizitätstests mit drei Photosensibilisatoren (PS) durchgeführt: den kationischen 5,10,15,20-Tetrakis(1-methylpyridinium-4-yl) porphyrintetra(p-toluenesulfonate) (TMPyP) und and 5,10,15-tris-(1-methylpyridinium-2-yl) corrolato-(trans-dihydroxo) phosphorus(V) (PCor+) sowie dem anionischen 4',5',7'-tetrabromo-3',6'-dihydroxyspiro[2-benzofuran-3,9'-xanthene] -1-one (Eosin G). Neben den Phototoxizitätstests wurden zeitaufgelöste Singulettsauerstoff-Lumineszenz Scans aufgenommen, die zur Verifizierung der PDI Effizienz genutzt wurden. Dabei wurde die Forschung zunächst mit i*n-vitro*-Experimenten an Sporensuspensionen und Oberflächen begonnen, gefolgt von *ex-vivo*-Tests an infizierten menschlichen Nägeln. Für jedes dieser Stadien wurden die Ergebnisse der Phototoxizität mit der Effizienz der Singulettsauerstoff-Lumineszenz korreliert. Alle drei PS zeigen *in vitro* eine hohe phototoxische Wirkung gegen die drei Pilzarten. Diese konnte mit Singulettsauerstoff-Lumineszenzmessungen korreliert werden, bei denen ein hohes Singulettsauerstoff-Lumineszenzsignal erfasst wurde. Entgegen den Erwartungen aus den *in-vitro*-Experimenten gestalteten sich die Ergebnisse der *ex-vivo*-Versuche: An infizierten menschlichen Nägeln konnten die PS keinen phototoxischen Effekt induzieren. Singulettsauerstoff-Scans, die für einen Einblick in die zugrundeliegenden Ursachen durchgeführt wurden, zeigten fast kein Singulettsauerstoff-Lumineszenzsignal an menschlichen Nägeln. Eine Anreicherung der Atmosphäre mit Sauerstoff führt zu einer leichten Verbesserung des Signals. Könnten die verschiedenen bekannten Herausforderungen im Zusammenhang mit PDI an infizierten menschlichen Nägeln - wie die Steifigkeit der Nagelplatte und ihre chemische Zusammensetzung – bewältigt werden, indem die Permeabilität der Nagelplatte erhöht und die Sauerstoffversorgung verbessert wird, hätte die PDI das Potenzial, eine schnellwirkende

Behandlungsmethode dieser Pilzinfektion im Zehennagel zu werden. Diese Studie zeigt erstmals den Zusammenhang zwischen der PDI-Behandlung von Onychomykose und Singulettsauerstoff.

Abstract

Onychomycosis is a very common illness that befalls an increasing number of individuals worldwide and involves a fungal infection of the nails. Currently, orally or topically administrated antimycotics are in use for the treatment of onychomycosis. However, these current treatments are unsatisfactory regarding efficiency, safety and costs. This justifies the efforts to look for alternative treatment modalities. This dissertation investigates the impact of photodynamic inactivation (PDI) against dermatophytes and molds. Three of the causing pathogens of the dermatological disease onychomycosis are under investigation: *Trichophyton rubrum (T. rubrum)*, *Trichophyton interdigitale (T. interdigitale)* and the mold *Scopulariopsis brevicaulis (S. brevicaulis)*.

To assess the potential of PDI against onychomycosis causing pathogens, phototoxicity tests were performed using three photosensitizers (PSs): the cationic 5,10,15,20-Tetrakis(1-methylpyridinium-4-yl) porphyrintetra(p-toluenesulfonate) (TMPyP) and 5,10,15-tris-(1-methylpyridinium-2-yl) corrolato-(trans-dihydroxo) phosphorus(V) (PCor+) as well as the anionic 4',5',7'-tetrabromo-3',6'-dihydroxyspiro[2-benzofuran-3,9'-xanthene]-1-one (Eosin Y). Alongside the phototoxicity tests, time resolved singlet oxygen luminescence scans were conducted to serve as a control method of PDI. The research strategy was to start with *in vitro* experiments on spore suspensions and on surfaces followed by *ex vivo* tests on infected human nails. For each of these stages, the results of phototoxicity were correlated with the singlet oxygen scans. All three PSs proved to have a high phototoxic effect against the three fungi species *in vitro*. Those could be correlated with singlet oxygen measurements, where a high singlet oxygen luminescence signal was acquired. Contrary to the expectations from the *in vitro* experiments were the results obtained *ex vivo*: On infected human nails, the PSs were not able to induce a phototoxic effect. Singlet oxygen scans conducted to get insight into the reasons behind these results showed nearly no singlet oxygen luminescence signal on human nails. Enrichment of the atmosphere with oxygen lead to a slight improvement of the signal. Addressing the various known challenges associated with PDI on infected human nails - like the nail plate rigidity and its chemical composition - by enhancing the permeability of the nail plate and additional oxygenation, PDI would have a great impact within short time on treating the toenail fungal infection. This study, for the first time, shows the correlation between PDI treatment of onychomycosis and singlet oxygen.

Schlagwörter:

Onychomycosis, Photodynamic inactivation (PDI), Dermatophytes, Singlet oxygen.

Keywords:

Onychomycosis, Photodynamic inactivation (PDI), Dermatophytes, Singlet oxygen.

Contents

Dedication

To my parents for their love, prayers and encouragement.

To my beloved husband, who encouraged me each step of the way and gave me the support and willingness.

To my brothers and sisters, who gave me the motivation and encouragement.

To my family and friends for their unrestricted support. I will always appreciate all they have done.

To everyone who supported me I dedicate this work.

List of abbreviations

PDI	Photodynamic inactivation
PDT	Photodynamic therapy
T. rubrum	*Trichophyton rubrum*
T. interdigitale	*Trichophyton interdigitale*
S. brevicaulis	*Scopulariopsis brevicaulis*
PS	Photosensitizer
TMPyP	5,10,15,20-Tetrakis(1-methylpyridinium-4-yl) porphyrintetra(p-toluenesulfonate)
PCor+	5,10,15-tris-(1-methylpyridinium-2-yl)corrolato-(trans-dihydroxo)phosphorus(V)
Eosin Y	2',4',5',7'-tetrabromo-3',6'-dihydroxyspiro[2-benzofuran-3,9'-xanthene]-1-one
HOMO	Highest Occupied molecular Orbital
LUMO	Lowest Unoccupied Molecular Orbital
O_2	Molecular oxygen
$^1O_2$	Singlet oxygen
HPD	Hematoporphyrin derivative
ALA	Aminolevulinic acid
E. coli	*Escherichia coli*
HIV/AIDS	Human immunodeficiency virus infection and acquired immune deficiency syndrome
DLSO	*Distal and lateral subungual onychomycosis*
PSO	*Proximal subungual onychomycosis*
SO	*Superficial onychomycosis*
C. albicans	*Candida albicans*
T. violaceum	*Trichophyton violaceum*
DMSO	Dimethyl sulfoxide

NAC	N-acetyl-cysteine
MPG	N (2-mercaptopropionly) glycine
PTO	Pyrithione (2-mercatopyridine-1-oxide)
SDA	Sabouraud dextrose Agar
TRSOL	Time resolved singlet oxygen luminescence
NIR	Near infrared
SNR	Signal-to-noise ratio
PBS	Phosphate-buffered saline
OD	Optical Density
CFU	Colony Forming Unit
PORTHE	5,10,15-tris(4-N-methylpyridinium)-20-(4-(butyramido-methylcysteinyl)-hydroxyphenyl)-[21H,23H]-porphine trichloride

1. Introduction

1.1 Motivation

Dermatophytes are a group of fungi causing infections to hair, nail and skin because of their ability to metabolize keratin. They secrete proteolytic enzymes which help them to metabolize keratin and thus invade any keratinous structures (1). As with other microorganisms, moist, warm and dark places are the best environment for their growth, as is the case inside of shoes and socks. Dermatophytes get under the nail fold and cause infection of the toenail, often rapidly spreading to neighbouring nails, fingernails and skin. Fungal infection of the toenail - or onychomycosis - is considered a serious health problem, especially in Europe and North America (2). The infection causes excessive thickness as well as discoloration of the nails and reduces the quality of life for the patients (3–6). Old people and immunocompromised patients like diabetics and AIDs patients are the ones most susceptible to the infection (7; 8). The main causative pathogens of onychomycosis are *Trichophyton rubrum (T.rubrum)* , *Trichophyton interdigitale (T.interdigitale)* and less frequently molds like *Scopulariopsis brevicaulis (S. brevicaulis)* or *Aspergillus spp (9).* In most countries, *T. rubrum* is responsible for about 90% of cases, followed by *T. interdigitale* with 8% (2). Oral or topical administered antifungals are currently used for the treatment of onychomycosis. In some cases, both treatment modalities are used simultaneously to increase the cure rate of the infection. Current therapy includes different antifungals like azoles and terbinafine (10; 11). Most antifungals have a fungistatic rather than a fungicidal effect. The antifungal's sites of action are the metabolic parts of the fungal cell. For example, azole's site of action is the ergosterol on the cell membrane. Thus the conidia are left unaffected which may cause recurrences of the infection. In addition to being rather inefficient, the currently available antifungals are very expensive, associated with several side effects and a long treatment period of up to 18 months (8). A further point is the resistance to antifungal drugs i.e. in case of the dermatophyte *T. rubrum* which raises the question of alternative treatment options. The negative image associated with onychomycosis treatment justifies the efforts to look for alternative treatment modalities.

Over the last ten years, several studies investigated the potential of photodynamic inactivation as a new antimicrobial tool. It was shown that photodynamic inactivation (PDI) is an efficient modality to kill several microorganisms such as bacteria, mold fungi and green algae (12–16). However, pathogenic fungi – particularly dermatophytes – have been rather neglected by PDI research. Recently some investigations showed that PDI of the dermatophyte *T. rubrum* is

possible in principle (17–24). In this study, I test the possibility of PDI of three causative pathogens of onychomycosis: the dermatophytes *T. rubrum*, *T. interdigitale* and the mold *S. brevicaulis*. The photosensitizers used in this investigation are the cationic porphyrin 5,10,15,20-Tetrakis(1-methylpyridinium-4-yl) porphyrintetra(p-toluenesulfonate) (TMPyP) and 5,10,15-tris-(1-methylpyridinium-2-yl)corrolato-(trans-dihydroxo)phosphorus(V) (PCor+) as well as the anionic 4',5',7'-tetrabromo-3',6'-dihydroxyspiro[2-benzofuran-3,9'-xanthene]-1-one (Eosin Y).

1.2 Objective of the PhD thesis

The difficulties associated with onychomycosis current treatment justify current efforts to develop new treatment modalities like biophysical treatments. In this study, photodynamic inactivation of dermatophytes is investigated for its potential to overcome the drawbacks of conventional treatments. Photodynamic treatment of onychomycosis is a promising treatment modality aimed to be a fast, efficient and cheap treatment.

Three fungi species and three photosensitizes are involved in this study. *T. rubrum*, *T. interdigitale* and *S.breivecaulis* were provided from the Department of Dermatology, university hospital in Greifswald, Germany. Fungi strains were isolated from patients diagnosed with onychomycosis. The PSs are the cationic TMPyP, PCor+ and the anionic eosin Y. They were chosen due to their efficiencies against bacteria, mold fungi and green algae.

This PhD thesis will begin with *in vitro* investigations followed by *ex vivo* investigation using human nails as an *ex vivo* model.

Not only the treatment development is to be investigated here but also singlet oxygen scans is to be applied in each part. Singlet oxygen scanning is a direct method to study the PSs behaviour in their microenvironment. It serves as control method to improve the conditions for better phototoxic action of the PSs against fungi.

2 Fundamentals

2.1 Photosensitization and singlet oxygen generation

As was proven, the use of light for medical treatment is historically founded. Ancient civilizations used light to treat various ailments, including skin diseases (25; 26). Nevertheless, photobiological research began no earlier than in the 19th century, when a medical student in Munich, Oscar Raab, discovered that the use of certain dyes such as eosin in the presence of certain wavelengths of light led to a fetal effect on protozoan. Raab's discovery was the key to a variety of research activities in the field of photodynamic action. Photosensitizers (PSs) are molecules that not only absorb light but are also excited to a long-lived, high-energy triplet state. The PS first absorbs a quantum of light and is excited from the base singlet state (S_0) to the higher singlet states (S_n). Then the relaxation of Sn takes place down to the lowest excited singlet state S_1. Intersystem crossing (ISC) generates the excited triplet state of the sensitizer. Since the relaxation of the singlet excited state into the triplet excited state is spin prohibited, the triplet lifetime is relatively long (μs). The long lifetime of the triplet-excited state of the sensitizer allows various interactions. Two of interactions allow for photosensitization: electron transfer or energy transfer (27-31).

Via electron transfer reactions (type I or type III photosensitization), an electron or hydrogen atom is transferred to a substrate or to molecular oxygen, creating free radicals. The high reactivity of the radicals leads to further interactions with other biological substrates in the vicinity, leading to structural or functional changes. These reactions require a direct interaction between the sensitizer and the substrate and are beneficial in environments with low oxygen concentrations.

In the energy transfer reaction (or Type II photosensitization) energy is transferred from the sensitizer to molecular oxygen resulting in the generation of singlet oxygen.

The Jablonski diagram (Figure 1) gives a clear explanation of all steps involved in the photosensitization process.

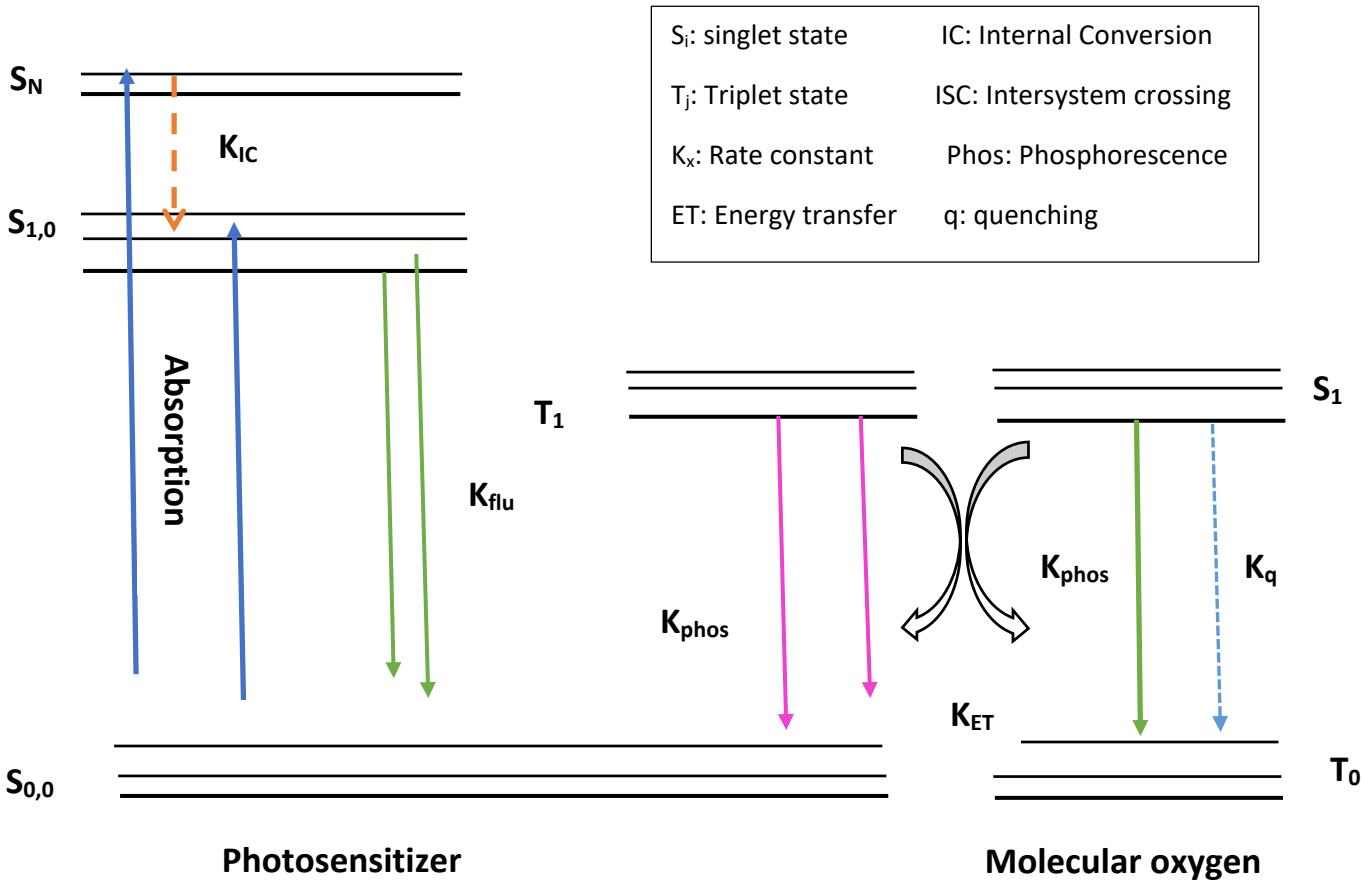

Figure 1: Jablonski diagram showing all electronic and vibronic states of the photosensitizer and the molecular oxygen and all relevant processes.

Steps involved in photosensitization:

1. Absorption (PS excitation):

In their ground state, PSs are in the singlet state. When the PS absorbs a quantum of light it is excited to a higher energy level as absorption lifts an electron from the ground singlet state to a higher molecular orbital without changing in its spin. As a result, the PS molecule reaches an excited singlet state ($S_0 \rightarrow S_n$).

$$PS + h\upsilon_{exc} \longrightarrow {}^1PS^*$$

2. Internal conversion (radiationless relaxation)

Some PSs are generally excited to higher vibrionic singlet states S_n and not directly to the first excited state $S_{1,0}$, so they exhibit a radiationless relaxation decay within picoseconds to aforementioned state ($S_n \rightarrow S_{1,0}$) in a process called internal conversion.

$$^{n}PS^{*} \longrightarrow {}^{1}PS^{*} \qquad : -K_{IC}[S_1]$$

3a. Fluorescence (PS deactivation):

The excited PSs can decay directly back to the ground state emitting light with an energy equal to the energy difference between the ground state and the excited states. The light emitted here spontaneously in such a process is called fluorescence.

$$^{1}PS^{*} \longrightarrow PS + h\nu_{flu} \quad \mathbf{: -K_F\,[S_1]}$$

3b. Intersystem crossing (ISC) (Other deactivation pathway of the PS):

In ISC, the PS in the singlet excited state undergoes multiplicity change. This results in occupation of its first excited triplet state. The short energy gap between S1 and T1 and the strong spin orbital coupling result in high quantum yields of ISC. The decay from the excited triplet state back to the ground singlet state is spin forbidden so the triplet excited state has a longer lifetime which extends to microseconds allowing for several reactions.

$$^{1}PS^{*} \longrightarrow {}^{3}PS^{*} \quad \mathbf{: -K_{ISC}\,[S_1]}$$

4a. Phosphorescence (Radiative decay back to the ground state):

As the energy gap between T_1 and S_0 is too high, the transition between them is unlikely. However, the triplet excited state PS might decay back to its singlet ground state. This comes along with phosphorescence emission.

$$^{3}PS^{*} \longrightarrow PS + h\nu pho \quad \mathbf{: -K_P\,[T]}$$

4b. Energy transfer from the PS to molecular oxygen:

When a type II reaction takes place, the PS in its excited triplet state interacts with molecular oxygen via Dexter energy transfer (Figure 2). Herein, a lowest unoccupied molecular orbital (LUMO) electron from the PS is transferred to molecular oxygen and a highest occupied molecular orbital (HOMO) electron from the oxygen is in turn transferred to the PS. This process requires adjacency of both PS and molecular oxygen in order to occur. Energy transfer from the triplet excited state PS to a molecular oxygen leads to singlet oxygen generation.

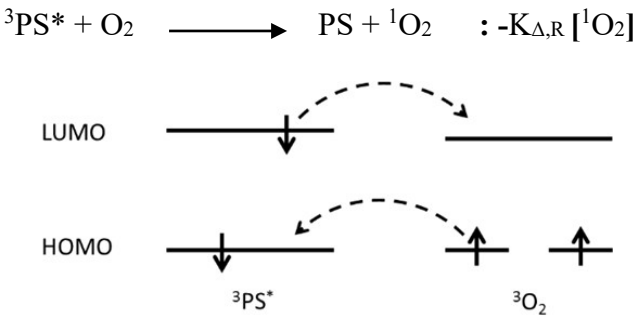

Figure 2: Dexter energy transfer between PS* and molecular oxygen.

2.2 Deactivation of singlet oxygen

Singlet oxygen possesses various deactivation channels after excitation. These either belong to monomolecular deactivation or to physical and chemical quenching. The monomolecular deactivation of singlet oxygen is associated with a phosphorescence emission at a wavelength of 1270 nm. Thus it is called radiative deactivation.

$$^1O_2 \longrightarrow O_2 + h\nu$$

The intensity of phosphorescence depends on the singlet oxygen quantum yield Φ_Δ and the singlet oxygen decay rate $K_{\Delta,R}$. Since the microenvironment has a large influence on singlet oxygen decay kinetics, $K_{\Delta,R}$ also depends on the microenvironment (37; 38).

The decay rates of singlet oxygen K_Δ and the singlet oxygen lifetime τ_Δ allow to study the decay kinetics in different media. The microenvironment in which singlet oxygen is located has great potential in terms of its kinetics. The singlet oxygen decay rate K_Δ represents all decay paths of singlet oxygen (36).

$$K_\Delta = K_{\Delta,R} + K_{\Delta,NR} + K_{\Delta,R}$$

Where:

- $K_{\Delta,R}$ is the rate constant of the singlet oxygen radiative decay.
- $K_{\Delta,NR}$ is the rate constant of the physical quenching of singlet oxygen.
- $K_{\Delta,R}$ is the rate constant of the chemical quenching of singlet oxygen.

The physical quenching of singlet oxygen has different channels: Energy transfer, charge quenching and electronic-vibrational energy transfer (25–28). These processes require collision between singlet oxygen and acceptor molecules.

$$K_{\Delta,NR} = K_{\Delta,ET}[Q_{ET}] + K_{\Delta,CT}[Q_{CT}] + K_{\Delta,e\text{-}v}[S]$$

Where

- $K_{\Delta,ET}$ is the rate of the energy transfer deactivation.
- $K_{\Delta,CT}$ is the rate of charge transfer deactivation.
- $K_{\Delta,e\text{-}v}$ is the rate of electronic vibrational energy transfer deactivation.
- [Q] is the concentration of quenchers.
- [S] is the concentration of solvent.

Charge transfer takes place in the presence of quenchers with an energetically high triplet state and a low oxidation potential like vitamins E and B12 (29). If the quenchers have a lower energetic triplet state than singlet oxygen, excitation energy transfer occurs. In the electronic-vibrational pathway, singlet oxygen converts its energy to vibrational modes of the acceptor. Good matching between the vibrational mode of the acceptor and the energy of singlet oxygen is required. In O-H containing solvents, better matching occurs and thus the process is more likely. In C-H containing solvents it is less favorable due to poor matching. Figure 3 (30) shows a comparison between the energy levels of singlet oxygen and different solvents (31–33).

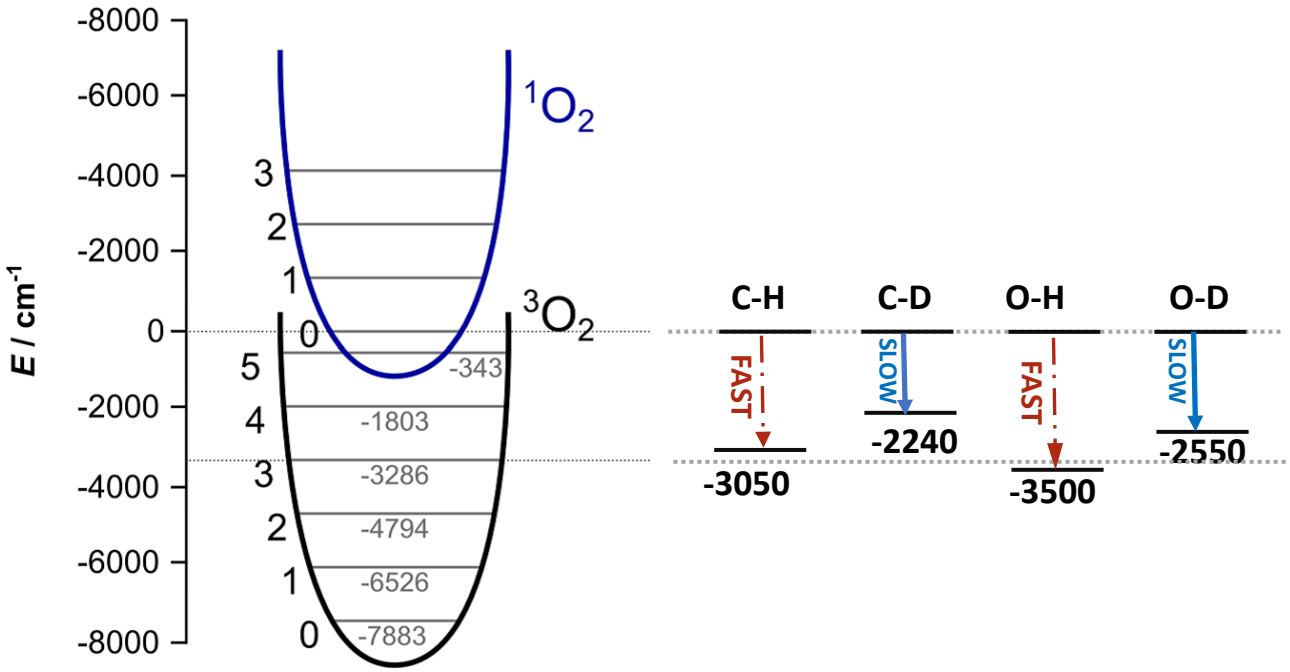

Figure 3: The energy levels of singlet oxygen and different solvents showing vibrational transition (after 30).

The third pathway of singlet oxygen deactivation is the chemical quenching. Chemical quenching is a dominant process in many systems. In chemical quenching, singlet oxygen reacts with a quencher molecule and the result of the chemical reaction is the consumption of both the quencher and singlet oxygen - in contrast to physical quenching where no consumption of oxygen occurs (34). The different deactivation channels compete with each other. In gas phase, radiative deactivation is dominant. In solvents, physical and chemical quenching are more probable. In biological systems, the deactivation mechanism depends on the site where singlet oxygen is produced.

2.3 Detection and characterization of singlet oxygen

Detection of singlet oxygen is very important to prove the generation of singlet oxygen and to quantify the amount of oxygen in addition to gaining information about singlet oxygen kinetics and its parameters. It can be observed directly by spectroscopic methods i.e. the detection of singlet oxygen phosphorescence at 1270 nm. Furthermore, limited information about singlet oxygen could be observed chemically by the use of singlet oxygen quenchers for example. In this section, a brief description of both direct and indirect singlet oxygen will be given.

Indirect singlet oxygen detection

Chemical indirect singlet oxygen detection is an old method for the observation and detection of singlet oxygen. Indirect detection only provides information about the generation of singlet oxygen and its amount. A secondary reporter or sensor molecule in addition to singlet oxygen chemical quenchers can be used for singlet oxygen identification. The use of chemical quenchers and secondary reporters could interfere with the investigated system and the required proximity between sensor molecule and PS is difficult to achieve in heterogeneous environments. Despite the limitations of indirect detection methods mentioned above, it continues to be used. (45–47).

Direct singlet oxygen detection

Identifying and quantifying singlet oxygen without spoiling the system under investigation is of a great importance. Therefore, detection without adding any additional substance is preferable, which is possible by direct detection of the characteristic weak NIR luminescence of singlet oxygen at 1270 nm. The luminescence is characteristic in both, kinetics and spectral

distribution. As a consequence, there are two principle options, spectrally resolved or time resolved detection. Good spectral resolution often results in a reduced sensitivity and was therefore usually performed in steady state manner. Only very recently, it was possible to combine the advantages of both methods, using a tiltable Interference filter for wavelength discrimination in a setup for time-resolved detection (35–37).

Spectrally resolved (steady state) detection provides spectral information that is important when singlet oxygen lifetime is much shorter than the triplet lifetime and short time artifacts masks the rising flank, hence, especially in biological systems. It is also easier to perform. Spectrally resolved detection offers higher sensitivity but usually with lower SNR unless block-in system is applied. The main limitation of spectrally resolved detection is the lack of temporal information and thus no kinetics is provided. The need to resolve the kinetics and its characteristic parameters come up later with time resolved detection. With more complex electronics, time resolved detection could be performed at a fixed wavelength. This method gives information about the kinetics and its characteristic parameters and thus follow the effect of the PS's microenvironment and any changes therein (38–42; 35). For this reason, time resolved detection was conducted in this investigation. It was important to observe the effect of the presence of fungi in the PS's microenvironment on the kinetics. Table 1 summaries the advantages and limitations of spectrally and time resolved detection methods.

	Spectrally resolved detection	Time resolved detection
Advantages	• Higher sensitivity • Easier to perform • Spectral information	• Time resolution information • Better SNR • Observe the effect of the PS's microenvironment
Limitations	• usually lower SNR • No temporal information	• Technically more difficult • Measurements at a fixed wavelengths

Table 1: Comparison between spectrally and time resolved singlet oxygen detection.

2.4 Singlet oxygen kinetics

The analysis of singlet oxygen kinetics is very important to understand the behavior of a PS in its microenvironment. It is also important to obtain information about the generation, deactivation and diffusion of singlet oxygen. Since singlet oxygen kinetics is environment dependent, all these parameters about singlet oxygen generation and deactivation depend on the local environment of the system under study. In homogenous systems, such as PS in a solution, three rate-based processes are involved

- Dexter energy transfer from PS triplet excited state to molecular oxygen triplet ground state, K_{ET}.
- PS triplet excited state deactivation without singlet oxygen generation.
- All singlet oxygen quenching processes.

The kinetics of singlet oxygen in homogenous system can be described through the following rate equation

$$\frac{d[\Delta]}{dt} = +K_{ET}.[\mathrm{O_2}].[T] - (K_q.[Q] + K_{phos}).[\Delta]$$
$$\frac{d[T]}{dt} = -K_{ET}.[\mathrm{O_2}] + \left(K_{phos,T} + K_{ns}\right).[T] \quad (1)$$

Where [^{1}O$_2$] is the concentration of singlet oxygen, [T] is the concentration of PS triplet state, [O$_2$] is the concentration of molecular oxygen, [Q] is the concentration of singlet oxygen quenchers, K_{ET} is rate of energy transfer from PS triplet state to molecular oxygen, K_q is the rate of singlet oxygen quenching, $K_{phos,PS}$ is the rate of PS's phosphorescence, $K_{phos,\Delta}$ is the rate of singlet oxygen phosphorescence, $K_{n,s}$ is the rate of all non-radiative deactivation processes(43–45).

The solution of the rate equation gives us the concentration of singlet oxygen as follows:

$$[\Delta](\mathrm{T}) = [\mathrm{T}].\frac{K_{ET}.[\mathrm{O_2}]}{K_\Delta - \mathrm{K_T}}\left(e^{-K_T \mathrm{t}} - e^{-K_\Delta t}\right) \quad (2)$$

$$K\Delta = \mathrm{Kq}.[\mathrm{Q}] + \mathrm{Kphos}$$

$$KT = KET[O] + Kns + Kphos, ps$$

With: $\tau = K^{-1}$

$$[\Delta](t) = [T]\frac{\tau_\Delta}{\tau_T - \tau_\Delta}\left(e^{-t/\tau_T} - e^{-t/\tau_\Delta}\right) \quad (3)$$

Experimentally, the analysis of singlet oxygen kinetics is not easy. It is hard to distinguish triplet lifetime from singlet oxygen lifetime. Laser flash photolysis is usually used to determine PS triplet lifetime. however, flash photolysis is limited to homogenous systems like PS solution (46). An alternative method should be used in microheterogeneous systems such as biological samples. In heterogeneous systems, the characteristic parameters change within nanometers of the environment inside the same system. The inhomogeneity influences the radiative decay constant because it is highly environment-dependent. The quantum yield of singlet oxygen in biological systems is about 10^{-5}. To simplify the evaluation of the kinetics in complex systems, the system is divided into several homogeneous microenvironments. Subsequently, several experimental functions are superimposed. In the course of this work, singlet oxygen kinetics were observed on a system consisting of fungi grown on filter papers placed on the surface of Agar.

2.5 Singlet oxygen diffusion

The concentration of singlet oxygen and its ability to diffuse in the desired microenvironment has a major influence singlet oxygen kinetics (47). The diffusion of PS and molecular oxygen is essential for adequate singlet oxygen generation. The heterogeneity of the intracellular domain in addition to pH-level, viscosity and polarity influence the diffusion of the generated singlet oxygen (47; 48). The presence of singlet oxygen quenchers would largely affect its decay time and thus its diffusion (49). As mentioned in the previous section, complex systems are divided into several homogenous segmentations to simplify the heterogeneity of their complexity. The individual homogenous units make Fick's 2nd law of diffusion applicable to observe the concentration of singlet oxygen as a function of time and place in 1-D diffusion:

$$\frac{\partial[\Delta](x,t)}{\partial t} = D\frac{\partial\text{^}2\ [\Delta](x,t)}{\partial x\text{^}2} - K[\Delta](x,t) \quad (4)$$

Where [Δ] (x,t) is the place and time dependent singlet oxygen concentration, D is the diffusion constant, and K_{Δ} is the rate of singlet oxygen deactivation. This represents a Gaussian distribution that expands over time with rescaling of the x-axis by a factor of $1\backslash\sqrt{D}$ (50). Solving the previous equation gives:

$$[O](x,t) = \frac{1}{\sqrt{2\pi t}} e^{-\frac{\check{x}}{4t}} e^{-\frac{t}{\tau\Delta}} \quad (5)$$

$$\check{x} = \frac{x}{\sqrt{D}}$$

In this investigation, it is important to know whether the produced singlet oxygen would reach the region of interest, which, in this case, is the infection site within the nail plate. The percentage of singlet oxygen reaching a particular region is referred to as the relative impact (RI) and can be expressed by the following equation:

$$RI(l) = \int_{x=-l}^{l} C(x) cw, norm\, dx \quad (6)$$

Relative impact reduces by a factor $1\backslash e$ for length$\sqrt{D}\tau\Delta$, which means that the diffusion displacement of singlet oxygen before quenching is very low.

2.7 Applications of photodynamic effect: PDT and PDI

Singlet oxygen is the toxic agent of any PDT or PDI on the affected cancer cells or microorganisms. Each PS molecule has the ability to produce 10^3 to 10^5 molecules of singlet oxygen before degradation. Type II reactions are favorable in environments under physiological conditions. In addition to that, type II photosensitization reactions are favorable over type I in the application of PDT and PDI. In the current study, all involved PSs possess type II photosensitization. An ideal PS should have some characteristic properties:

- High triplet quantum yield
- High singlet oxygen quantum yield.
- Exhibit no dark toxicity.
- Should be photo-stable (51; 52).

According to their chemical structures, PSs can be divided into different groups such as porphyrins and corrols (53). The use of the photodynamic effect to remove harmful or undesirable cells in humans or animals is referred to as PDT while using it as antimicrobial agent it is termed PDI (54; 16). PDT and PDI are indeed very promising treatment modalities to overcome failure and difficulties associated with conventional treatments. This section provides a brief description of PDT and its use, as well as PDI.

PDT

The use of photoactivated dyes to kill harmful or unwanted cells like cancer cells is called PDT (55–57). The treatment protocol used involves PSs aimed at accumulating in the target cells and then illuminating them. After light absorption, singlet oxygen is produced, which has a toxic effect on the target cells. In recent years, the advantage of PDT over other treatment methods has become increasingly clear. Unlike conventional therapies such as chemotherapy and radiobiology, today PDT has no serious side effects (58). The toxic effect of PDT is limited to cancer cells where a combination of light and PS is present. The absence of light invalidates the action of the PS and light alone has no effect on cells, as the wavelength window used in PDT is (650-900 nm). Approved PSs for the treatment of cancer are hematoporphyrin derivative HPD (59), *Foscan* and *N*-aspartyl chlorin e6. PDT is limited to skin-, superficial-, and endoscopically accessible tumors. PDT shows a great potential in the treatment of bladder cancer, skin cancer, and lung and gastrointestinal cancer (60; 61). Aminolevulinic acid (ALA) as a precursor of protoporphyrin is used in dermatology for the treatment of skin disorders such as acne and psoriasis (62; 63).

PDI

The spread of antimicrobially resistant pathogens is currently one of the biggest threat to health worldwide. New strategies and new alternatives should be developed to tackle this accelerating problem (64; 65). Since the 1990s, it has been established that the photodynamic effect works not only on cancer cells but also on microorganism. PDI is considered an important approach to overcome antimicrobial resistance. PDI is the use of the photodynamic effect to achieve a photo-induced death of microorganisms. The ability of microorganisms to develop resistance against PDI is nearly non-existent (66–70). The cell wall of microorganisms serves as structural support and protection layer and any destruction of it leads to cell death. Cell walls of microorganisms mainly consist of chitin and glycan, which give it a negative charge (71). The negative charge of the microorganism’s cell wall makes positively charged PSs preferred.

Studies show that PDI has a great potential on bacteria and fungi. In the following, the current state of the art for each of them is given.

PDI of bacteria

Bacteria have a large pathogenicity profile on humans, animals and plants. A wide range of antibiotics is available to cure this pathogenicity (72; 73). However, the adaptability of bacteria makes them resistant to a wide range of antibiotics. The accelerated development of antibiotics resistance is alarming experts looking for alternatives to control the enlarging problem (74–78). PDI offers a great potential in bacterial inhibition, making it a promising alternative to conventional antibiotics (79). In the last ten years, the research activities on PDI of bacteria have been growing significantly. Very promising approaches have been developed. Gram-positive bacteria as well as gram-negative bacteria have been studied (80–85). It is known that gram-negative bacteria are associated with difficulties in treatment due to the structural features of their cell wall. Preuß et al. (12) showed inhibition of *E. coli* by PDI without cellular uptake of the PSs. This minimizes the ability of *E. coli* to develop a resistance against the inhibition method. The hypothesis behind it, the action of PDI is from the outside the cell wall of *E. coli* and therefore the possibility of resistance development is very low. Several investigations showed the great potential in inhibition of different bacterial species (13).

PDI of fungi

Fungi in general and dermatophytes in particular contribute to a variety of skin, hair and nail infections. Fungal infections range from simple superficial infections to complicated infections (86–91; 1). As the complexity and intensity of the infection increases, the efficiency of treatment becomes limited. Tinea corporis, Tinea Pedis (Athlete's foot) and Tinea virsocolor are common fungal skin infections. Onychomycosis is a fungal nail infection (2) and is the focus of the investigations presented in this thesis.

The challenge of fungal infections treatment is tough. Fungal infections take a long time to cure. A variety of antimycotics are currently in clinical use (92). The protracted treatment of fungal infections makes it expensive. The recurrence of the infection is common (93). The subversive effect of fungi is not limited to human and animals' infections. Molds, for example, pose a threat to the environment. Like other microorganisms, fungi develop resistance to antifungals (93- 96). These limitations in the available treatment of fungal infections require the development of new treatment methods. The success of PDI of bacteria promotes efforts to test the effect of PDI on fungi. The potential of PDI against fungi was neglected until recently.

Recent studies show that several PSs are photodynamically active against fungi (15). In this study, PDI will be tested on main causative pathogens of onychomycosis. Dermatophytes, nail fungal infections and its complications are described in the following section.

2.8 Dermatophytes

Dermatophytes are the most common cause of skin, hair and nail infections. These fungi thrive in dark environments where heat and moisture prevail (97). In the human body, they grow in the skin folds of breast and armpits. They also grow in mucous membranes such as the genital area and the mouth. Many of these fungi live in non-living tissues like the epidermis, the outer skin layer and nail tissue. Dermatophytes are not able to penetrate viable tissues, particularly in hosts with a healthy immune system (98-99). They secret proteolytic enzyme that break down keratin. Keratin is the main protein in hair, nail and skin. Through keratin digestion, dermatophytes penetrate the keratinized structures and cause infections (100). Classified according to their favored host, there are three major groups of dermatophytes (101):

- Geophilic organisms: reside in soil, occasionally infect human and animals.
- Zoophilic organisms: are ingested by animals and can infect humans on direct contact.
- Anthropholic organisms: are ingested by humans and cause numerous infections.

Dermatophytes include three genera of pathogens: Euascomycetes, Trichophyton and Microsporum (102). These pathogens cause a wide range of cutaneous infections. They infect the keratinized structure by hyphal adherence to them, followed with rapid germination (a few hours). The secretion of proteolytic enzymes speeds up the infection development through keratin layers (99). Most mycotic infections are caused by dermatophytes to human beings (99). The increasing prevalence of dermatophytosis is a worldwide health problem (103). The term tinea in general refers to a fungal infection and infections are differentiated according to their infection side. Tinea capitis refers to hair/hair scalp infection, Tinea pedis is athlete's foot infection and Tinea unguim (onychomycosis) is the term for nail infections (102). Onychomycosis and its possible treatment modalities will be discussed in more details here.

2.9 Onychomycosis

Tinea unguim or onychomycosis is a fungal nail infection. Dermatophytes get under the nail fold and start to penetrate into the keratin layers through protease enzymes, causing the infection of toe nails which can spread to finger nails and surrounding tissue (104; 5; 105; 90). The main pathogens causing onychomycosis are the dermatophytes *T. rubrum, T. interdigitale* and - less frequently - the non-dermatophyte mold *S. brevicaulis* (8; 9; 106; 107). Common

signs of infected nail are increased thickness, brittleness, shape distortion and discoloration (108). Onychomycosis is considered a serious health problem worldwide. The infection accounts for 50% of all nail disorders. Its prevalence has been increasing to reach 8% of the population in Europe and North America (109–111). The increasing incidence of the infection also increases the concerns for it, even if it is a non-fetal disease. The infection is more common in elderly individuals and occurs in males more often than females. Patients with other mycotic infections, immunocompromised patients (HIV/AIDS) or diabetic patients are more likely to get the infection (112; 5; 7). The life style also can influence the probability of infection. The modern life style in developed countries, where people wear tight, closed shoes for long time, capturing heat and humidity, is a factor promoting the infection. In addition, public swimming pools and fitness studios, where a full hygienic process is not guaranteed, are also contributing to an increasing risk of nail fungal infections. Depending on the site of the infection, Onychomycosis is clinically divided into different types, as shown in figure 4 (3).

The most common form of *onychomycosis* is *Distal and lateral subungual onychomycosis (DLSO)*. The sites of fungal invasion are the nail bed and the bottom of the nail. In this type of inflammation, the nail is often shows white or yellow discoloration and in some cases even brown or black pigments. The dermatophytes *T. rubrum*, *T. mentagrophytes, E. floccosum* and non-dermatophytes *S. brevicaulis* are prevalent in DLSO (8). The second type of onychomycosis is *proximal subungual onychomycosis (PSO).* With this type of infection, the invasion starts from the proximal end of the nail fold and extends towards nail plate. The nail appears with a white or yellow proximal end and a normal distal end. The fungi causing this type most often are *T. rubrum, Fusarium, C. albicans, and Aspergillus spp. (108).* In *superficial onychomycosis (SO)* the pathogens penetrate the superficial layer of the nail plate. The most common form is the white superficial onychomycosis, but when *T. rubrum* is the causative pathogen, then the infection rather presents as black superficial. *T. mentagrophytes* is the frequent pathogenic agent for superficial mycosis, along with *Fusarium, Acremonium and Scytalidium (4).* If the entire nail plate is attacked by the pathogens, then it is completely dystrophic onychomycosis. *T. rubrum* is the species most often isolated from such infection. *T. mentagrophytes, floccosum, Ttonsurans, Microsporum canis, T violaceum*, and other *Microsporum spp* may be also found (4). If the causative pathogen is *C. albicans,* the infection is called *Candida onychomycosis.* Candida onychomycosis is also referred to as secondary infection or secondary onychomycosis (106).

			
(A) DLSO	(B) PSO	(C) SO	(D)Candida onychomycosis

Figure 4: Types of onychomycosis (after 11).

2.9.1 Onychomycosis and quality of life

Nail plates play a protective role in the human body. The infection of the nail unit has negative effects on the well-being. Such infections make daily life very hard for activities such as wearing shoes, walking and even standing. Elderly patients usually suffer from walking difficulties and other disorders and onychomycosis makes life more difficult for them. Not only the mechanical side is a problem, but also the appearance of the infected nails. Fungal nail infections cause discoloration and thickness of the nail plate. For patients, showing up with visibly infected nails is unpleasant and embarrassing in every aspect of social life, where the appearance of people is plays an important role. This anxiety and self-consciousness affects the social life of patients, especially female ones. Taking social and clinical complications associated with the infection into account, a strict therapeutic modality should be found for it (113–117).

2.9.2 Onychomycosis treatment

Oral and topical antifungal agents are the oldest and most popular methods so far. The severity and the type of the infection determine the treatment modality. In severe cases, surgery may be required, where complete separation of the nail is needed. In this section, the different treatment possibilities will be discussed.

Antifungals

The treatment of onychomycosis with antifungal agents by systemic administration is the most popular method. The antimycotic agent diffuses systemically to reach the nail bed and subsequently the underside of the nail plate. The low solubility of the drugs and a low permeability of the nail plate weaken the efficiency profile of oral antifungals and prolong the

treatment. The treatment period might last up to 6 months for finger nails and 12 months for toenails (118; 119).

Several factors must be taken into consideration before prescribing the appropriate antifungal. The type of pathogens, the patient's state of health, severity of the infection, the type of the infection, the interaction with other medicaments taken simultaneously, and the age of the patient are all to be considered (6). There are two families of systemic antimycotics available, namely oral allylamine antifungals and oral azole antifungals. Terbinafine is an allylamine oral antifungal and is one of the most frequently used systemic antimycotics (6). From the azole family, triazole antifungals including Iitraconazole, fluconazole, voriconazole and posaconazole are currently in clinical use (120).

The antifungal site of action is the ergosterol biosynthesis. Ergosterol maintains the integrity and fluidity of the fungal cell membranes and stimulates fungal growth. The destruction of ergosterol stops fungal fertility and causes cell death (93; 96). Nevertheless, oral antifungals are associated with several clinical concerns. The risk of drug-drug interactions is relatively high, therefore becoming more important with old patients, who usually use other medications. Patients with cardiovascular diseases or immunosuppressed patients are more likely to have serious complications. Liver function must be monitored during and after the treatment. Heart failure and hepatotoxicity are rare but serious complications. Other common side effects that are associated with azoles are headaches, rash, gastrointestinal disorders and sometimes loss of taste (121).

The use of topical antifungals is preferable to oral administration as there is no chance of drug-drug interaction (6). Efinaconazole is one of the commercially available antifungals. Topical treatment may be effective with superficial onychomycosis where the infection is on the surface of the nail plate and does not penetrate to the nail bed or the matrix (119). When the infection penetrates the nail bed or nail matrix as is the case in distal subungual onychomycosis, then it is better to combine the local treatment with oral treatment to increase the cure rate of the infection (11). Local treatment is limited to the range of nail permeability. The condense keratin content of the nail makes its diffusion very difficult (119).

Biophysical treatment methods

The development of resistance of dermatophytes and other onychomycosis causing pathogens to current treatments, in addition to the numerous side effects of antifungals justify the need to find alternative treatment methods. Possible novel treatment modalities are laser treatment and PDI.

Laser treatment of onychomycosis

Laser treatment is a safe and cost effective treatment method that is used clinically to treat a variety of skin lesions and for cosmetic purposes. The potential of lasers to treat toenail fungal infection has been investigated in the recent years. Different types of laser have been used, including long and short pulse Nd:YAG, Q-switched Nd:YAG, fractional lasers, diode lasers and mode-locked lasers. Most laser-treatment-studies have been carried out clinically. In most cases, the nails present onychomycosis-free after several applications. Fungi are heat sensitive microorganisms and the thermal energy from the absorption of laser light has a lethal effect on them. The limitations of laser treatment lie in the fact, that the thermal effect of the laser beam is not selective so the laser beam does not only affect the fungal species but any tissue in their way (122–128).

Photodynamic inactivation (PDI) of onychomycosis

As mentioned previously, PDI could become an attractive alternative to antibiotics and antifungals. In the case of onychomycosis, research into the development of PDI as a treatment method has recently started. The number of studies is increasing from year to year. Most of the studies are *in vitro,* while few of them are *ex vivo* and *in vivo*. Most of the tested PSs are cationic PSs and show good a phototoxicity on suspension cultures of onychomycosis causative pathogens, especially *T. rubrum* (17; 19; 21-24; 129-131). *Ex vivo* studies were conducted with powders of human nails (132) or with human nail clippers (20). Minor studies were performed testing PDI activity clinically on patients, some of them showing interesting results (132-134).In this work, the potential of the cationic TMPyP, PCor+ and the anionic eosin Y has been tested against *T. rubrum*, *T. interdigitale* and the mold *S. brevicaulis*. The tests were performed on suspension and on surfaces as well as *ex vivo* on human nail clippers.

2.10 Nail structure

The administration of medication throughout the nail has recently received a great deal of attention. An adequate amount of the PS should reach be the right place at the right time to show its effect. To achieve this, it is necessary to understand the anatomical and physiological structure of the nail barrier.

2.10.1 Nail anatomy

Human nails are horn-like structures that cover the tip of fingernails and toes. Human nails consist mainly of three structures; nail plate, nail bed and nail matrix (see figure 5). These main parts are the goal of onychomycosis treatment (135; 136).

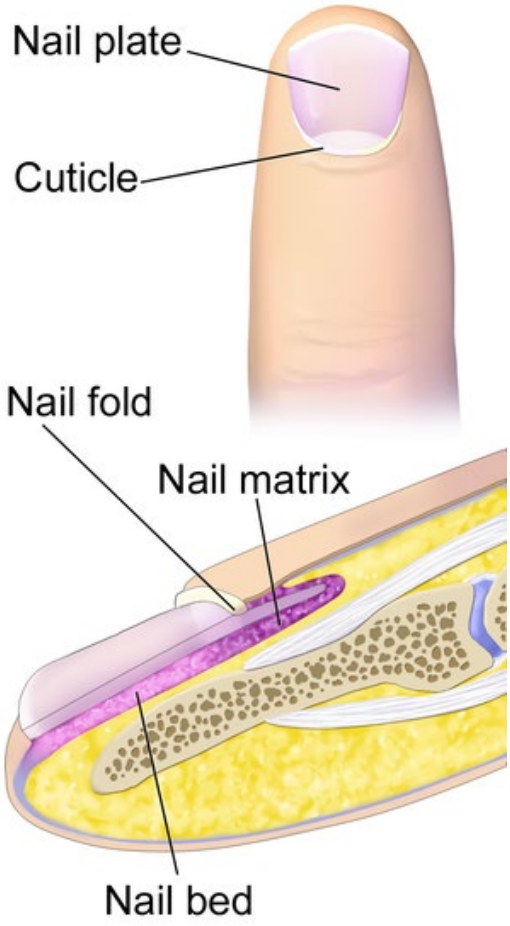

Figure 5: Nail anatomy showing the main parts of human (137).

The thickness of healthy human nails ranges from 0.25-0.6 mm for fingernails and up to 1.3 mm for toenails. The growth rate of fingernails is 3mm per month, while that of toenails is 1 mm per month. The growth rate varies from person to person. For healthy fingernails, it takes 6 months for them to grow out completely and one year for toenails. The thickness of the nail plate is defined by the thickness of its matrix (138; 136). The nail matrix nourishes and produces

the nail plate. The nail plate consists of three layers; dorsal, intermediate and ventral with a thickness ratio of 3:5:2. The dorsal layer forms the main nail barrier with dominant sulfhydryl groups. The amino acid cysteine is dominant in the intermediate layer which contains the disulfide bonds responsible for keratin stability (137).

2.10.2 Physical properties of nails

Nail plates consist of α-keratin helix, 20% soft α-keratin and 80% hard α-keratin. The alignment and orientation of keratin fibers in the intermediate layer is perpendicular to the axis of nail growth. In the dorsal and ventral layers, the keratin fibers are oriented randomly and do not follow a defined direction. This alignment of keratin in the three layers gives the nail plate its stiffness. The other source of nail toughness is the large number of cross-linked di-sulfide bonds. In addition to cysteine (half-cystine), several amino acids contribute to the nail plate, see table 2 (137; 139). The nail plate is the barrier that faces any treatment modality either oral or topical (140; 141).

Amino acid	pI[a]	Nail (%)
Lysine	9.74	3.1
Histidine	7.59	1.0
Arginine	10.76	6.4
Aspartic acid	2.77	7.0
Threonine	5.60	6.1
Serine	5.68	11.3
Glutamic acid	3.22	13.6
Proline	6.30	5.9
Glycine	5.97	7.9
Alanine	6.00	5.5
Valine	5.96	4.2
Methionine	5.74	0.7
Isoleucine	6.02	2.7
Leucine	5.98	8.3
Tyrosine	5.66	3.2
Phenylalanine	5.48	2.5
Half-cystine	5.07	10.6

Table 2: Nails' content of amino acids (137).

2.10.3 Differences between nails and stratum corneum

Despite both nails and stratum corneum being keratinized and dead tissue, there are remarkable differences between both. Nails are much thicker and harder than skin. They contain disulfide linkage cysteine and are 100 fold thicker than stratum corneum. The differences between both are not only the thickness but also their chemical composition. The Nails' lipid domain ranges from 0.1 to 1% while in the stratum corneum it is around 10%. The water content is 7-10% in nails compared to 25% in the stratum corneum (137). These differences indicate the differences in permeability of both tissues. These differences are also the reasons for the low efficacy of topical antifungals on nails. The chemical enhancers of skin permeability like dimethyl sulfoxide (DMSO) also have no effect on nails. Skin penetration enhancers work through the use of lipid pathways. Due to the lack of a lipid domain in nails, skin enhancers have no impact on nail permeability. The principle of action of nail penetration chemical enhancers is the cleavage of disulfide bonds. This makes the nails very elastic and permeable (142–144). More details will be discussed in the following section.

2.10.4 Nail permeability and possible enhancement methods

The chemical composition of nails is responsible for the basic rigidity of the nail unit and its low permeability. Diseased nails are found to be even less permeable than healthy nails. Onychomycosis is always associated with over-thickness as shown in Figure 6. This increment in thickness makes the task of topical treatments more difficult. Permeability modifiers are required for successful treatment (145; 146). There are a lot of factors that improve nail permeability. pH-value and molecular weight of the drug and water hydration may help slightly in increasing the penetration (144).

Figure 6: Over-thickness onychomycosis diseased nail (108).

The penetration enhancement can be achieved physically or chemically. Examples of physical enhancement are nail abrasive through using lacquers or electrical drills like dental drills. Laser or low frequency ultrasound can be used as well. Chemical enhancement modalities are less aggressive. There are some chemical enhancers that act on the nail unit directly and more efficiently. Thiol compounds which contain (-SH) groups are considered to be very efficient enhancers. N-acetyl-cysteine (NAC), mercaptoethnol, N (2-mercaptopropionly) glycine (MPG) are examples of thiol enhancers. The enhancement effect is proportional to the enhancer concentration (145). Some enhancers possess a fungistatic effect like pyrithione (2-mercatopyridine-1-oxide, PTO). Sulfites and bisulfite compounds have the ability to reduce disulfide linkages (147). Enhancement of the permeability is important for any treatment methodology of onychomycosis.

3. Experimental (Materials, Method)

3.1 Materials

Fungal strains

Three kinds of fungal species were isolated from patients in the Department of Dermatology, university hospital in Greifswald, Germany. The three fungi are *T. rubrum*, *T. interdigitale* as models of dermatophytic pathogens of fungal infections and *S. brevicaulis (Sb)* as model of non-dermatophytic mold fungi. Fungi strains were cultivated on Sabouraud dextrose Agar (SDA 4%) at 28 ºC to get fungal spores for suspension preparation.

PSs

The PSs being used in this investigation are 5,10,15,20-Tetrakis(1-methylpyridinium-4-yl) porphyrintetra(p-toluenesulfonate) (TMPyP), Sigma-Aldrich Chemie GmbH (Munich, Germany) , 5,10,15-tris-(1-methylpyridinium-2-yl)corrolato-(trans-dihydroxo)phosphorus(V) (PCor+) which was synthesized according to (15) and 2',4',5',7'-tetrabromo-3',6'-dihydroxyspiro[2-benzofuran-3,9'-xanthene]-1-one (Eosin Y), Sigma-Aldrich Chemie GmbH (Munich, Germany).

1. TMPyP

TMPyP is a very famous (Figure 7), commercially available porphyrin based PS. The high phototoxic effect of TMPyP on bacteria, its stability and its high quantum yield(~ 72% in water) make it a good choice to test for its impact on dermatophytes and mold fungi(7).

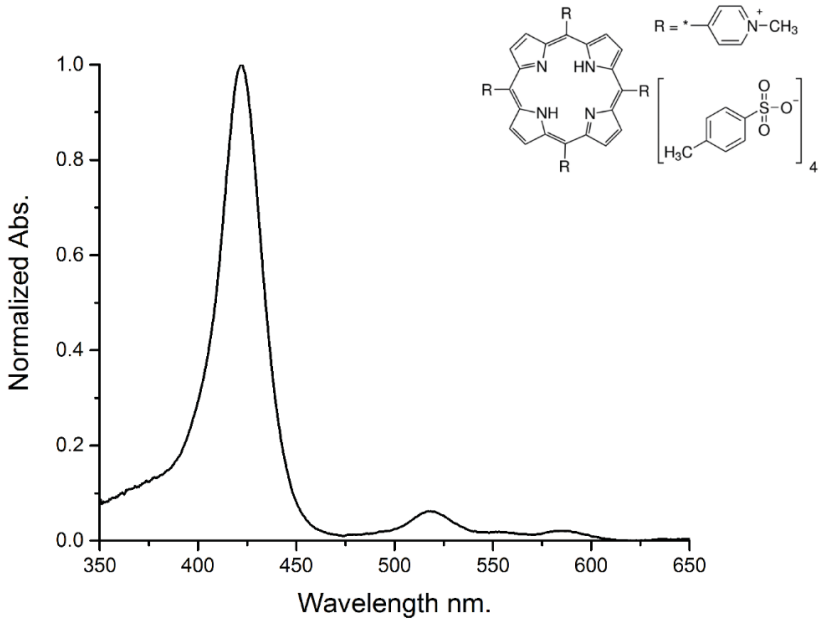

Figure 7: TMPyP normalized absorbance spectrum and chemical structure.

2. PCor+

The second PS involved in this investigation is the corrole based PS PCor+ (Figure 8). It was first produced in 2013 by Gross and his co-workers. PCor+ also has a good singlet oxygen quantum yield of about 81% in water. It offers high phototoxicity against molds, bacteria and with less impact against green algae (15).

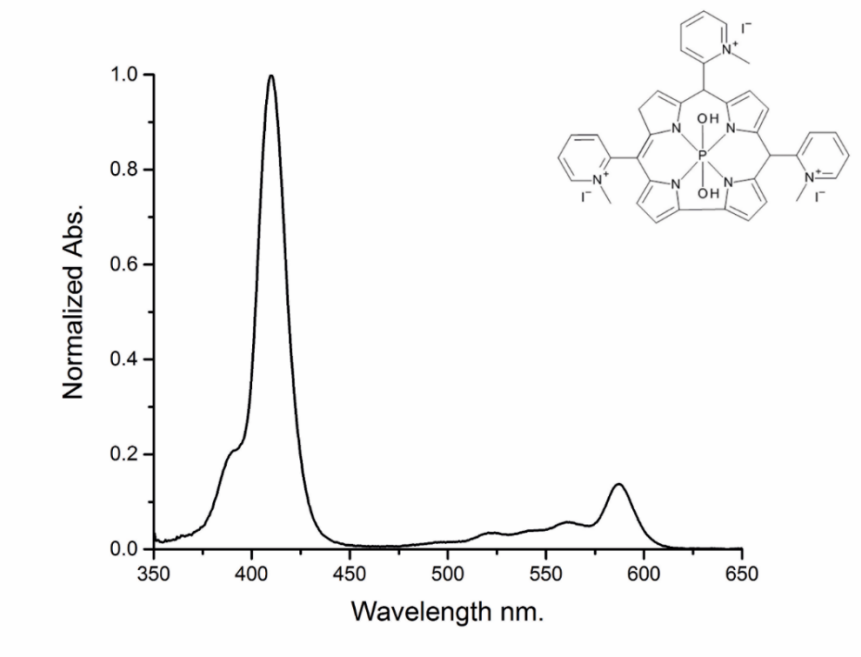

Figure 8: PCor+ normalized absorbance spectrum and chemical structure.

3. Eosin Y

Despite its negative charge, eosin Y (Figure 9), the red acid stain, was used due to its availability. Its singlet oxygen quantum yield is approximately 72% (148).Eosin Y has a great potential against gram-positive bacteria. It is one of the oldest PSs being used clinically (not as a PS). Using clinically approved PSs for the treatment of onychomycosis facilitates any future application for the treatment of nail fungal infection.

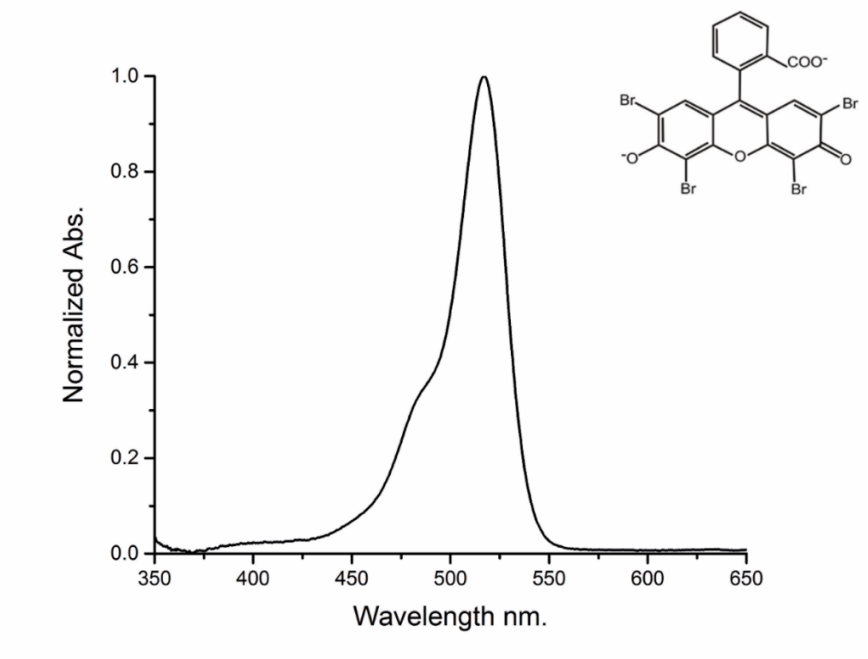

Figure 9: Eosin Y normalized absorbance spectrum and chemical structure.

Illumination

- **White Illumination**

  In this study, a customized illumination setup containing white light LEDs (Osram, Munich, Germany) was used. Each setup consists of eight 3500 K LEDs and eight 6500 K LEDs placed alternating in a square arrangement. The LEDs illuminate an opal glass plate from below, guaranteeing a uniform irradiation of the cell samples in the well plates at an intensity of 12 mW/cm^2 for phototoxicity in suspension cultures and 8 mW/cm^2 for phototoxicity on agar surfaces.

- **Green illumination**

  A customized illumination setup containing Green light LEDs (523 nm) (Osram, Munich, Germany) was used for the illumination in the *ex vivo* investigation. The Setup comprises 48 LEDs in a square arrangement. The LEDs illuminate an opal glass plate from below and ensure a uniform irradiation of the cell samples in the well plates with an intensity of 10 mW/cm^2.

Nails

Clippers of healthy human nails were collected from a group of volunteers with ages ranging from 24 to 65 years. Nails were immersed in 70% ethanol (v/V) for 30min for disinfection purposes. Clean nails were stored in plastic tubes until use within one month of collection.

Singlet oxygen detection

- **Time resolved singlet oxygen luminescence (TRSOL) (*in vitro*)**

  The scans were performed with a customized set-up reported in (149). The set-up consists of a cross table moving in x and y directions to allow scan over samples with 15 cm in both directions. Movable optics in Z-direction are used for optimal overlap of excitation and imaging spot. For detection of singlet oxygen luminescence, an imaging spot of 300 µm on 2000 µm fiber was used. A modulated LDM-405D (Omikron-Laserage, Rodgau-Dudenhofen, Germany) diode laser is used as excitation laser. The excitation laser is focused in an angle of 40° on the imaging spot. All presented measurements were performed with excitation pulses with a temporal width of 240 ns and a pulse energy of 0.3 µJ at 405 nm. This wavelength is suitable to excite both tetrapyrrol PSs in the respective Soret peak.

  A C10083CAH Spectrometer (Hamamatsu, Shizuoka, Japan) was used for spectrally resolved visible luminescence measurements with an Integration time of 200ms. For time resolved near infrared (NIR) luminescence measurements, TCMPC-1270 Singlet Oxygen Luminescence Detection System (SHB Analytics, Berlin, Germany) was used with a bandpass filter of 1270+15 nm. A Bandpass filter with a center wavelength of 1230 nm was used as well to differentiate singlet oxygen luminescence from possible PS phosphorescence or disturbance signals of unknown sources.
  The fluorescence and singlet oxygen luminescence scans were performed sequentially. An area of 6 x 2 cm including all six sample sections (see Figure 11) was scanned several times over a period of up to 24 days.

- **Singlet oxygen detection (*ex vivo*)**

  Measurements were taken using the compact table-top $^1O_2$ luminescence detection system developed in the Group of photobiophysics, Humboldt Universität zu Berlin. Excitation was done using a frequency doubled Nd3+-YAG Laser Vector from Coherent, Germany. Samples were excited with 5 mW at 532 nm, 10 ns pulses with a

repetition rate of 12 kHz for 100 s when the 1270 nm filter was used (37). Bandpass filters with center wavelengths at 1230 nm and 1300 nm were used to separate singlet oxygen from PS- phosphorescence or any other disturbance signals. Molecular oxygen was blown on the samples during the scan in an alternating on/off regime to see the effect of oxygenation in singlet oxygen generation on nail microenvironment.

Microbiology laboratory tools

Equipment	Company
Sterile Bank	BDK Luft- und Reinraumtechnik GmbH
Micropipettors (10-100 µl, 20-200 µl , 100-1000 µl)	Eppendorf Research
Barrier pipette tips sterile (20 µl, 300 µl, 1000 µl)	Sorenson BioScience
Sterile pipettes (5 ml,10 ml, 25 ml)	Greiner Bio-One: GBO
1,5 ml Caps	Greiner Bio-One: GBO
Sterile Tubes (15 ml, 50 ml)	Greiner Bio-One: GBO
6, 12, 24, 96 well-plates (transparent)	Greiner Bio-One: GBO
Syringe filters, CME, sterile, pore size 0.22µm	International - Carl Roth
Single use syringes, 2 pieces (5 ml, 10 ml)	B BRAUN
Filter papers	
Petri dishes sterile	Greiner Bio-One: GBO
Inculcation loop sterile	Greiner Bio-One: GBO
Cell spreader	ISOLAB Laborgeräte GmbH
Cell scarper	ISOLAB Laborgeräte GmbH
Forceps	ISOLAB Laborgeräte GmbH
Sterile cotton swab, 15 ml long, small head	Hubei Haige Medical Instrument Co
Sterile Disposable Reagent Reservoirs	Fisher Scientific

Table 3: Microbiological laboratory tools.

3.2 Methods

Spore suspension preparation

The protocol used for suspension preparation is given in (150) , with the small modification of using sterile gauze compresses instead of 8µm filter. 10 ml of phosphate-buffered saline (PBS) with 10% of tween 80 were added to the surface of 2-3 weeks old culture before gently brushing the spores of the surface with a glass rod. The filtrate gained from this step was centrifuged at 3400 g (10 ºC) and the supernatant was discharged and washed again with PBS. For singlet oxygen measurements, spore suspensions were prepared in a different way. 3-4 weeks old plate cultures with sufficient spore amount were used. In 1ml of PBS, pH 7.2 with 1% of tween spores harvested with an inoculation loop were suspended. To get homogenous spore suspensions, the mixture was gently shaken.

Optical density and biomass of the biological samples

In this study, optical density (OD535) was used to reflect the biomass of the biological samples. The concentrations of the spores' suspensions are expressed as relative concentration in term of OD535 and not as absolute cell number. The correlation between the optical density and colony forming unit (CFU) is difficult to achieve because of the fungal morphology. The spore suspension may include hyphal fragments beside fungal cells so that a precise counting could not be observed. Figure 10 shows the OD535 of *S. brevicaulis* in different incubation periods (0 h, 3 h,7 h, 24 h). *S. brevicaulis* was chosen as example. For the phototoxicity experiments the high concentrations was chosen for fast experiments while the low concentration was chosen to start the long-time experiments (2 weeks on).

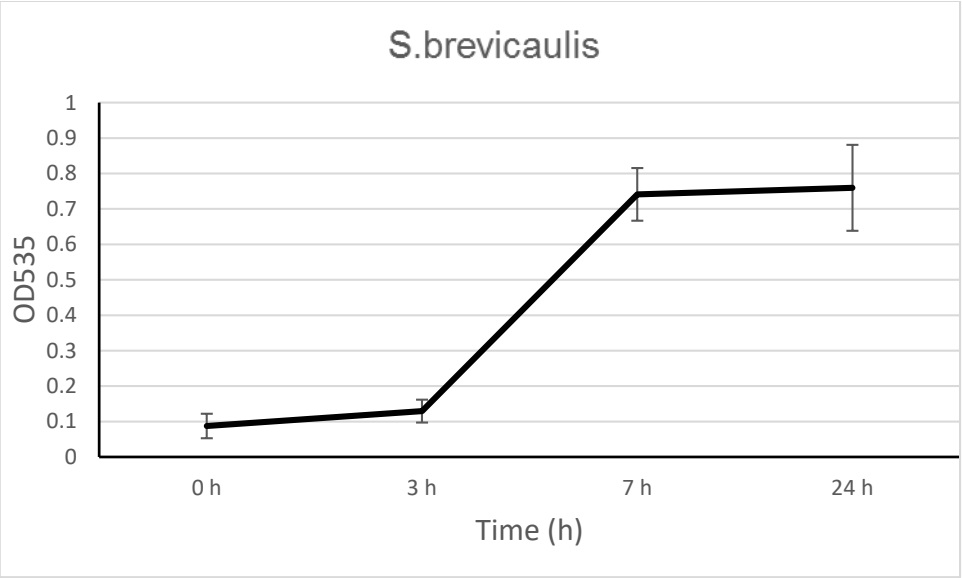

Figure 10: The optical density OD535 of spore suspension of S. brevicaulis at different incubation periods (0 h, 3 h, 7 h and 24 h).

3.2.1 Phototoxicity tests

The investigation of the phototoxic effect of the three PSs was carried out in three stages: first, phototoxicity on suspension cultures as preliminary tests, then the investigation on surfaces and finally *ex vivo* phototoxicity tests on human nails.

Phototoxicity tests on suspension cultures

As preliminary step, the phototoxicity test was started on suspension cultures. It was performed on 96 well plates. To each well, 50 µl of spore suspension and 50µl of PS were added. The biomasses of the spore suspensions were determined at the beginning of the experiment using optical density at 535nm. OD535of the spore suspensions of *T. rubrum*, *T. interdigitale* and *S. brevicaulis* was 0.7, 0.48 and 0.87, respectively. As mentioned previously, the phototoxicity on spore suspension was started with high concentrations as it consider a fast experiment. In addition, the start with high concentration of living cells results in high signal of MTT and the ration between dead and living cells will be much higher. MTT assay was used as viability evaluation method after phototoxicity tests (see section 3.2.3).

Three different concentrations of TMPyP and PCor+ (5 µM, 10 µM and 20 µM) were applied. For a control group, SD broth was used instead of PSs.

Before the illumination, samples were incubated for 30 min at 28 ºC. Subsequently, the samples were illuminated for 30 min, 60 min and 90 min whereby 30 min, 60 min and 90 min were

selected as different illumination periods. After illumination, all samples were kept in the incubator for an additional 24 h. The applied source of illumination is white LEDs with an intensity of 12 mW/cm^2.

Phototoxicity tests on cultures on surfaces

This part was conducted using 6 well plates. Per well, 2 ml of SDA agar was added. On sterilized (1.5 cm * 1 cm) filter papers, two different amounts per PS (0.5 µmol and 0.1 µmol) were used. After drying, each filter paper was placed on each well of the 6 well plates. 10 µl of suspension cultures were added to each filter paper. For the control group, no PS was added to the filter paper (0 µmol). The concentration of spores in the suspensions of *T. rubrum*, *T. interdigitale* and *S. brevicaulis* was determined using optical density at 535 nm amounting to 0.1, 0.087 and 0.108 at the beginning of the experiments respectively. The phototoxicity on surfaces experiments extended for two weeks and for this reason the low concentration was chosen to start with.

Samples were continuously illuminated for 48 h using white LEDs illumination from a customized setup (mentioned previously) with a total illumination intensity of 8 mW/cm^2. After illumination, samples were kept in the incubator at 28 ºC for two weeks.

Phototoxicity tests on human nails as ex vivo model

To test the potential of the three PSs in cases closer to reality, human nails were used as *ex vivo* model. Nails were termed to get flat rectangular shapes. The clipped nails were incubated in 2 ml of spore suspension of T. rubrum for two hours on a shaker at room temperature. The nails were then removed and kept in 24 well plate with 100 µl of Sodium chloride solution (NaCl 0.9) in each well. Sealed well plates with infected nails were stored in the incubator at 28 ºC to be used within one month.

For the PDI tests, two weeks and four week old infected nails were used. As pretreatment step, infected nails were immersed in water for 2 h on a shaker at room temperature for hydration purposes. Afterwards, the hydrated infected nails were also immersed in 2 ml of eosin Y solution with concentrations between 1 mM and 4 mM for 2 h on a shaker at room temperature. Samples were removed from eosin Y solution and placed in 24 well plate for illumination. The final concentration of eosin Y taken up by the infected nails could not be determined. Different illumination times of 30 min, 60 min and in some cases 48 h of continuous illumination were used. Green LEDs (at 523 nm) illumination from a customized setup (mentioned previously) with a total illumination intensity of 10 mW/cm^2 was used.

Phototoxicity tests on infected socks' textiles

Socks textile with 80% cotton and 20% polyester was used for this part. The socks were cut into rectangular pieces with dimensions (1.5 cm*2 cm). 10 µl of suspension cultures of T.rubrum were added to each piece. 20 µl of two different concentrations of eosin Y (3 mM and 10 mM) were added to the infected textiles. For the control group, no PS was added to the filter paper (0 mM). Samples were continuously illuminated for 90 min using green LEDs (at 523 nm) illumination from a customized setup (mentioned previously) with a total illumination intensity of 10 mW/cm^2. After illumination, samples were kept in the incubator at 28 ºC for two weeks.

3.2.2 Dark toxicity

In every investigation, equivalent samples were prepared for dark toxicity tests. Samples were kept in darkness at room temperature for time intervals corresponding to those of the phototoxicity experiments.

3.2.3 Viability evaluation

Depending on the type of phototoxicity tests, suitable viability evaluation was carried out. The MTT assay was used to check the viability of the suspension cultures after dark and phototoxicity tests (151; 152). 24 h after the end of illumination, 10 µl of MTT (5 mg/ml) was added to each well. After addition of MTT, samples were kept in the incubator for 2 h or less until the interaction had taken place and purple formazan was formed. Then 200 µl of DMSO were added. To keep the optical density within the linear region, samples are diluted accordingly.

To check the efficiency of photodynamic inactivation on surfaces and on nails, samples were kept in the incubator at 28 ºC for two weeks following the illumination. Samples were scrutinized every three days. Photographs were taken after one week and after two weeks. Hereby, no fungi growth on agar represents efficient photodynamic effect of the PS on fungi. Normal fungi growth on treated samples represents an inefficient phototoxic effect.

3.2.4 Singlet oxygen luminescence kinetics detection

Any change in the microenvironment of the PS can affect the generation of singlet oxygen, its reactivity and diffusion. Here, singlet oxygen kinetics were observed twice for two different experimental setups, on surfaces and on human nails. First, we studied the impact of the presence of fungi in the PS's microenvironment on singlet oxygen kinetics. 2DTRSOL scans in the presence of the three fungi species involved in this investigation and the PSs TMPyP and

PCor+ were conducted. The samples were kept in the darkness at all time to allow proper growth of the fungi to study the kinetics throughout different fungi growth stages.

The second part was performed to study the behavior of the PS and to gain information about the generation of singlet oxygen in the microenvironment of human nails. Here, healthy human nails were used instead of infected nails to prevent any possible contamination with spores when blowing oxygen. The PS used was eosin Y.

Sample preparation

For singlet oxygen kinetics measurements on surfaces, M9 Agar (153) replaces the mostly used SDA (154) as earlier preliminary measurements showed a high singlet oxygen luminescence quenching effect of SDA (42) 75 ml of M9 were pipetted in each petri dish. 5 µl of 1 mM stock solution of each PS was added to sterile filter papers of 5 mm diameter. After drying, the filter paper was placed onto the M9 Agar Petri dishes as shown in Figure 11 and consecutively 5 µl of each dilution of spore suspension of T. *rubrum* and *S.brivecaulis* were pipetted. PSref: PS without spore suspension; C1: 1/1000 + PS, C2: 1/100 + PS, C3: 1/10 + PS, C4: original suspension + PS, Fref: original suspension only. While in case of T. interdigitale, 5 µl of the 1/100 dilution of spore suspension was only used for statistical purposes.

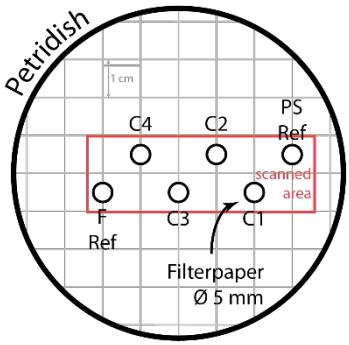

Figure 11: Sketch of the sample geometry of Petri dish used in the 2DTRSOL kinetics experiments: PSref: PS without spore suspension; C1: 1/1000 + PS; C2: 1/100 + PS; C3: 1/10 + PS; C4: original suspension + PS; Fref: spore suspension without PS.

The configuration of nail samples was different. Since no area scan was carried out and only single point scans were conducted, there is no need for a special configuration. Nails' samples were placed on the top of M9 agar petri dish and arranged according to eosin Y concentration and enhancer (see figure 12).

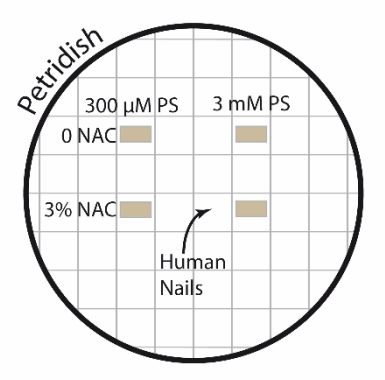

Figure 12: Sketch of the sample geometry of Petri dish used in the singlet oxygen luminescence kinetics on the surface of human nails experiment.

Singlet oxygen luminescence observation

Data processing

Fluorescence and singlet oxygen luminescence were conducted consecutively. The scanning area was divided into six segmentations according to the filter paper configuration as shown in Figure 11 and thus the scanning data. Data processing is shown in Figure 13. For each pixel, both fluorescence and singlet oxygen luminescence were observed described below.

Fluorescence

For the correction of the observed technical spectra, a subtraction was done of a spectrum measured in the dark before each scan. The fluorescence intensity for each pixel was observed by integration over the range of the PS fluorescence. With PCor+ from 550 nm to 750 nm and for TMPyP from 600 nm to 830 nm.

Singlet oxygen luminescence

All time resolved NIR luminescence curves, determined at 1270 nm were fitted by the bi-exponential model in traduced in (155) but with some modifications. Bi-exponential model describes singlet oxygen luminescence in homogeneous systems. As a precise description of the kinetics in complex systems is unlikely to succeed. The aim is to describe the kinetics with fewest fitting parameters, two mono-exponentially decaying compartments with additional compartment for the disturbance signal. A significant fast decaying disturbance signal from unknown source was dominant to all measured kinetics at 1270 nm and 1230 nm. With the consideration of emission spectrum of singlet oxygen, any luminescence at 1230 nm is either a

PS phosphorescence or disturbance signal. In this work, the signal is out to be disturbance signal as the kinetics do not follow the PS's kinetics.

A stretched exponential decay as described in (156) is used to describe the disturbance signal. Whereby the values of τ, β were set to 0.3 µs, 0.7 respectively with amplitude exception. An independent decaying compartment was used to include the disturbance signal to the fitting model with the following distribution

$$f(t) = e^{-\left(t/0.3\mu s\right)^{0.7}}$$

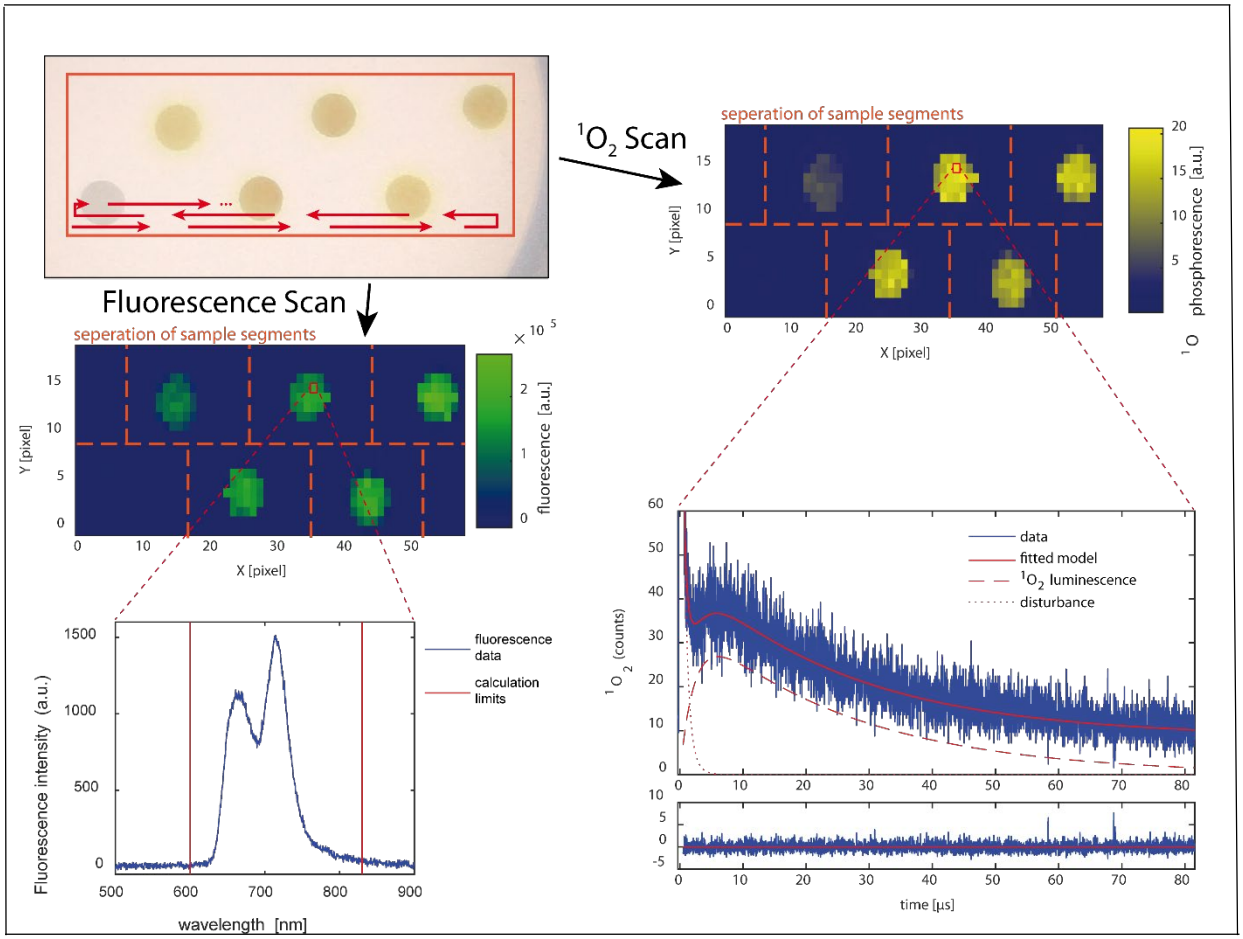

Figure 13: Illustration of data processing (42).

The scanned area was divided into six segmentations after obtaining the fluorescence and singlet oxygen luminescence kinetics as shown in Figure 11 and Figure 13. The intensity of fluorescence per segment as well as its uncertainty were calculated by the average value and the standard deviation of all pixels in that segment. For *T. interdigitale* data, the error-weighted

mean value and standard deviation of the fitted values of all pixels of the six segments were used.

Singlet oxygen luminescence amplitude, rise and decay time of each segment were determined by error-weighted mean value and standard deviation of the fitted values of all pixel in that segment (157). Consequently, the confidence intervals of the fitted values were used to express the error of the corresponding value of each pixel.

Singlet oxygen kinetics on the surface of nails' samples were not analyzed. They are only shown to describe the difference of the signal between aerated samples and those under oxygen atmosphere. Signals show a combination of PS' phosphorescence, singlet oxygen phosphorescence and short artefacts. Singlet oxygen luminescence is a very week component and for that reason it is difficult to analyse. It is difficult to distinguish singlet oxygen lifetime and triplet lifetime. In addition to that, scattering is dominant which is normal in biological samples.

4. Results

4.1 Time resolved singlet oxygen luminescence detection (2DTRSOL)

The investigation was started with 2DRSOL detection. It is important to study the behaviour of the PS in the presence of fungi, and to gain information about the kinetics of singlet oxygen, its generation and diffusion in an environment with fungi growing on agar surfaces. Such information would help to know whether our PSs are able to produce singlet oxygen in such microenvironment. Another point of interest is, if the amount of the generated singlet oxygen would be enough to induce high phototoxicity. In this part, the used PSs are PCor+ and TMPyP.

2DTRSOL in the presence of *T. rubrum*

T. rubrum is the most prevalent onychomycosis causative pathogen. For this reason, the study was started with *T. rubrum.* Four different samples with four different spore suspension concentrations were investigated here. In addition, two references, one the PS without *T. rubrum* and the other *T. rubrum* spores without PS, were included in the study. The sample configuration is shown in figure 11. The samples were incubated for one hour before the first scan. The samples were scanned on a daily basis over a time of 24 days. To induce proper fungi growth, they were kept in the incubator in between scans. Figure 14 and figure 15 show the normalized fluorescence and singlet oxygen luminescence amplitude of PCor+ and TMPyP in the presence of fungi. In samples kept in darkness, *T. rubrum* grew normally during the investigation time. *T. rubrum* is known for its slow growth. Spores could be detected only after 8-9 days. The growth of *T. rubrum* results in the formation of water drops on the inner top cover of the Petri dish. The water drops formed causes scattering during scans, which is visible at day 9. The Figures show the intensity plots of singlet oxygen luminescence and PS fluorescence signals over time. As can be seen, the intensities of both fluorescence and singlet oxygen luminescence decreases over time for TMPyP as well as PCor+. Comparison of figure 14 and figure 15 also show the difference in diffusion of the PSs. In figure 14, the localization of TMPyP is on filter paper or close by. In contrast to TMPyP, PCor+ diffuses rapidly away from the filter paper. The diffusion of PCor+ occurs rapidly and starts immediately, as can be seen clearly in figure 15, day 0 (measurements taken after one hour of incubation).

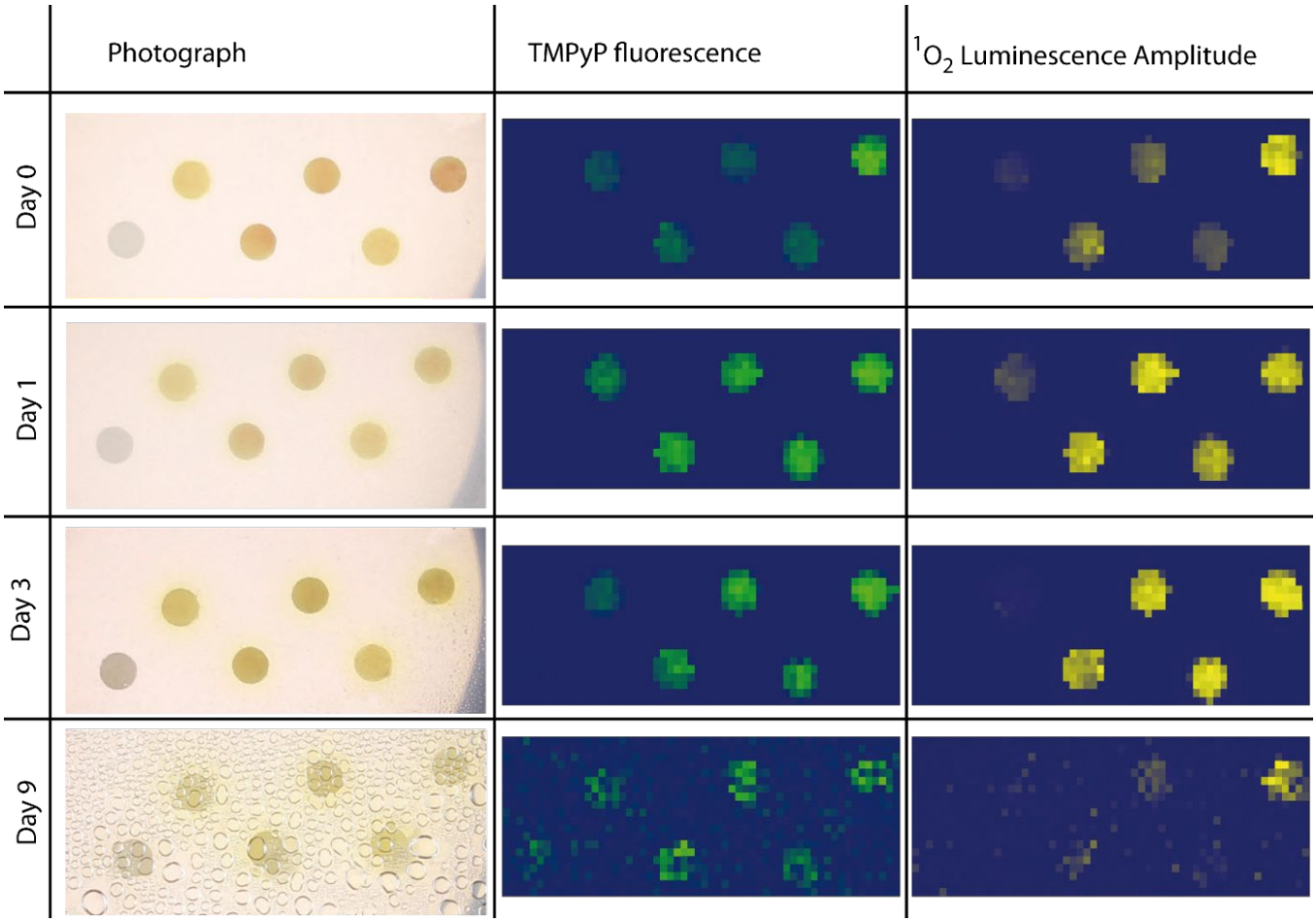

Figure 14: Photograph and normalized intensity plots of TMPyP fluorescence and $^1O_2$ luminescence of the TMPyP-*T. rubrum* sample.

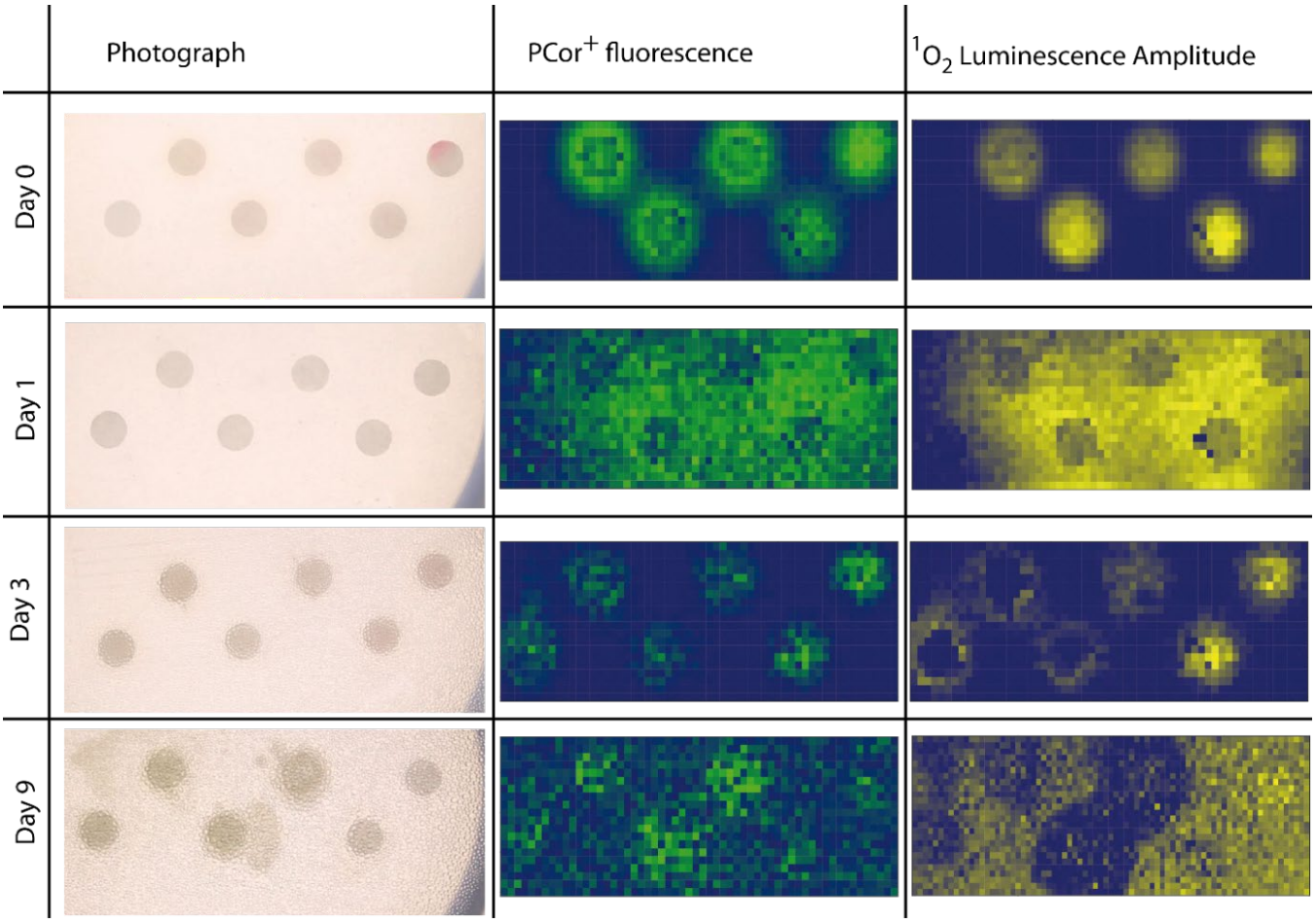

Figure 15: Photographs and normalized intensity plots of $PCor^+$ fluorescence and $^1O_2$ luminescence of the $PCor^+$-*T. rubrum* sample.

A correlation between the fungi growth stage and the lifetimes can be extrapolated from the comparison between the observed lifetimes on fungi samples and separated reference. From figure 16, the amplitude of the luminescence signal decreases with the growth of the fungi.

At day 0, a pronounced singlet oxygen kinetics signal is visible for TMPyP-*T. rubrum* sample, as shown in figure 16. Afterwards the singlet oxygen luminescence signal is superimposed by an interference signal. Figure 16 shows that the singlet oxygen luminescence amplitude decreases with fungi growth. After one week, hardly any kinetics signal could be detected.

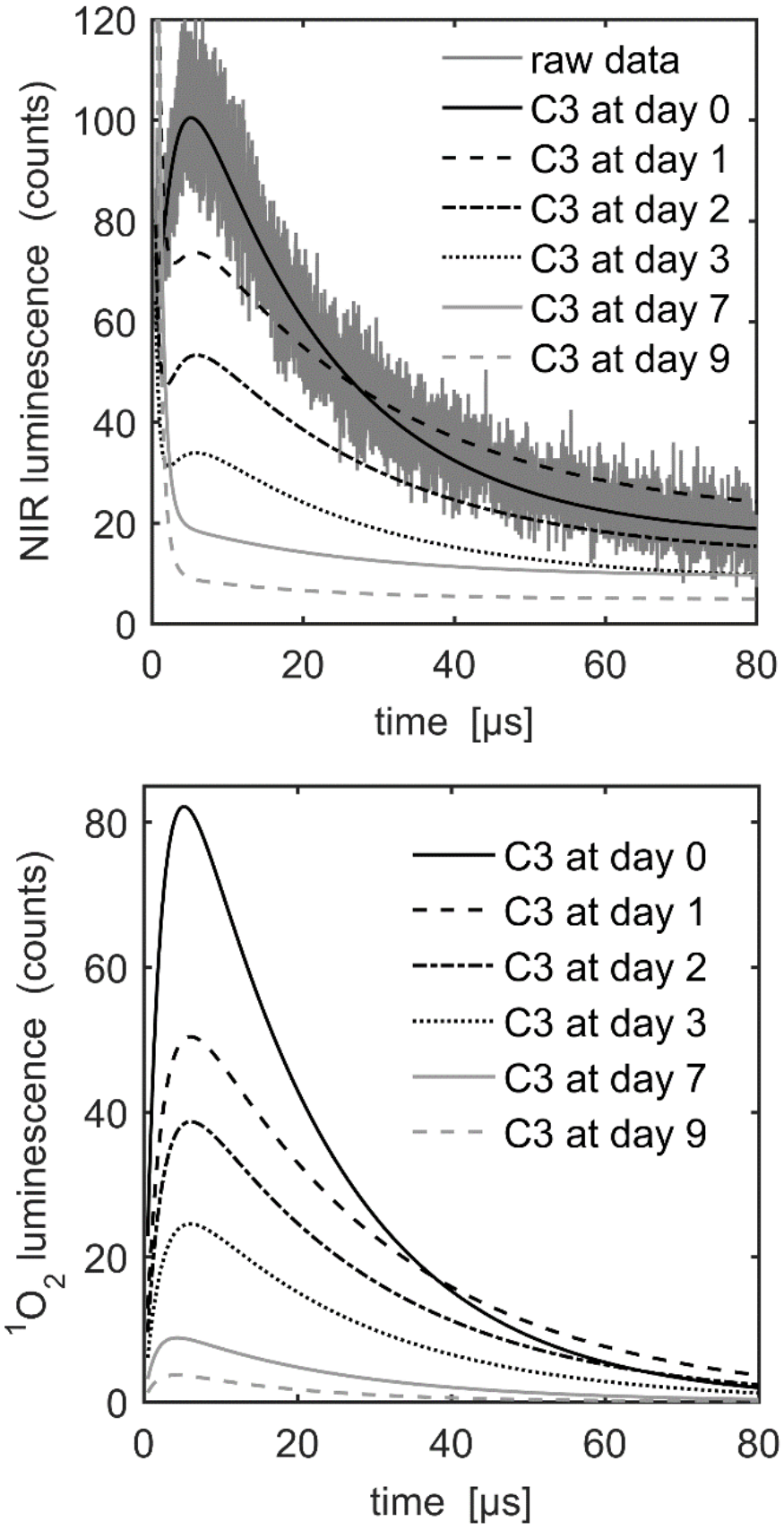

Figure 16: NIR luminescence kinetics and isolated $^1O_2$ luminescence kinetics part on the surface of the C3 area of the TMPyP - *T. rubrum* sample. The kinetics of $^1O_2$ can be determined up to day 7.

The development of the PS's triplet lifetime and the $^1O_2$ lifetime on the surface of the $PCor^+$-*T. rubrum* samples is shown in figure 17 and the TMPyP- *T. rubrum* in figure 18. The values represent the error-weighted mean values with corresponding error-weighted standard deviation of the fitted lifetimes of each area.

The rise and decay time of singlet oxygen and triplet lifetime of the PSs cannot be evaluated directly from the kinetics so an independent method for triplet lifetime determination, like flash-photolysis is required. Since laser flash photolysis methodology is inapplicable to the samples investigated in this work, due to their opalescence, indirect methods should be used. As there are two PSs in two similar microenvironments, the lifetimes of both PSs and the singlet oxygen lifetimes can be determined by comparison. From figure 17 and figure 18, we can find that the shorter lifetime is the singlet oxygen lifetime as it is nearly equal for TMPyP and PCor+. The lifetime of singlet oxygen is equal to 1.5 to 2.5 µs. The lifetime varying greatly from TMPyP to PCor+ samples is the triplet lifetime. The triplet lifetime of TMPyP decreases slightly over seven days in the presence of fungi. In contrast, the triplet lifetime of the TMPyP reference in a separate Petri dish (sep. PSref), hence without fungi, increases from the initial value at day zero to a constant triplet lifetime of about 24 µs on days 1-7. The triplet lifetime of $PCor^+$ shows a slight increase over seven days.

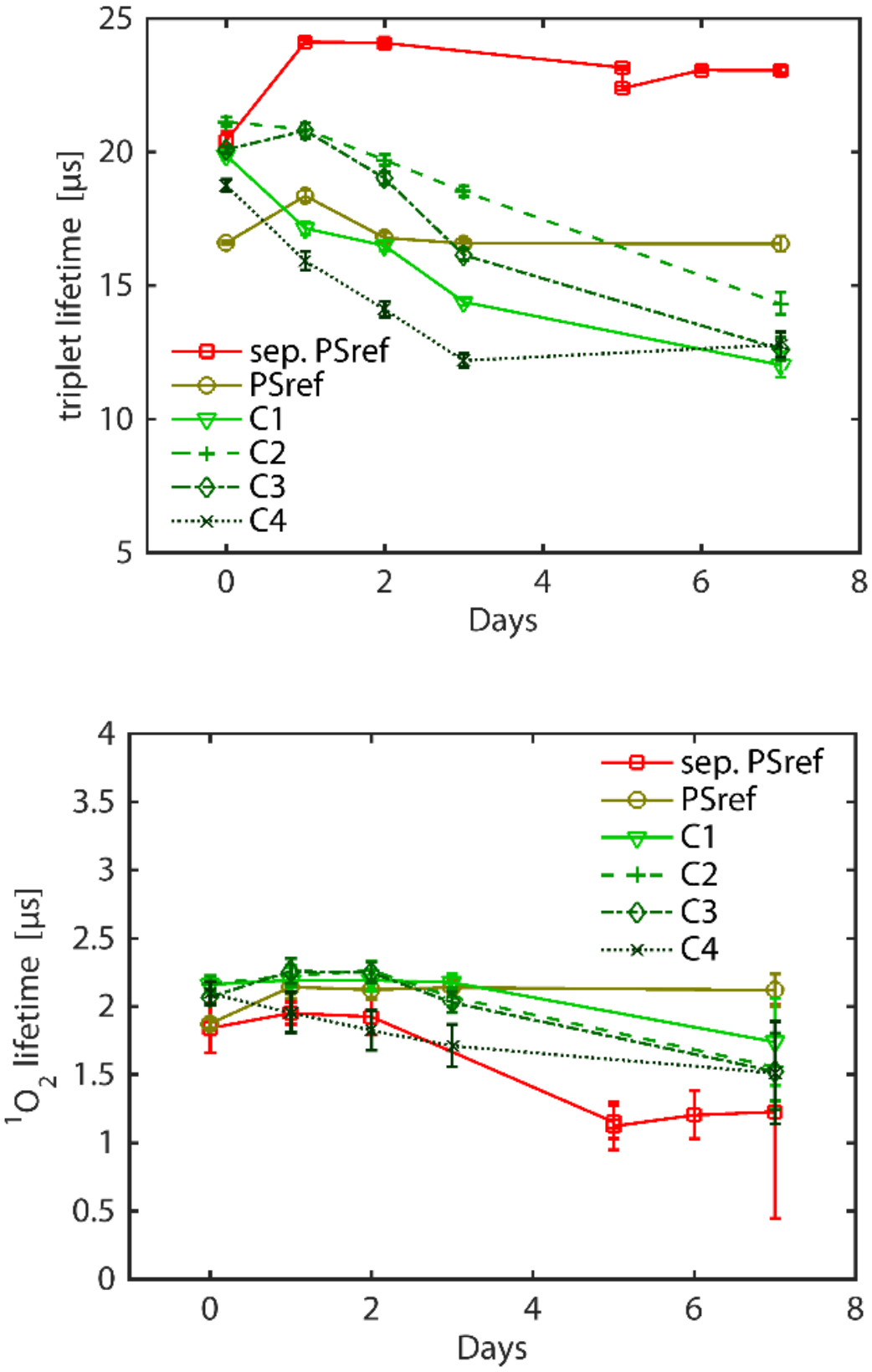

Figure 17: Development of the PS's triplet lifetime and the $^1O_2$ lifetime measured on the surface of the the TMPyP -*T. rubrum* sample. The value of each day represents the error weighted mean value of all pixels of each sample area. The error values are the corresponding error weighted standard deviations. "Sep. PSref" represents the PS reference on a separate Petri dish.

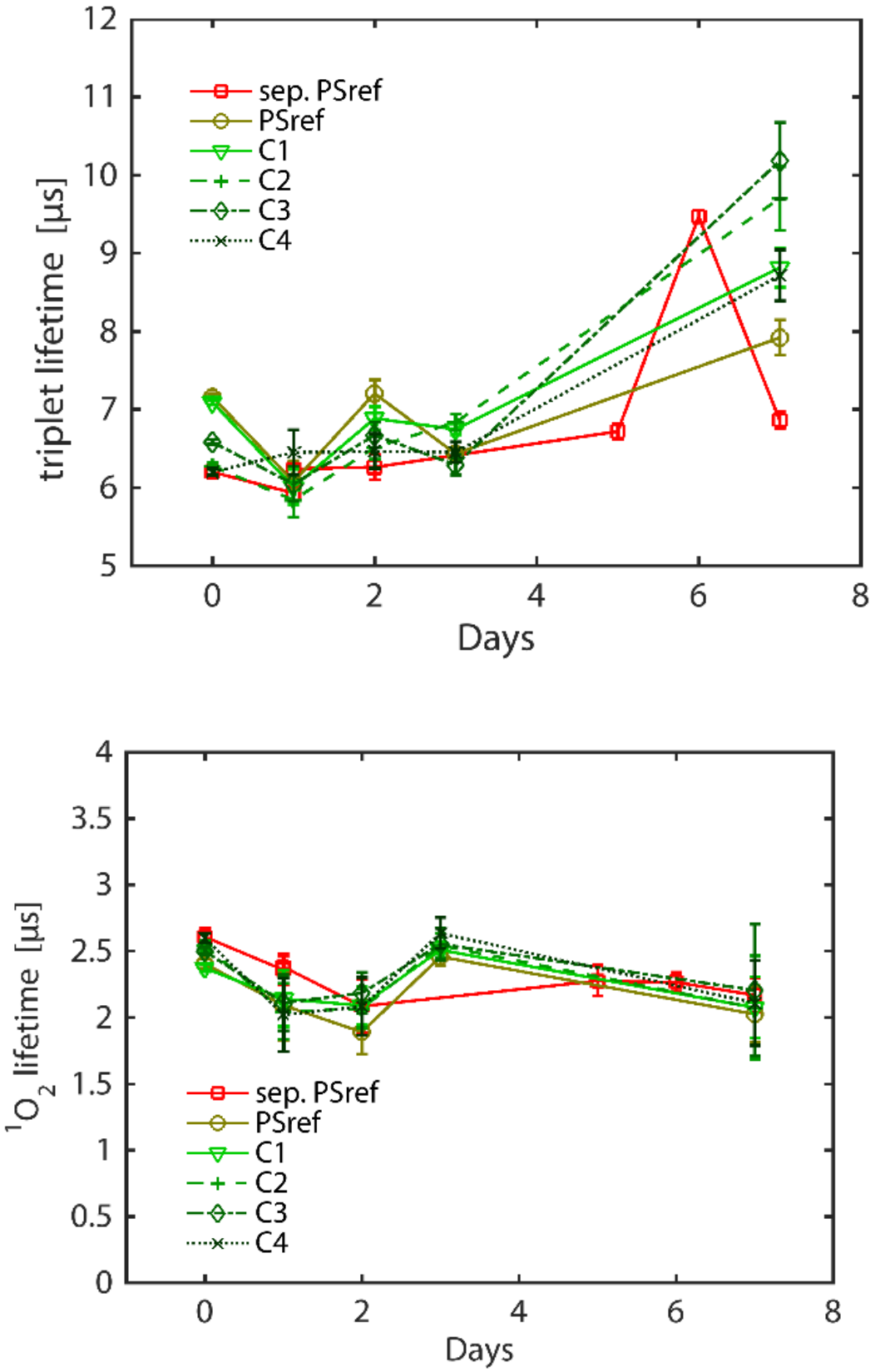

Figure 18: Development of the PS's triplet lifetime (left) and the $^1O_2$ lifetime measured on the surface of the PCor$^+$- *T. rubrum* sample. The value of each day represents the error weighted mean value of all pixels of each sample area. The error values are the corresponding error weighted standard deviations.

2DTRSOL in the presence of *S. brevicaulis*

To continue this study, 2DTRSOL has been investigated in the presence of *S. brevicaulis*. The conditions and sample configurations of the experiment were the same as in the *T. rubrum* test.

Figure 19 and figure 20 show photographs and normalized intensity plots of the PS fluorescence and the $^1O_2$ luminescence amplitudes of the *S. brevicaulis* samples with TMPyP (Figure 19) and $PCor^+$ (Figure 20).

The growth of the mold *S. brevicaulis* is fast, compared to that of the dermatophyte *T. rubrum* as can be seen in the photographs. *S. brevicaulis* started to form spores on the third day after incubation. After two weeks, the spores almost covered the entire surface, even near samples with low spore suspension concentration. As with other microorganisms, moisture is the result of their by-products during metabolism. This moisture turned to water drops covering the upper surface of the petri dish. Since the detection is performed through the upper surface of the petri dish, water drops cause scattering in luminescence signal. This effect is clearly visible at day 13 for the TMPyP- *S. brevicaulis* sample (Figure 19) and at day 12 for the $PCor^+$- *S. brevicaulis* sample (Figure 20).

The species of the fungus investigated had no influence on the behaviour of the PS. The intensity plots show that PS fluorescence and singlet oxygen luminescence intensities decrease over time. A good signal of both can be acquired for up to one week. After four weeks, the luminescence signal was barely detectable.

The diffusion behaviour of the PSs seen on *S. brevicaulis* samples equals that on *T. rubrum* samples.

The figures also show a correlation between the growth stage of *S. brevicaulis* and the intensity of signals. In the first days, between day 0 and day 3, both fluorescence and singlet oxygen luminescence signal have a high intensity. After two weeks, only a weak signal was detected. Interestingly, after sporulation of *S. brevicaulis*, the observed intensity after four weeks was higher. However, it has to be pointed out, that both the PS fluorescence and the singlet oxygen luminescence are very weak after about seven days. The development of the $^1O_2$ luminescence kinetics over the period of days in this experiment will be discussed in detail in the following.

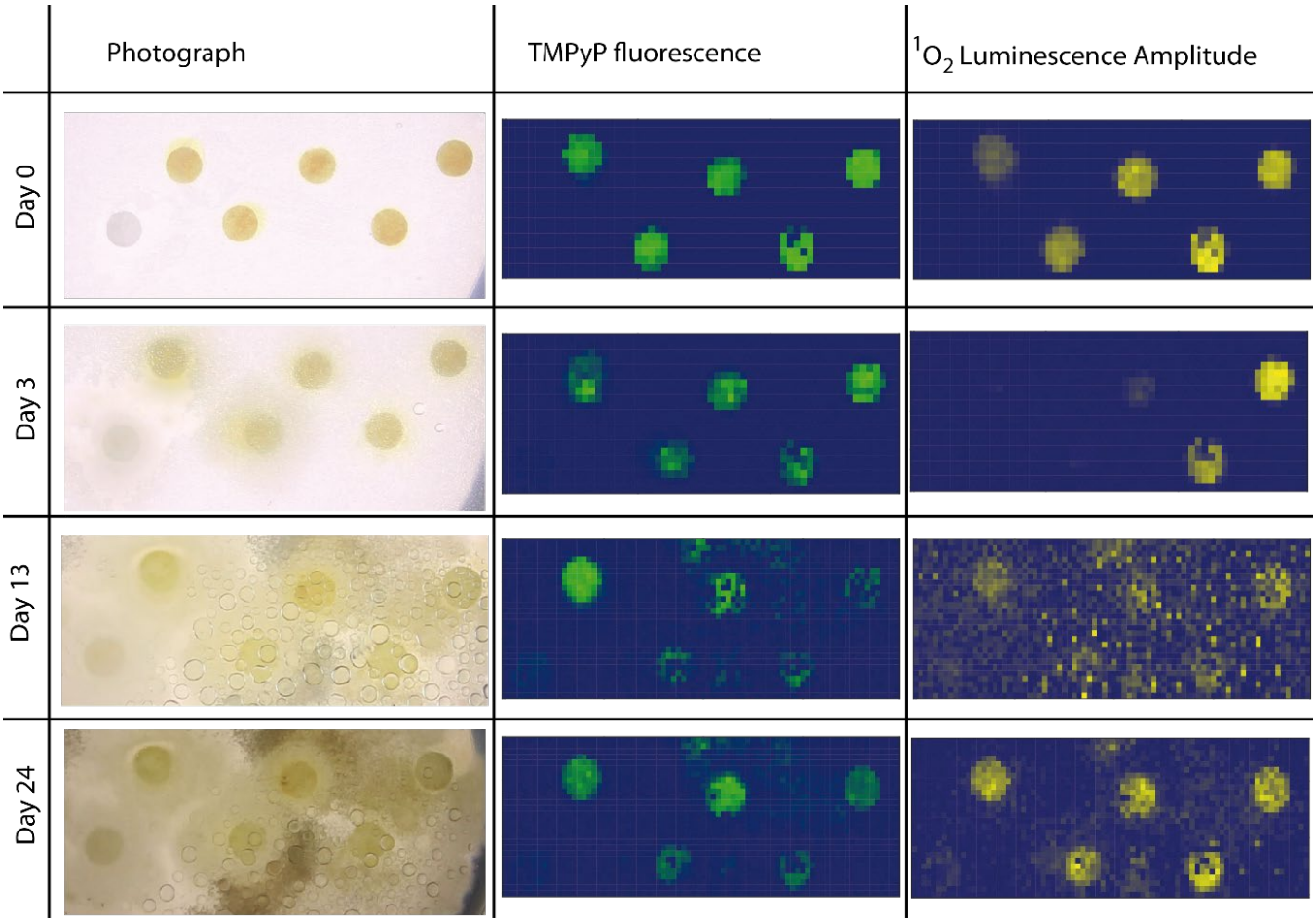

Figure 19: Photograph and normalized intensity plots of TMPyP fluorescence and $^1O_2$ luminescence of the TMPyP-*S. brecivaulis* sample.

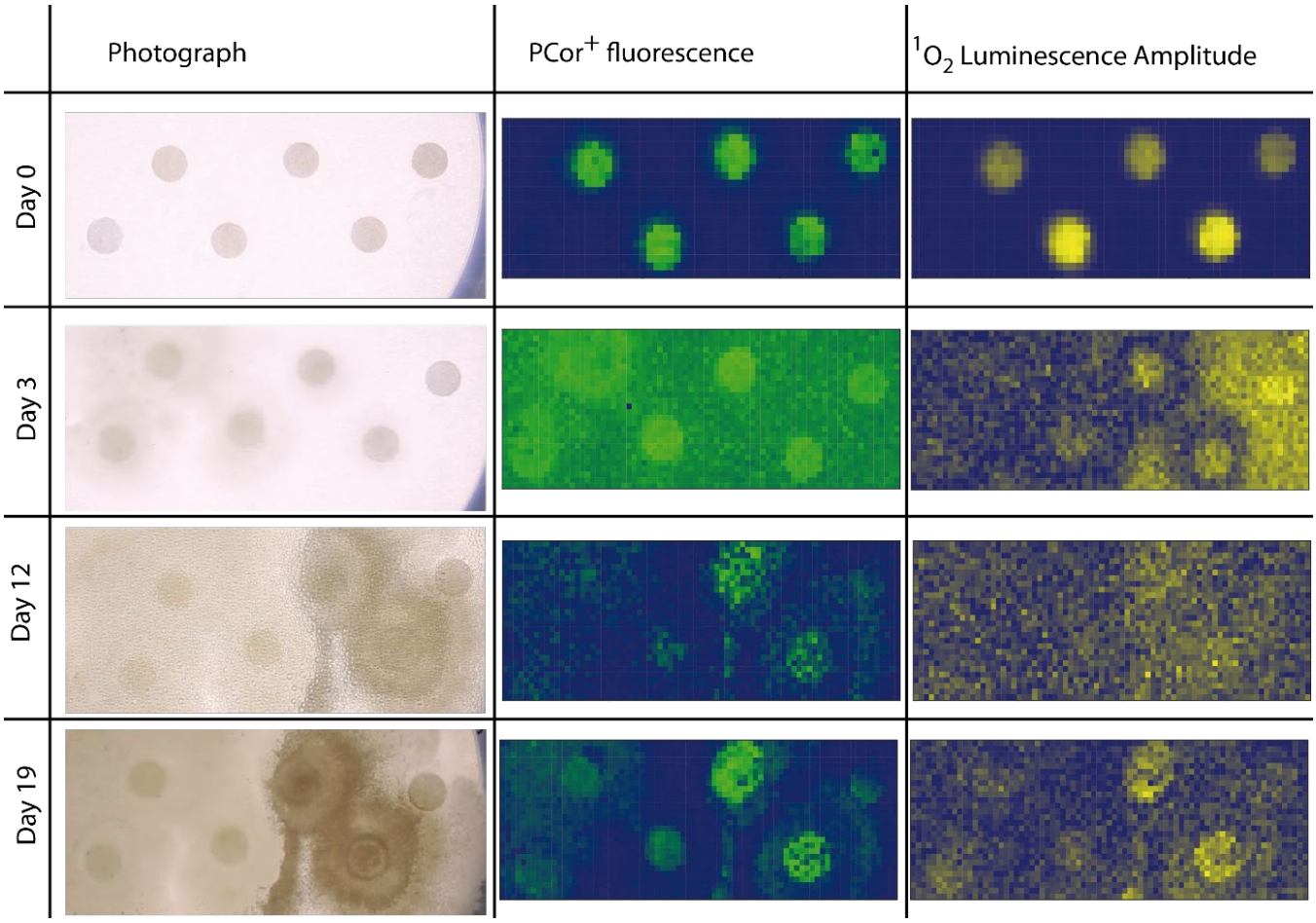

Figure 20: Photograph and normalized intensity plots of $PCor^+$ fluorescence and $^1O_2$ luminescence of the $PCor^+$-*S. brevicaulis* sample.

The NIR luminescence kinetics related to the $^1O_2$ luminescence intensity plots in figure 19 and figure 20 are shown in figure 21. The curves represent the NIR luminescence kinetics of the pixels of highest amplitude on the surface of C1 area of the TMPyP- *S. brevicaulis* sample and C4 area of the PCor+-*S. brevicaulis* sample.

In figure 21a, the singlet luminescence kinetics of the TMPyP sample is shown. On day 0, one hour after preparation, a clear singlet oxygen luminescence kinetics can be seen. On the third day, a disturbance signal overlays the luminescence signal. On day 13 and 24, hardly any luminescence kinetics could be observed. Figure 21b shows the singlet oxygen luminescence kinetics of the PCor+ sample. At day 0, a distinct singlet oxygen luminescence kinetics is observed. From day 3 on, a disturbance signal dominates the NIR kinetics

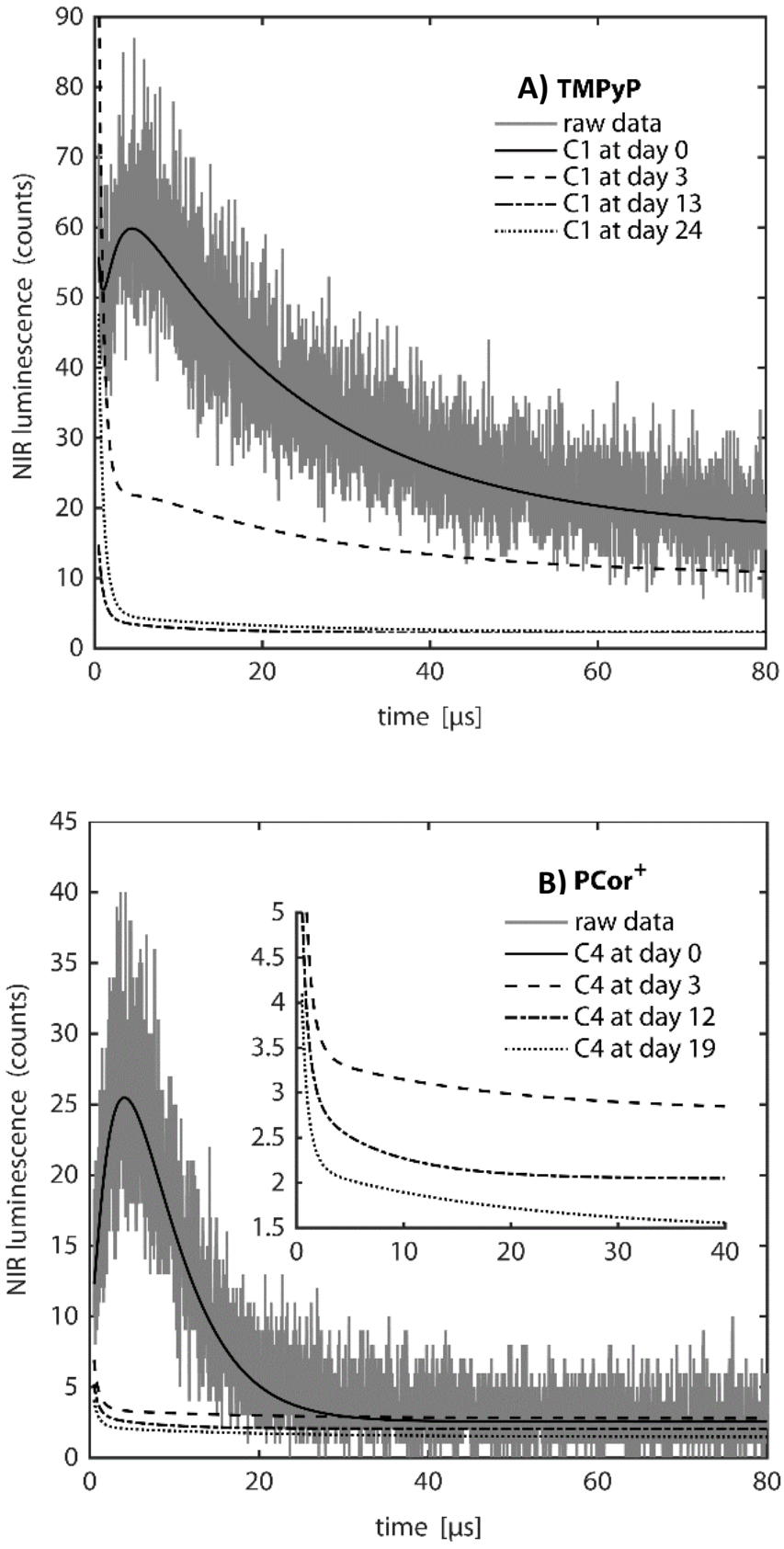

Figure 21: NIR luminescence kinetics corresponding to the $^1O_2$ intensity plot of figure 19and figure 20. The NIR luminescence kinetics on the surface of the C1 area of the TMPyP-S. brevicaulis sample and the C4 area of the $PCor^+$-*S. brevicaulis* sample were chosen exemplary. The kinetics of the pixels of highest amplitude are shown.

The development of the PS's triplet lifetime and the $^1O_2$ lifetime on the surface of the TMPyP-*S. brevicaulis* and the $PCor^+$- *S. brevicaulis* sample are shown in figure 22 and figure 23. The values represent the error-weighted mean values with corresponding error weighted-standard deviation of the fitted lifetimes of each area.

A comparison between TMPyP and PCor+ samples is the principle of choice for assigning the $^1O_2$ lifetime and the PS's triplet lifetime. Since both PSs are subject to almost identical microenvironments, the comparison method is valid here. As seen in figure 22 and figure 23, the shorter of the two lifetimes is almost the same for both photosensitizes, while the longer lifetime shows a significant difference. For this reason, the shorter lifetime was assigned to the $^1O_2$ lifetime. Under this assumption, a $^1O_2$ lifetime of about 1.5 to 2 µs was found.

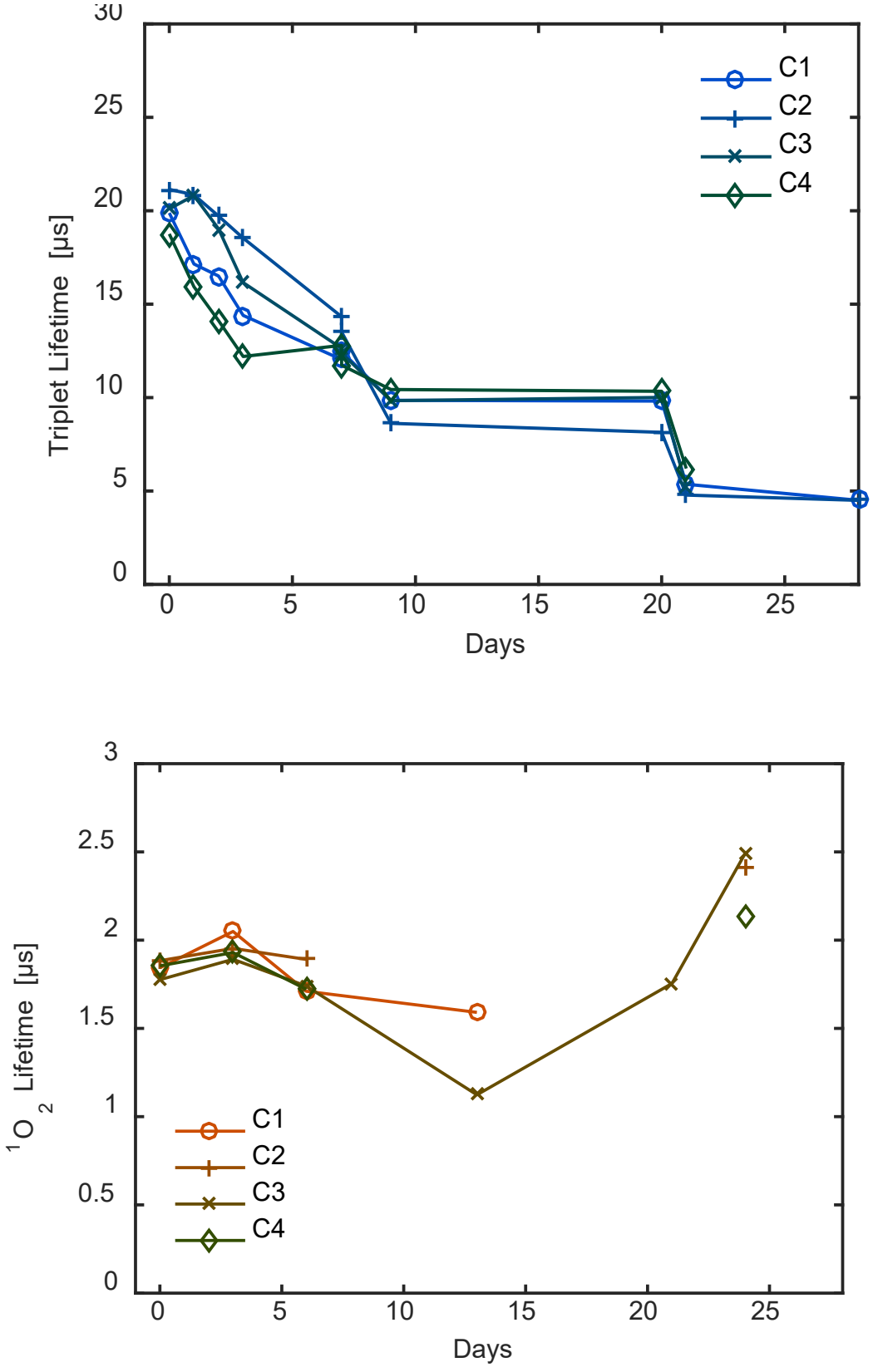

Figure 22: Development of the PS's triplet lifetime and the $^1O_2$ lifetime measured on the surface of the TMPyP-*T. rubrum* sample. The value of each day represents the error weighted mean value of all pixels of each sample area. The error values are the corresponding error weighted standard deviations.

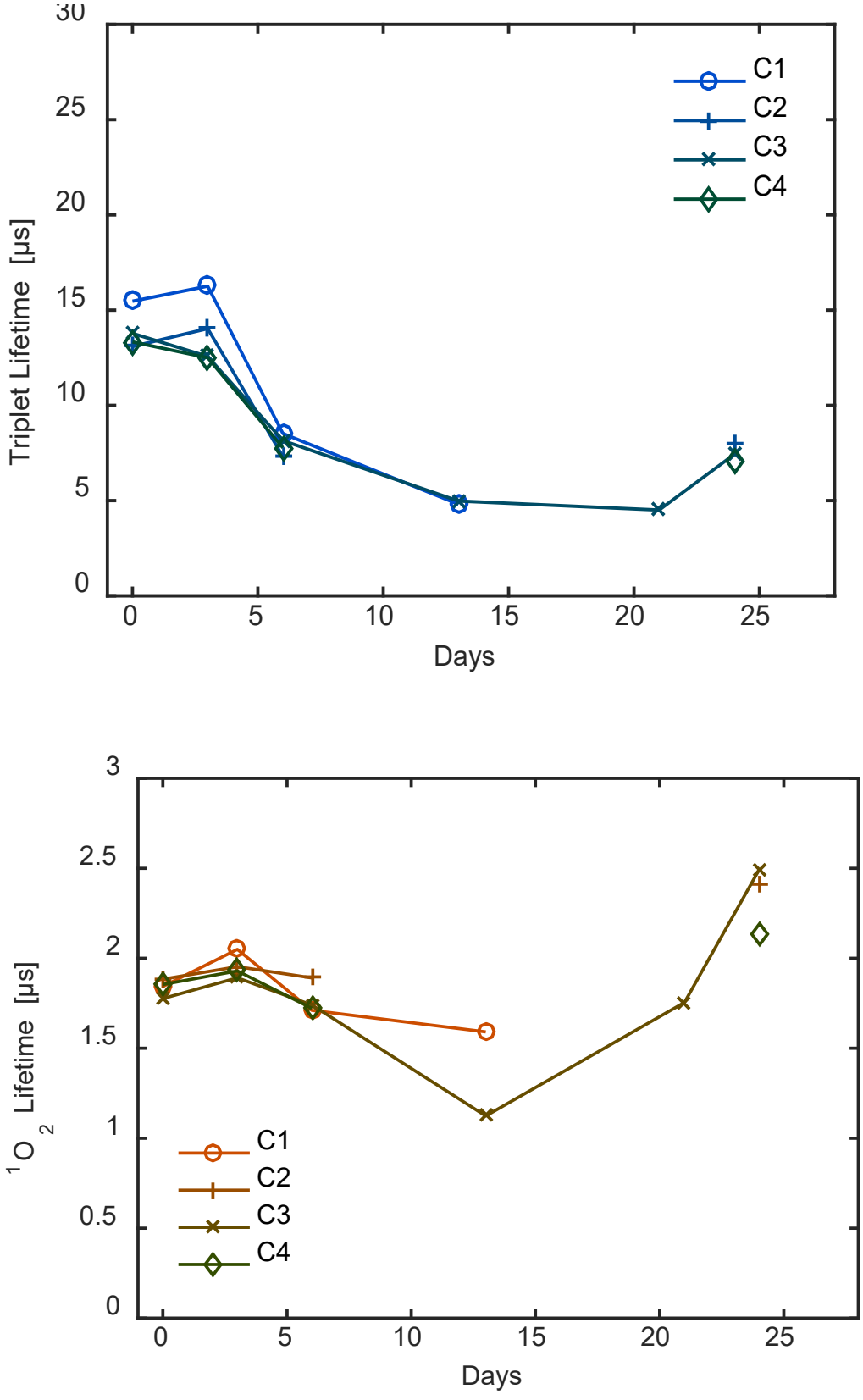

Figure 23: Development of the PS's triplet lifetime and the $^1O_2$ lifetime measured on the surface of the PCor$^+$- *T. rubrum* sample. The value of each day represents the error weighted mean value of all pixels of each sample area. The error values are the corresponding error weighted standard deviations.

2DTRSOL in the presence of *T. interdigitale*

Since the significance of the development of the kinetics has to be validated by statistics over several samples, 2DTRSOL in the presence of *T. interdigitale* was performed over 6 samples. For *T. interdigitale* samples, the same concentration of spore suspension was used for six filter papers placed on the surface of agar. The references were prepared on separate petri dishes. Figure 24 and figure 25 show the photographs of *T. interdigitale* samples and the corresponding intensity plots of fluorescence and singlet oxygen luminescence. For PCor+, the intensity plots show that it diffuses rapidly away from filter papers to the surrounding agar. On day 0, only one hour after preparation, PCor+ started to diffuse. After seven days of luminescence it became barely detectable. TMPyP in contrast shows a high localization with nearly no diffusion. A good luminescence signal could be shown for up to one week.

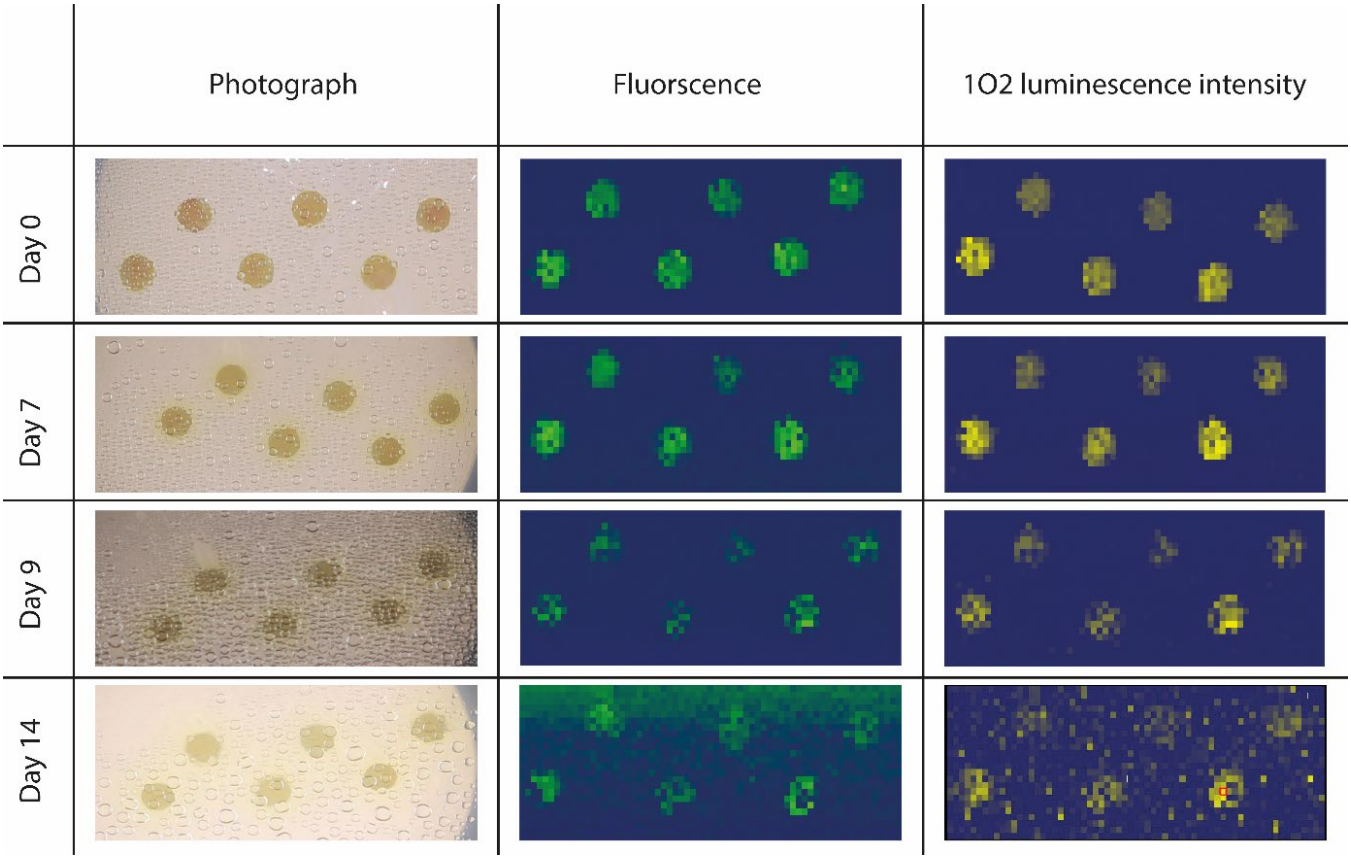

Figure 24: Photograph and normalized intensity plots of TMPyP fluorescence and $^1O_2$ luminescence of the TMPyP-*T. interdigitale* sample.

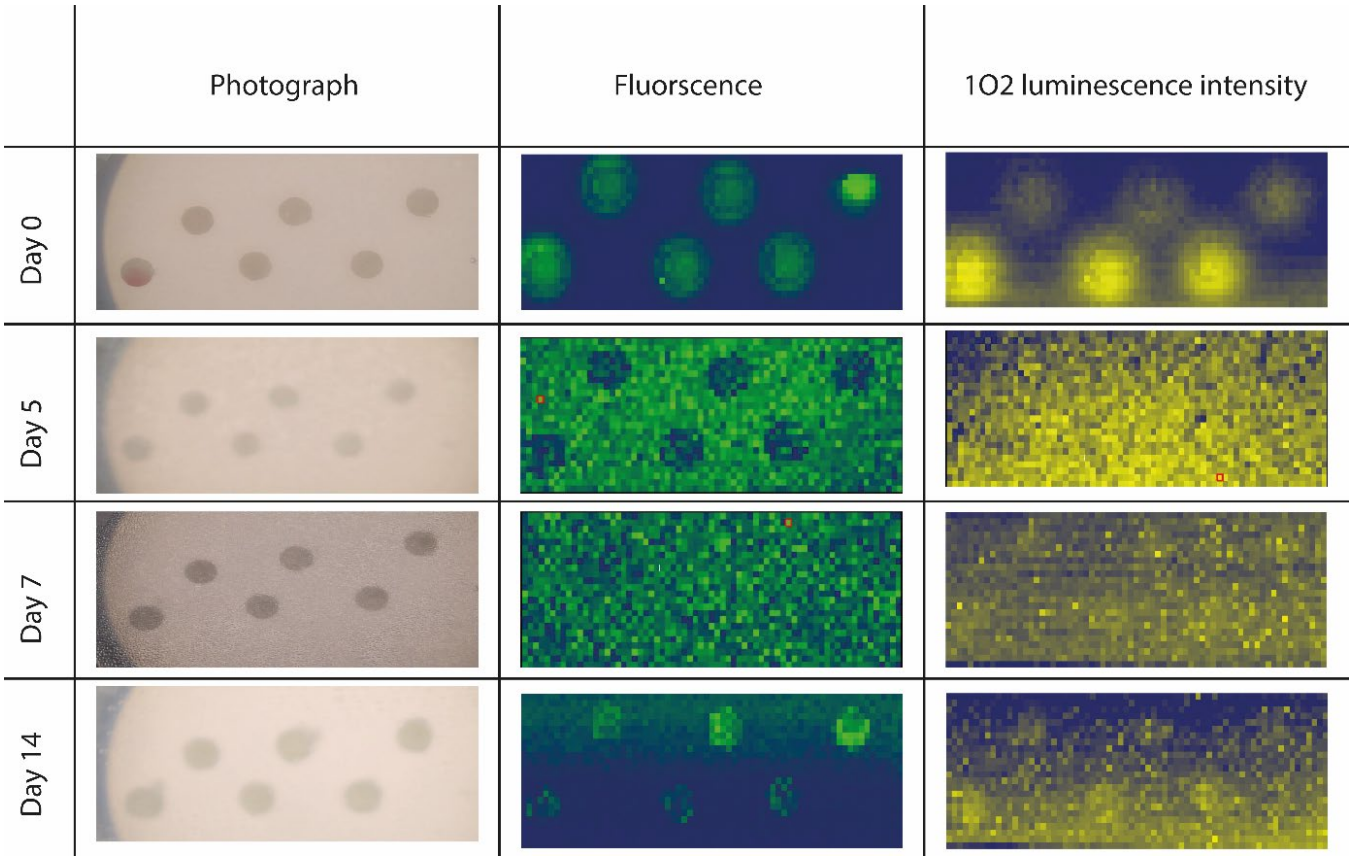

Figure 25: Photograph and normalized intensity plots of $PCor^{+}$ fluorescence and $^{1}O_2$ luminescence of the $PCor^{+}$-*T. interdigitale* sample.

Figure 26 and figure 27 show the photographs and the corresponding intensity plots of the fluorescence and luminesce of the reference samples in separate petri dishes. Without the involvement of fungi, nearly the same behaviour of both PSs was observed, albeit demonstrating a higher stability.

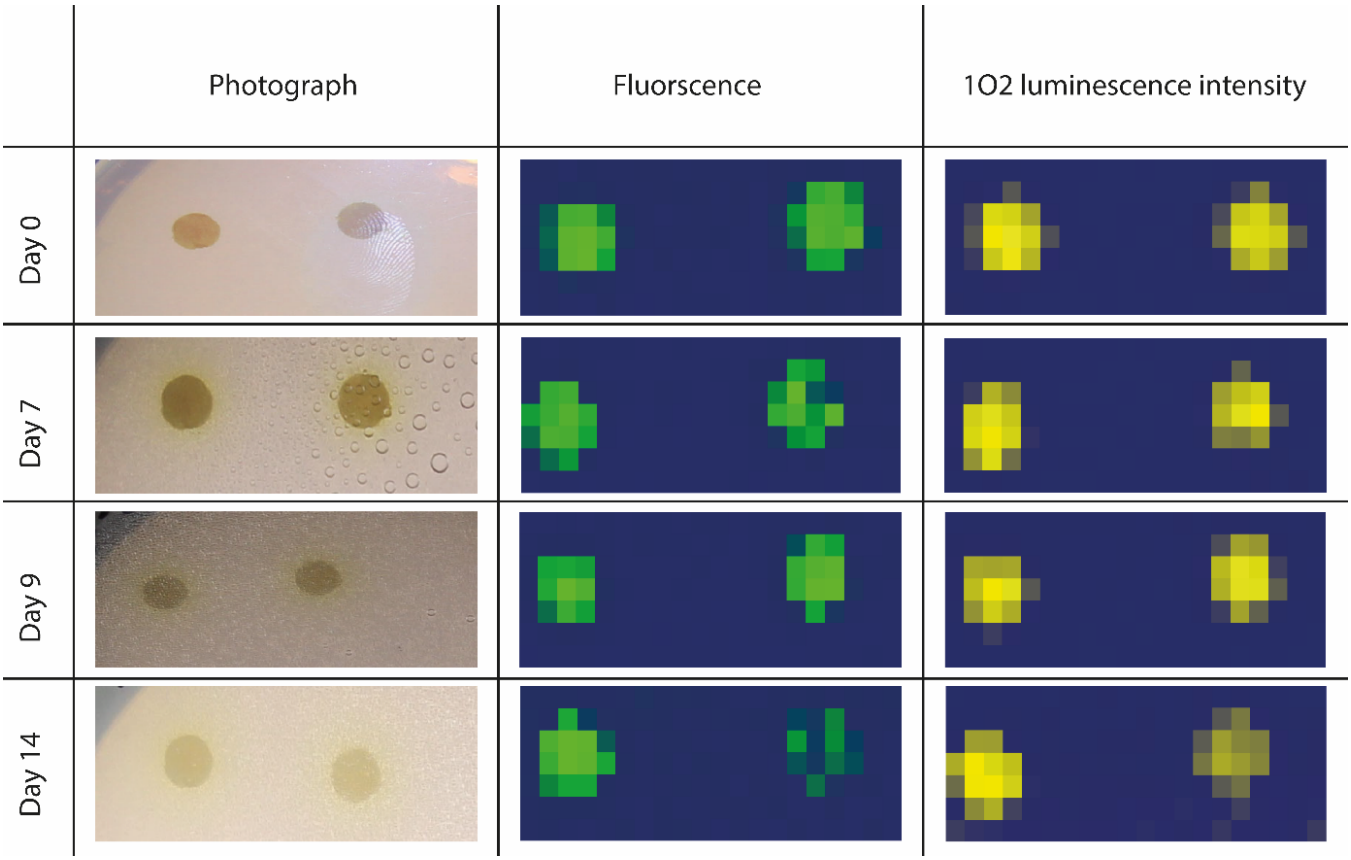

Figure 26: Photograph and normalized intensity plots of TMPyP fluorescence and $^1O_2$ luminescence of the TMPyP reference sample.

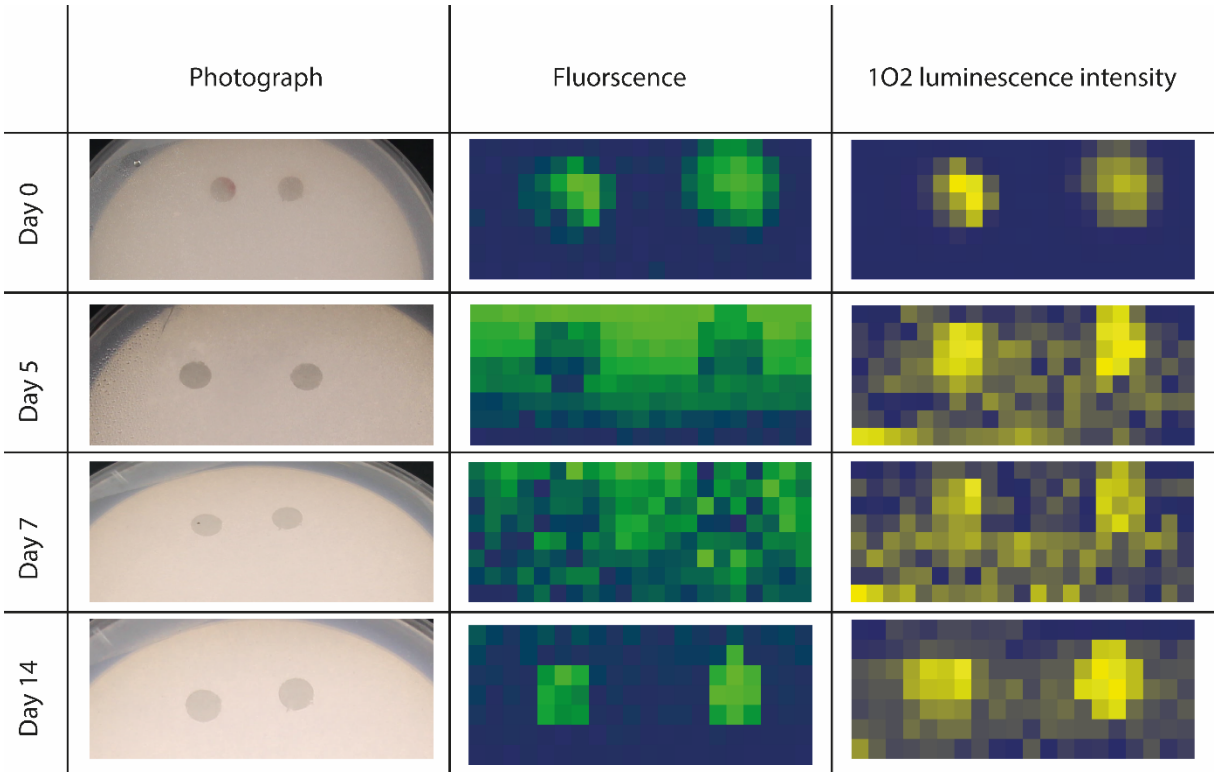

Figure 27: Photograph and normalized intensity plots of $PCor^+$ fluorescence and $^1O_2$ luminescence of the $PCor^+$ reference sample.

Figure 28 and figure 29 show the NIR luminescence kinetics corresponding to the $^1O_2$ luminescence intensity plots in figure 24 and figure 25. The development of the kinetics is validated by statistics over six samples. The curves represent the NIR luminescence kinetics of the pixels of highest amplitude on the surface of the respective area. The days were selected according to the days of the intensity plots in figure 24 and figure 25. On day 0, singlet oxygen kinetics is evident. After 7 days, hardly any kinetics could be determined and a disturbance signal dominates the measured luminescence.

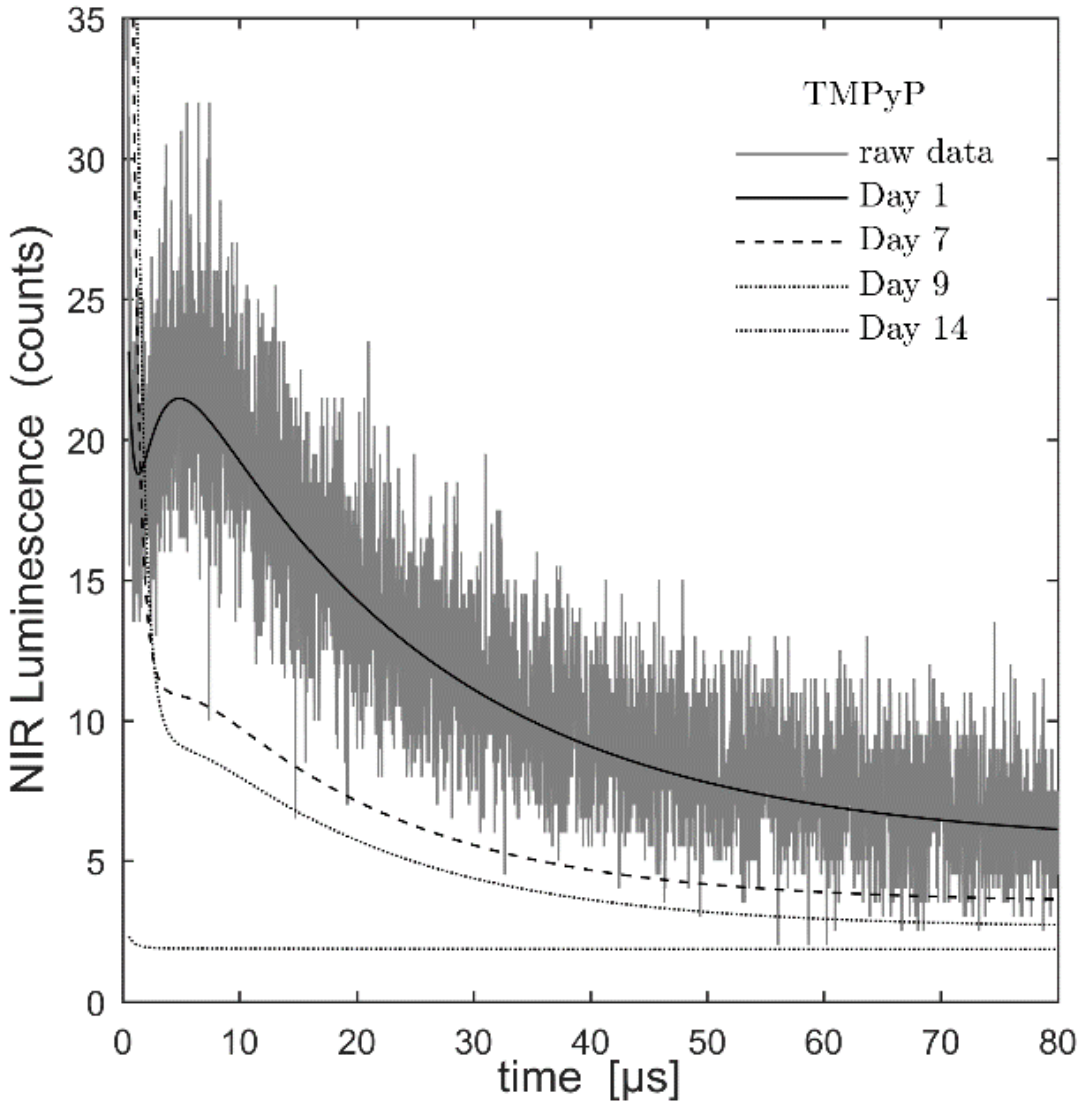

Figure 28: NIR luminescence kinetics corresponding to the $^1O_2$ intensity plot of Figure 28 and Figure 29 . The NIR luminescence kinetics of the TMPyP-*T. interdigitale* sample was chosen exemplary. The kinetics of the pixels of highest amplitude are shown.

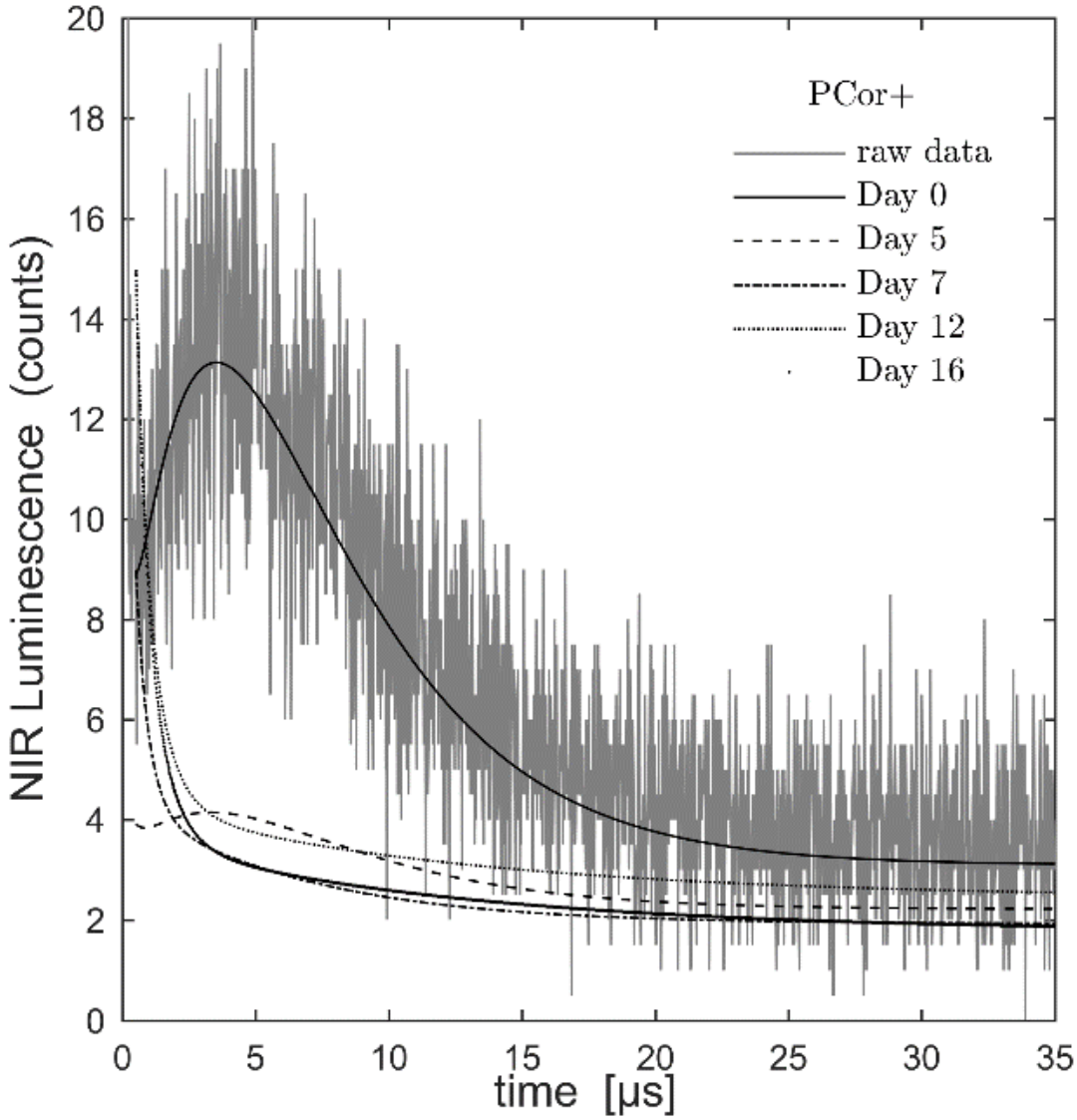

Figure 29: NIR luminescence kinetics corresponding to the $^1O_2$ intensity plot of Figure 28 and Figure 29 . The NIR luminescence kinetics of the PCor$^+$-*T. interdigitale* sample was chosen exemplary. The kinetics of the pixels of highest amplitude are shown.

Figure 30 and figure 31 show the fitted singlet oxygen luminescence over the range of the experiment for both PSs in the presence *of T. interdigitale*. It can be seen, that the amplitude of the luminescence signal decreases dramatically over a period of 4 to 6 days. The reduction of the luminescence signal may be related to the growth of the fungi.

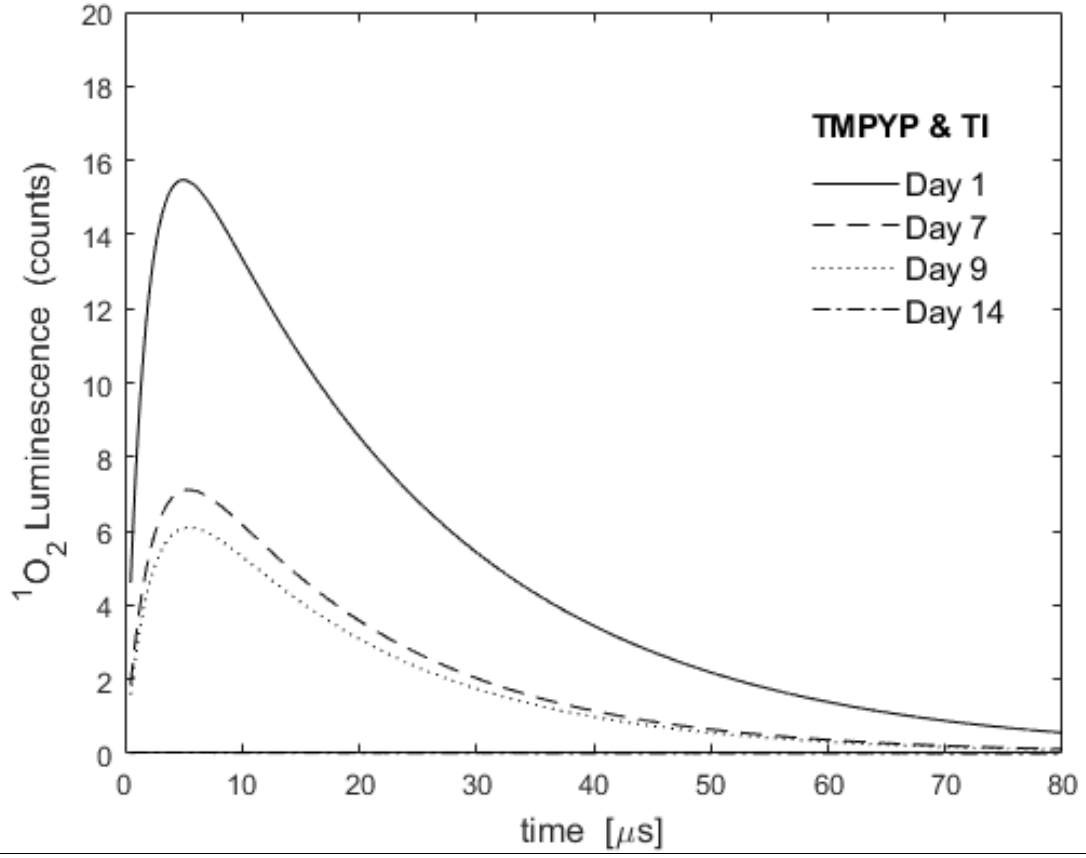

Figure 30: Isolated $^1O_2$ luminescence kinetics on the surface of samples TMPyP - *T. interdigitale* sample.

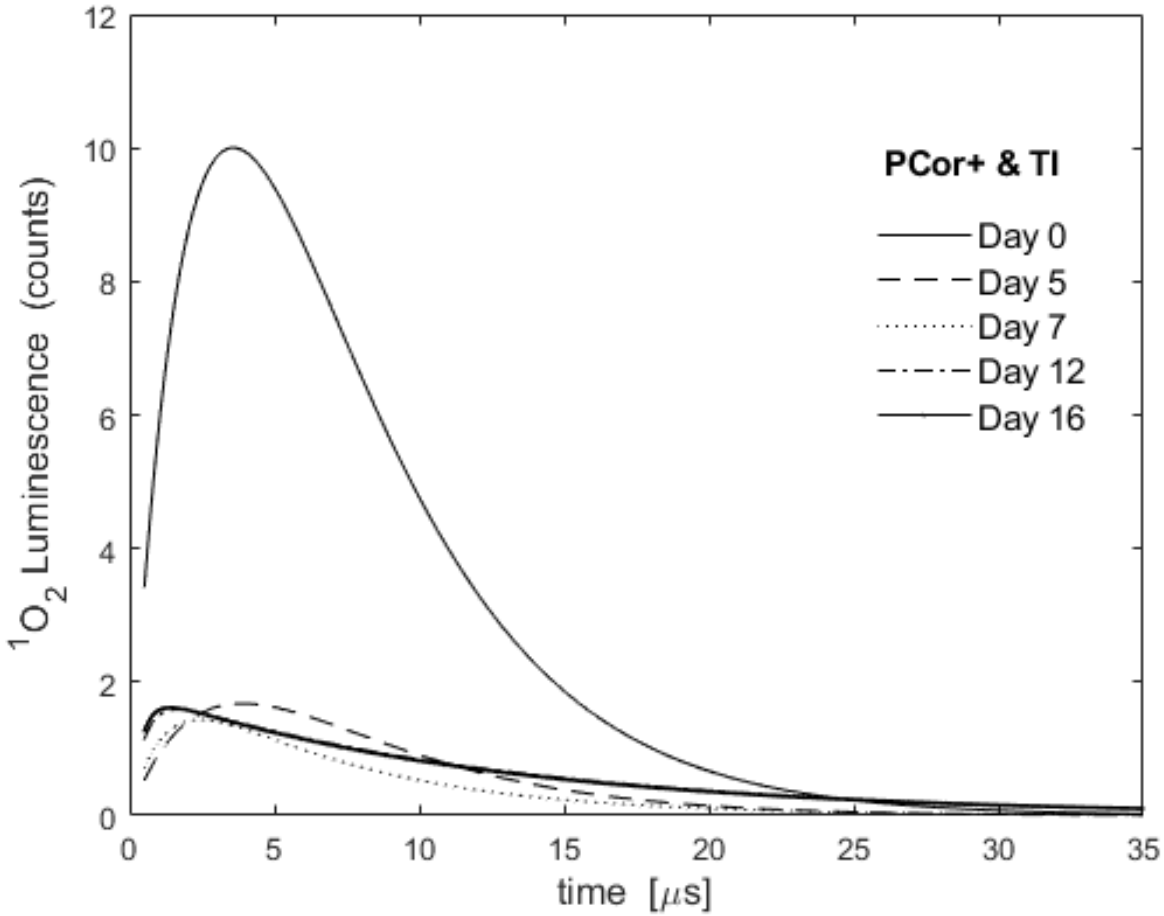

Figure 31: Isolated $^1O_2$ luminescence kinetics on the surface of $PCor^+$ - *T. interdigitale* sample.

Figure 32 and figure 33 show the singlet oxygen luminescence kinetics of the separate reference PS samples (without fungi) over the time period of the experiment. Figure 32 shows the reduction of luminescence amplitude of the TMPyP reference. The reduction of the luminescence signal here is not as fast as in the presence of fungi as shown in figure 30 and figure 31. As no fungi are present in the sample, the reduction of the signal might be attributed to bleaching of TMPyP over several days of illumination. Figure 33 shows the reduction of luminescence amplitude of the PCor+ reference. A very rapid reduction is shown over 6 days. The stability of PCor+ is lower compared to TMPyP.

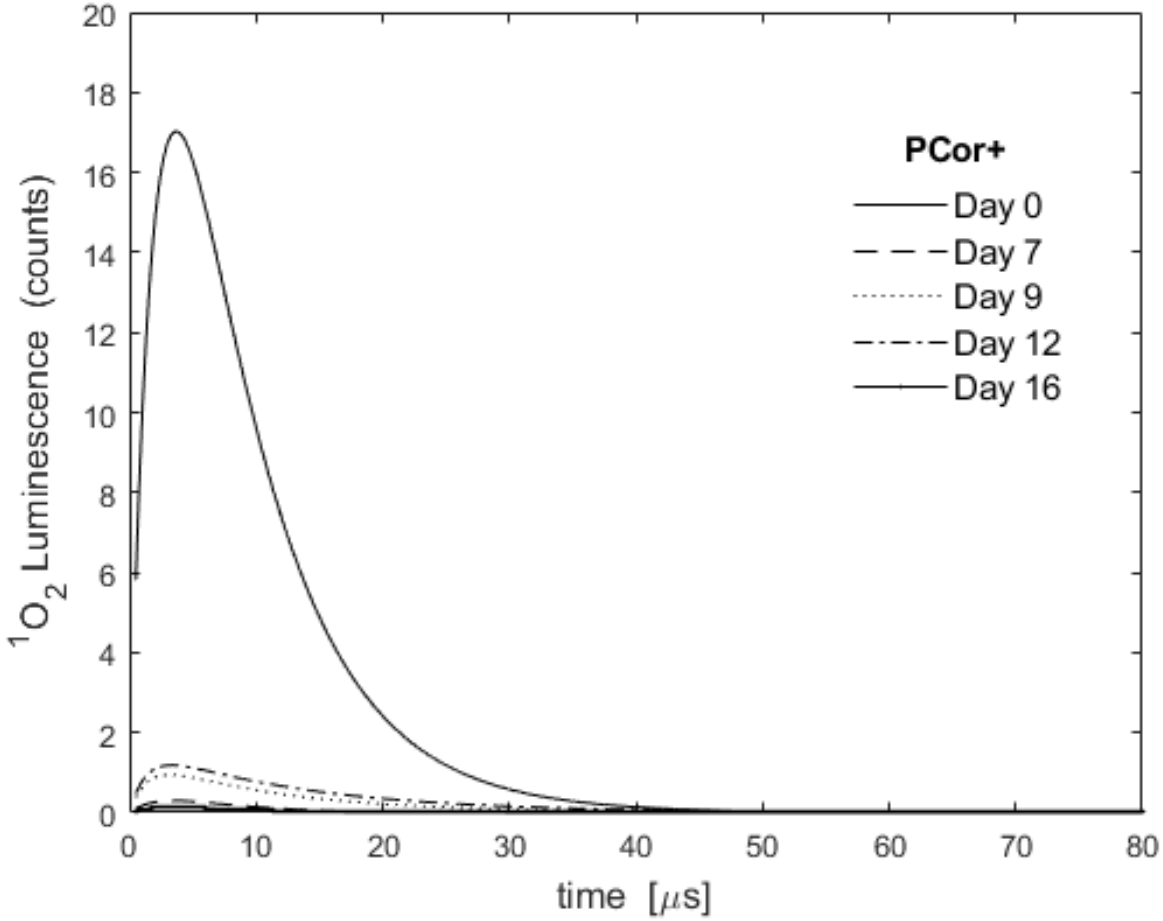

Figure 32: isolated $^1O_2$ luminescence kinetics on the surface of $PCor^+$ - reference samples.

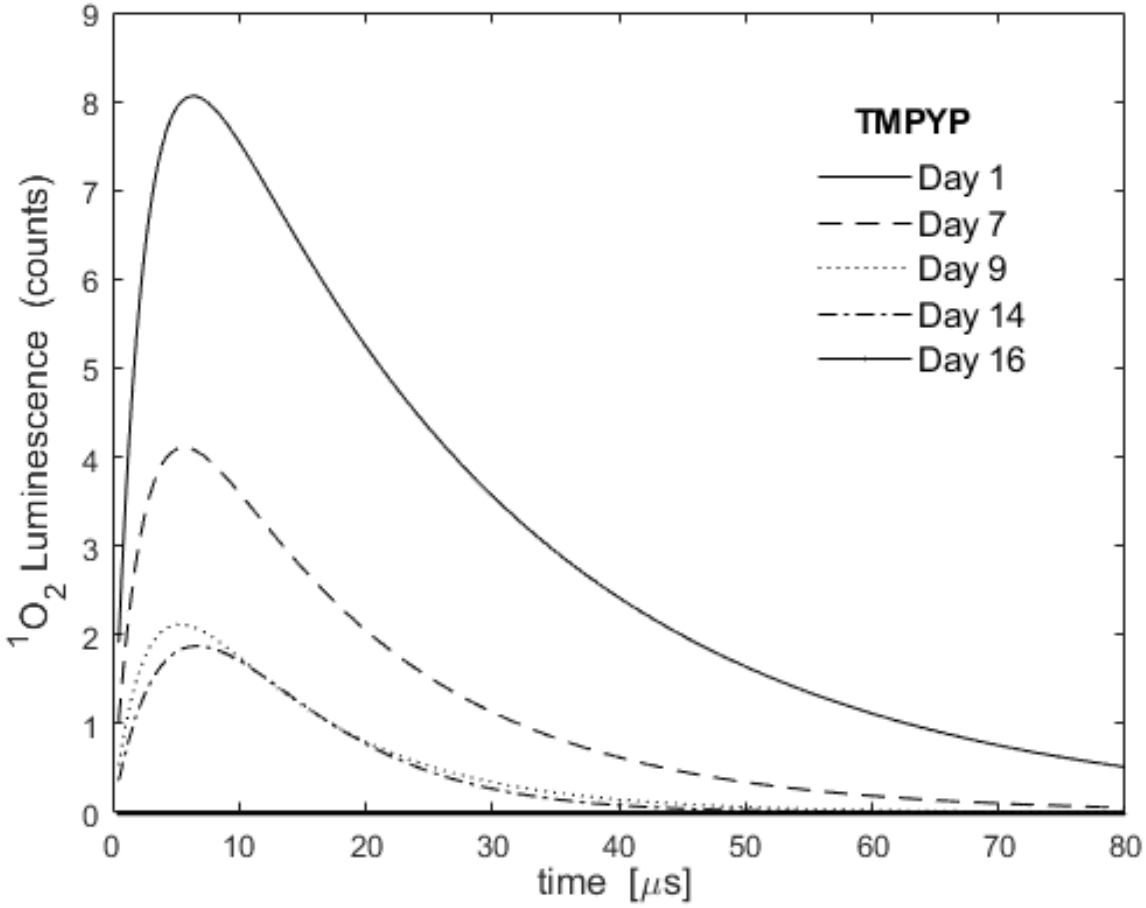

Figure 33: isolated $^1O_2$ luminescence kinetics on the surface of TMPyP - T. reference samples.

Using the same assumption as in the previous part, the rise and decay time was determined. Figure 34 and figure 35 show the triplet lifetime of both PSs and singlet oxygen lifetime as determined from both samples. The shorter lifetime is almost the same in both TMPyP and PCor+ samples and thus, the shorter lifetime is singlet oxygen lifetime. The determined value of the singlet oxygen lifetime was about 2 µs. The longer lifetime with significant difference between the two PSs is the triplet lifetime. The triplet life time of TMPyP decreases over time in the presence of *T. interdigitale*, while the triplet lifetime of PCor+ increases over time in the first 10 days. The TMPyP triplet lifetime has an initial value of 17 µs and dropped to less than 10 µs in the first week. The PCor+ triplet lifetime increased from 6 µs up to 7.6 µs during the first 10 days.

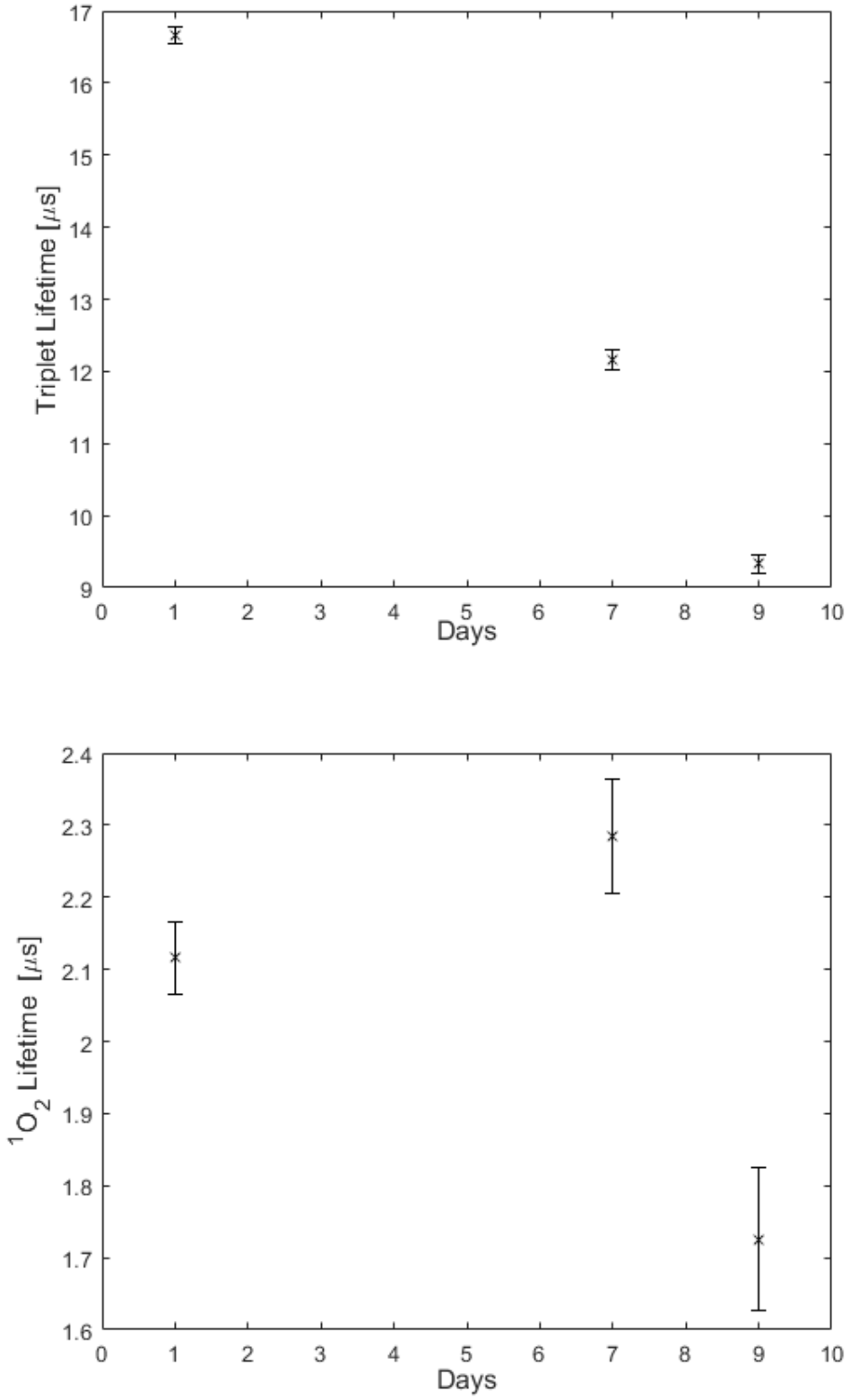

Figure 34: Development of the PS's triplet lifetime and the $^1O_2$ lifetime measured on the surface of the TMPyP-*T. interdigtale* sample. The value of each day represents the error weighted mean value of all pixels of each sample area. The error values are the corresponding error weighted standard deviations.

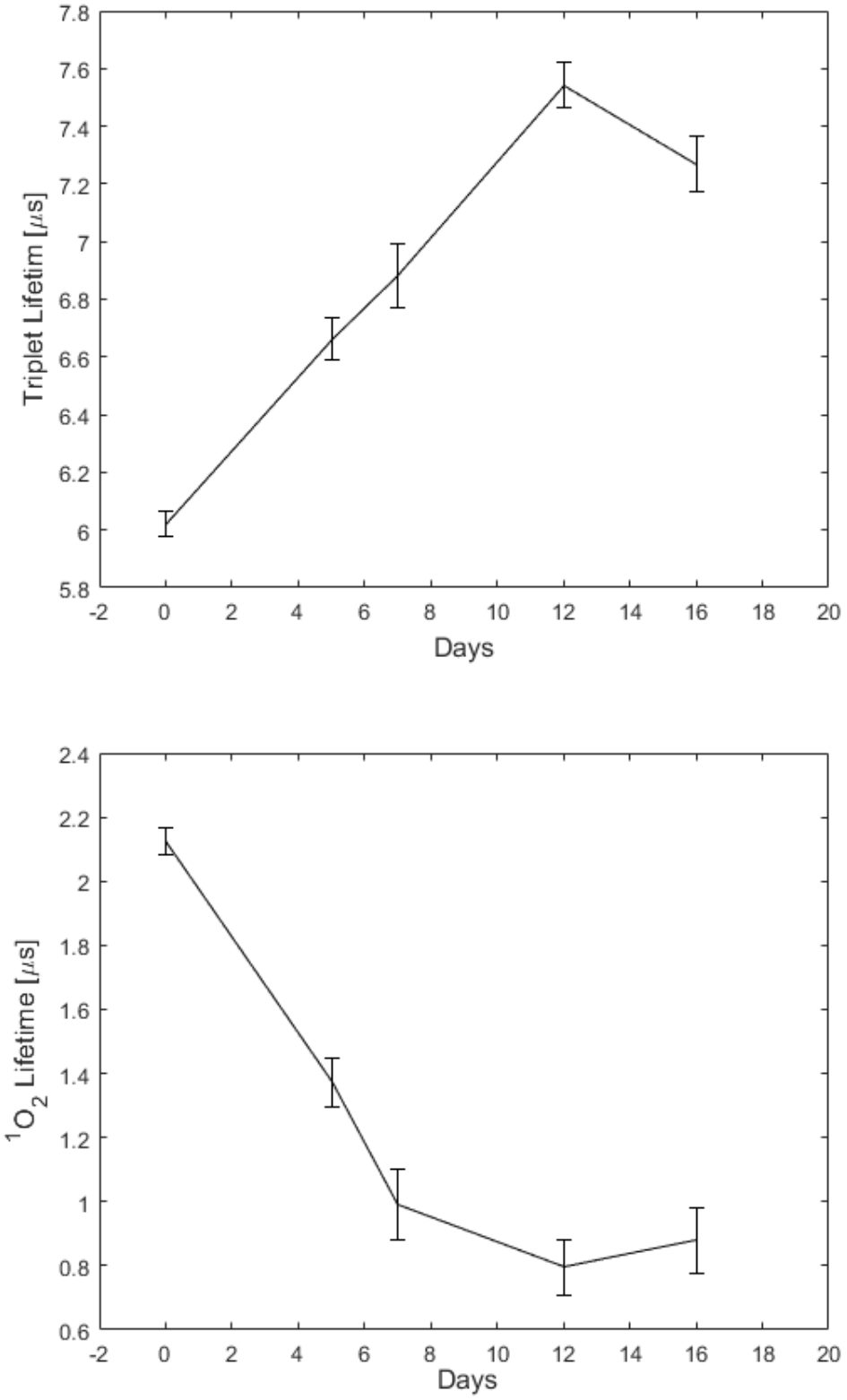

Figure 35: Development of the PS's triplet lifetime and the $^1O_2$ lifetime measured on the surface of the $PCor^+$- *T. interdigitale* sample. The value of each day represents the error weighted mean value of all pixels of each sample area. The error values are the corresponding error weighted standard deviations.

Figure 36 and figure 37 shows the singlet oxygen lifetime and triplet lifetime of both PSs in the separate reference. The value of the singlet oxygen lifetime is around 2 µs. The triplet lifetime of TMPyP and PCor+ follows the same pattern as in the presence of fungi (see figure 34 and figure 35). The triplet lifetime of TMPyP decreases over time while the lifetime of PCor+ increases slightly. The triplet lifetime of TMPyP decreases from 17 µs to nearly 8 µs over a time of two weeks. The initial value of the triplet lifetime of PCor+ was about 6 µs, increased up to 7.5 µs after 5 days and decreased again after two weeks.

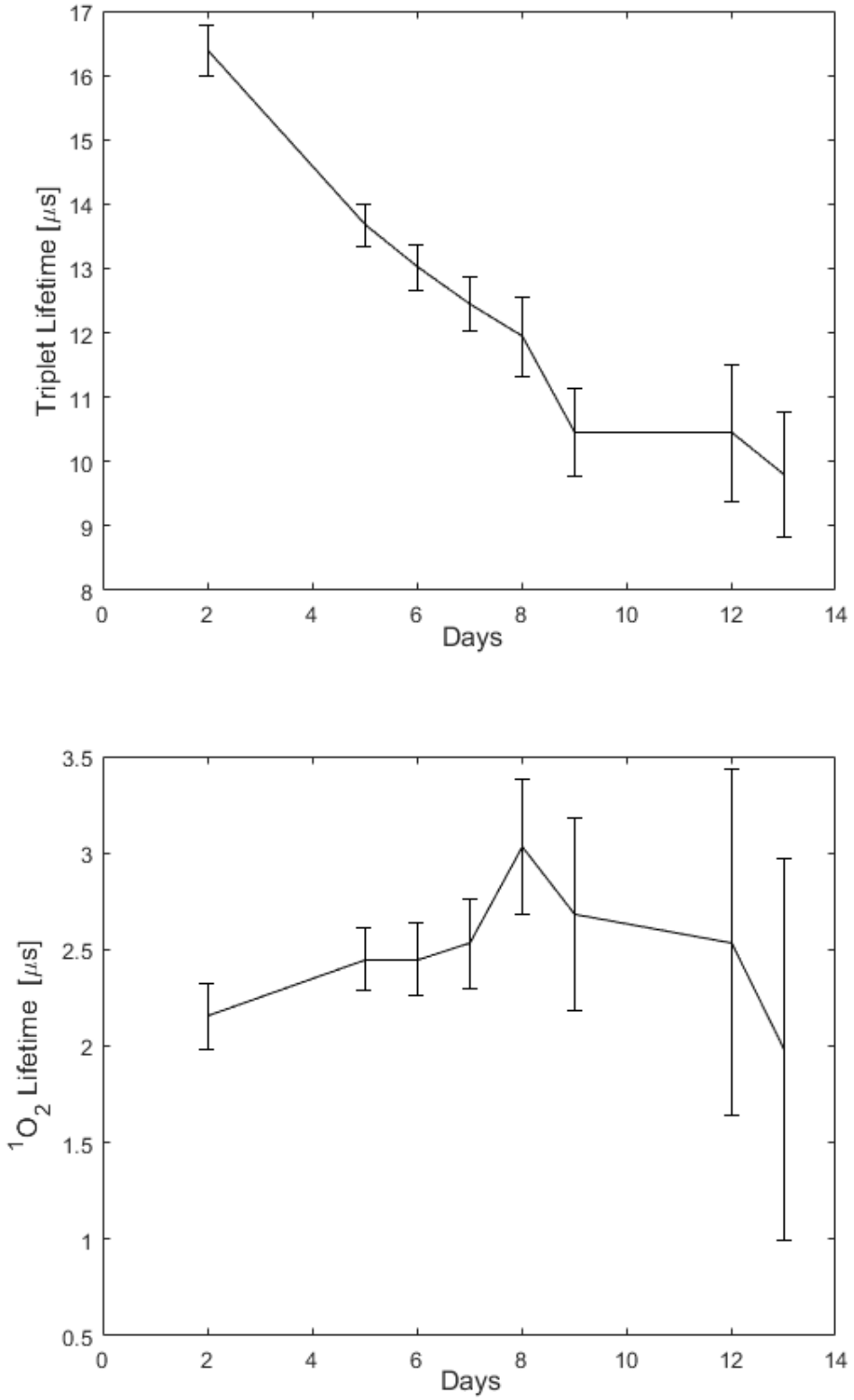

Figure 36: Development of the PS's triplet lifetime and the $^1O_2$ lifetime measured on the surface of the TMPyP-reference sample. The value of each day represents the error weighted mean value of all pixels of each sample area. The error values are the corresponding error weighted standard deviations.

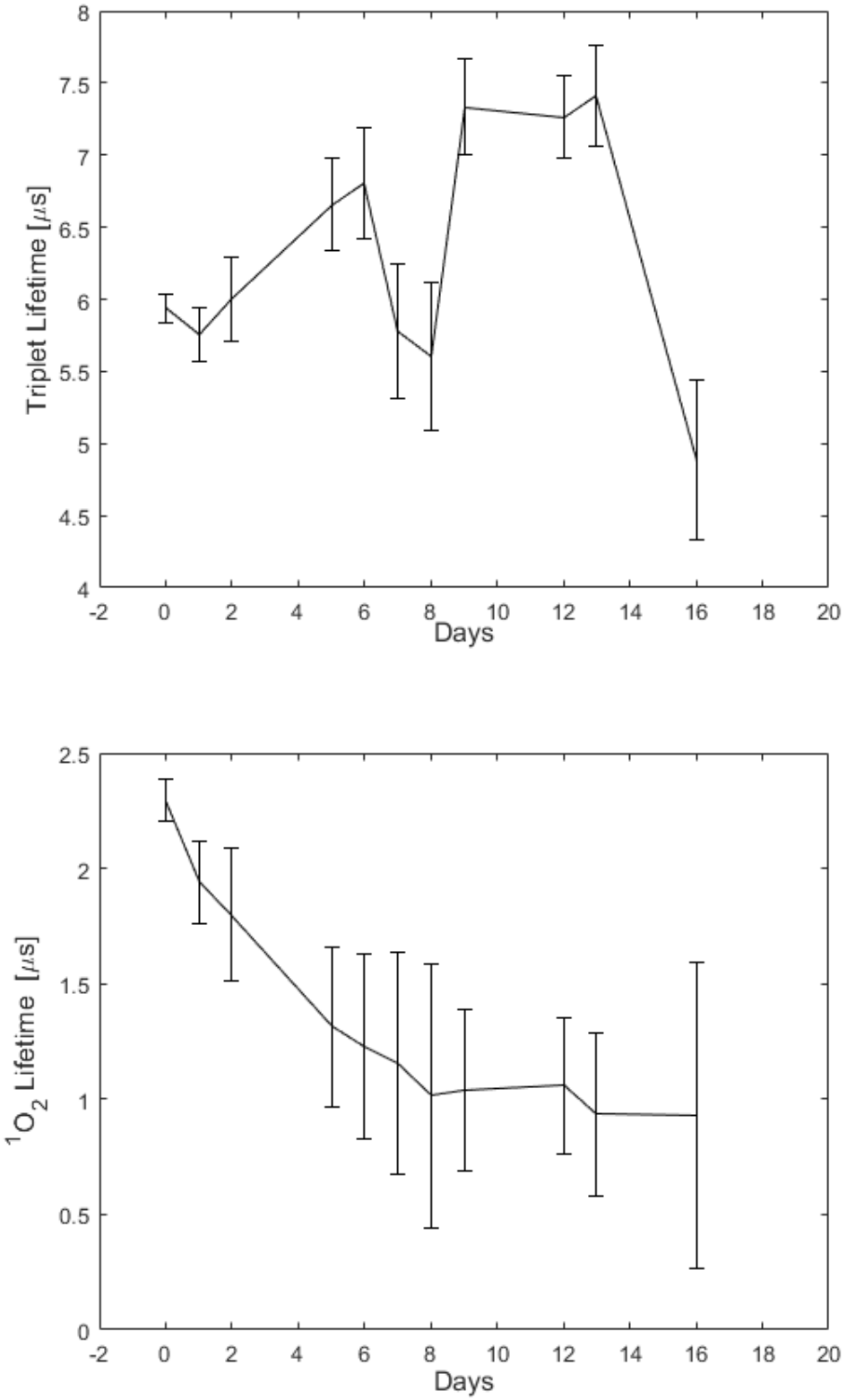

Figure 37: Development of the PS's triplet lifetime (left) and the $^1O_2$ lifetime measured on the PCor$^+$- reference sample. The value of each day represents the error weighted mean value of all pixels of each sample area. The error values are the corresponding error weighted standard deviations.

Discussion

2DTRSOL scans were performed of the PSs, TMPyP and PCor+ with the involvement of dermatophytes and mold fungus. The analysis of the kinetics helps to understand the behaviour of the PS in the presence of fungi. It helps to gain information about the stability of the PS and its diffusion, the generation of singlet oxygen and its reactivity. Those measurements help to determine any impact of the fungi on the behaviour of the PSs.

The intensity plots of PS fluorescence and singlet oxygen luminescence show the diffusion of the PSs. TMPyP is strongly localized while PCor+ tends to diffuse very fast to the surrounding agar. A correlation between the fungal growth stage and fluorescence and luminescence intensities was observed. The local humidity inside petri dishes due to fungi growth might be the reason for the change in signal intensities. A clear singlet oxygen kinetics was observed for up to seven days. This demonstrates the stability of the used PSs. A disturbance signal from unknown source was observed in all measurements. The disturbance signal was also shown with PS in a separate reference, which means that we cannot attribute the disturbance of the signal to the presence of the fungi. It might be an interaction of the PS with agar, that is the reason for this signal.

The results obtained with *T. interdigitale*, where the kinetics were validated by statistics over several samples, showed no difference from the results obtained in the first experiments. In fact, no great difference was observed by changing the type of fungi. All three fungi show similar behaviour under PDI treatment.

2DTRSOL detection is very important for the development of the conditions for PDI of onychomycosis. Scans show stability of the used PSs and good singlet oxygen generation, which means that the PSs might have a high phototoxic effect on the three fungi species. *In vitro* phototoxicity tests of the PSs on the three fungi species are the next step of this project.

4.2 *In vitro* phototoxicity tests on suspension cultures

In order to test the phototoxic effect of the PSs investigated in this work, the investigation were started on suspension cultures.

4.2.1 The phototoxic effect of TMPyP PDI of *T. rubrum* suspension cultures

The potential of TMPyP as PS was tested on the suspension cultures of the dermatophytes *T. rubrum* and *T. interdigitale* and the molds *S. brevicaulis*. Three different concentrations of TMPyP with three different illumination times were used. The concentrations are 5 µM, 10 µM and 20 µM and the illumination times are 30 min, 60 min and 90 min.

Figure 38 shows the phototoxic effect of TMPyP on A) *T. rubrum* B) *T. interdigitale* C) *S. brevicaulis*. In figure 38a, 20 µM of TMPyP reduces the viability to 50% in 30 min of illumination, while additional 60 min of illumination reduce the viability to 15%. TMPyP shows a higher phototoxic effect on *T. interdigitale* and *S. brevicaulis* (Figure 38 b and c). Among 30 min illumination, the viability of both fungi is reduced to 25% in case of 20 µM and additional 30 min led to complete eradication of the suspension cultures. No dark toxicity was detected for TMPyP on the three fungi species.

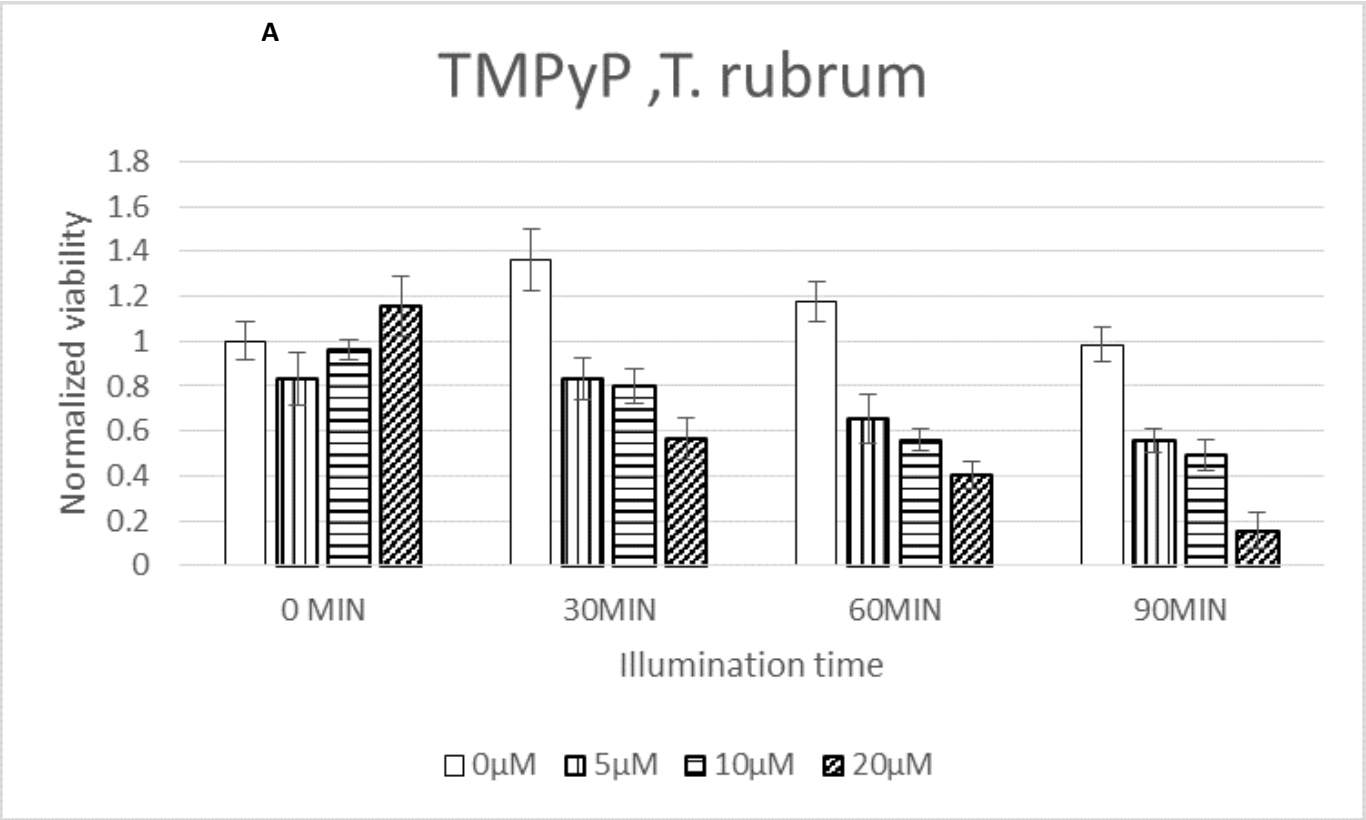

Figure 38a: The viability of the suspension cultures of *T. rubrum* after 24 h of phototoxicity test with TMPyP. Error pars represent the standard deviation of 8 samples (n=8). For dark control, samples kept in darkness at room temperature. 0 µM represents reference samples.

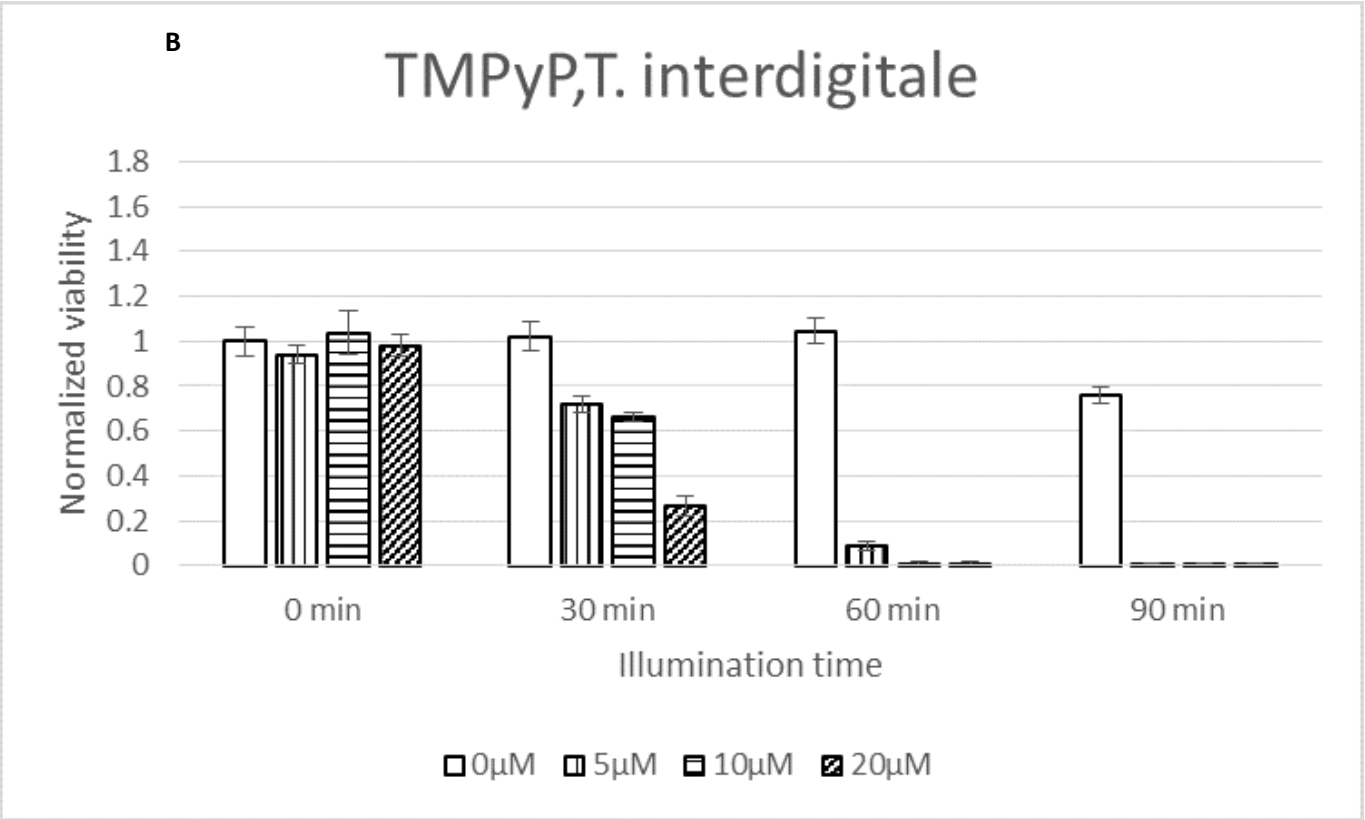

Figure 38b: The viability of the suspension cultures of *T. interdigitale* after 24 h of phototoxicity test with TMPyP. Error pars represent the standard deviation of 8 samples (n=8). For dark control, samples kept in darkness at room temperature. 0 µM represents reference samples.

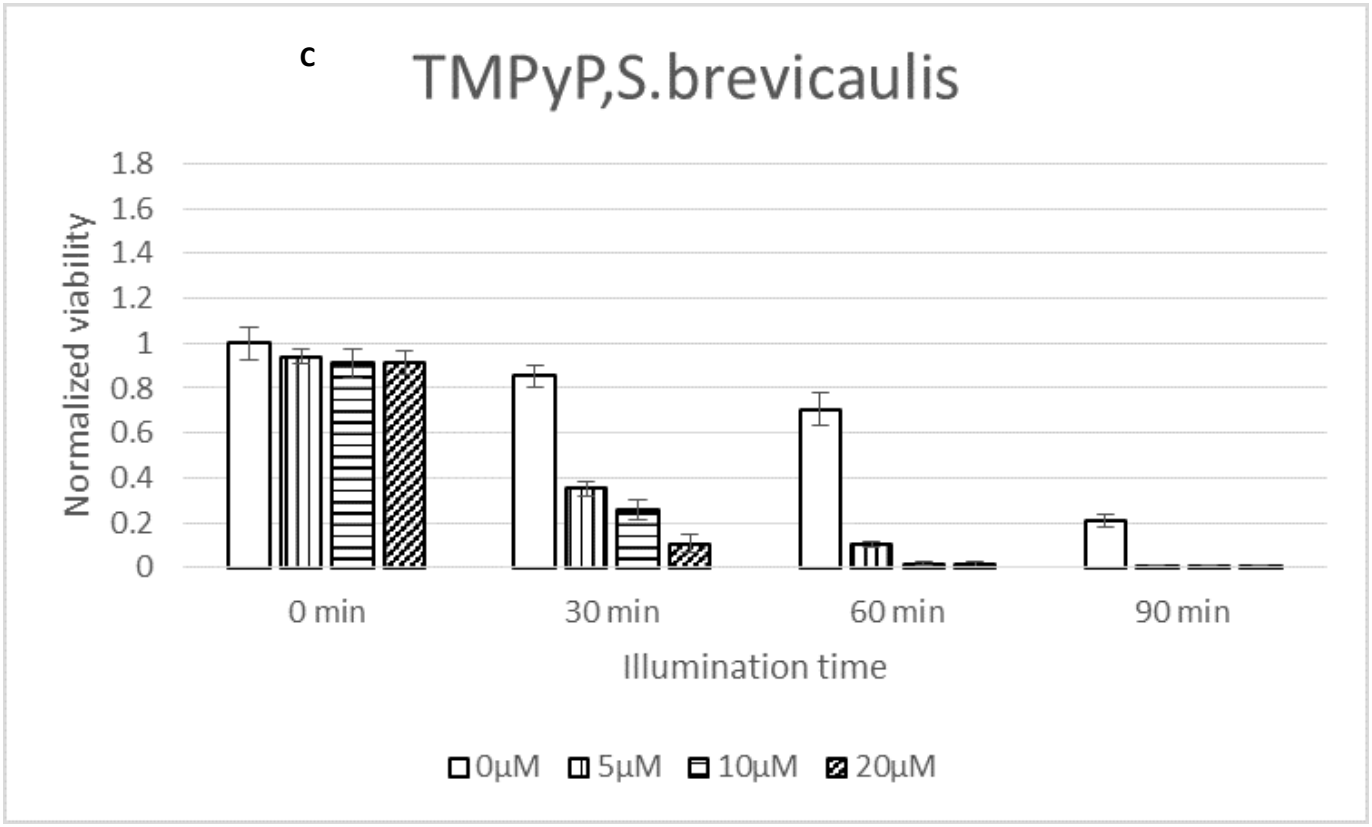

Figure 38c: The viability of the suspension cultures of *S. breivecaulis* after 24 h of phototoxicity test with TMPyP. Error pars represent the standard deviation of 8 samples (n=8). For dark control, samples kept in darkness at room temperature. 0 µM represents reference samples.

4.2.2 The phototoxic effect of PCor+

Besides TMPyP, PCor+ phototoxic effect was tested as well against the three fungi species on spore suspension cultures.

As with TMPyP, three concentrations with three different illumination times were tested against spore suspensions of the three fungi species. Figure 39 shows the phototoxic effect of PCor+ on the spore suspensions of *T. rubrum*, *T. interdigitale* and *S.breivecaulis*. Figure 39a, shows the phototoxic effect on *T. rubrum*. As is shown, the high phototoxicity of PCor+ was achieved with an illumination of more than 30 min. After 60 min illumination, the survival rate was nearly 10% in case of 5 µM PCor+ and nearly no survival was detectable using higher concentrations. After 90 min illumination, a complete eradication of the spore suspension was achieved even with the smallest concentration of 5 µM. With *T. interdigitale* and S. *brevicaulis* (Figure 39 b and c), the phototoxic effect of PCor+ appears in 30 min illumination. The proportion of surviving *T. interdigitale* spores was up to 50% with 10 µM and 20 µM while no survival was detected at all PCor+ concentrations an additional 30 min of illumination. Nearly the same results were shown with *S.brivecaulis* but the phototoxic effect of PCor+ was higher after 30 min illumination, the viability was reduced to 20% at 5 µM concentration and 10% with 10 µM and 20 µM. No viable spores were detected at all concentrations with additional 30 min illumination. PCor+ shows no dark toxicity at all concentrations.

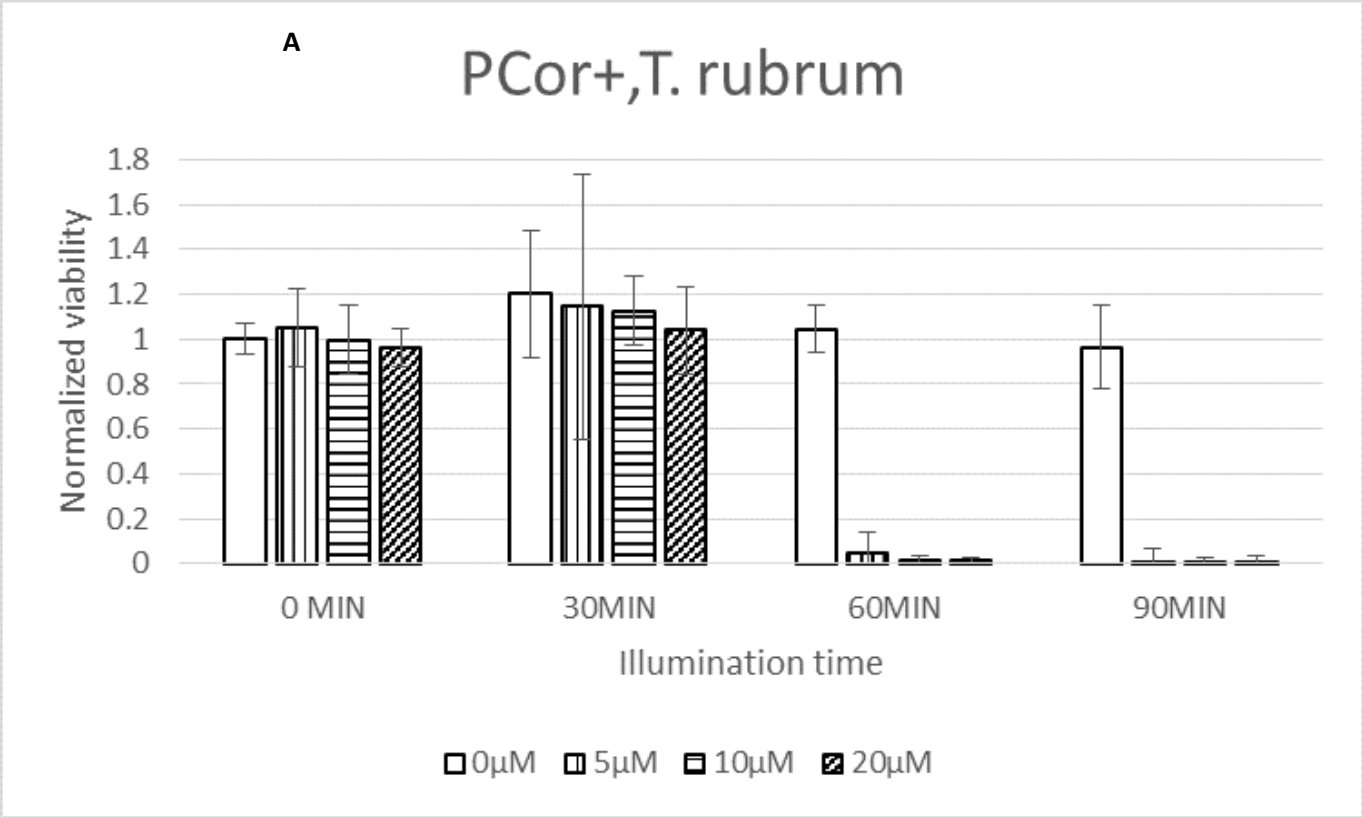

Figure 39a: The viablility of the suspension cultures of *T. rubrum* after 24 h of phototoxicity test with PCor+. Error pars represent the standard deviation of 8 samples (n=8). For dark control, samples kept in darkness at room temperature. 0 µM represents reference samples.

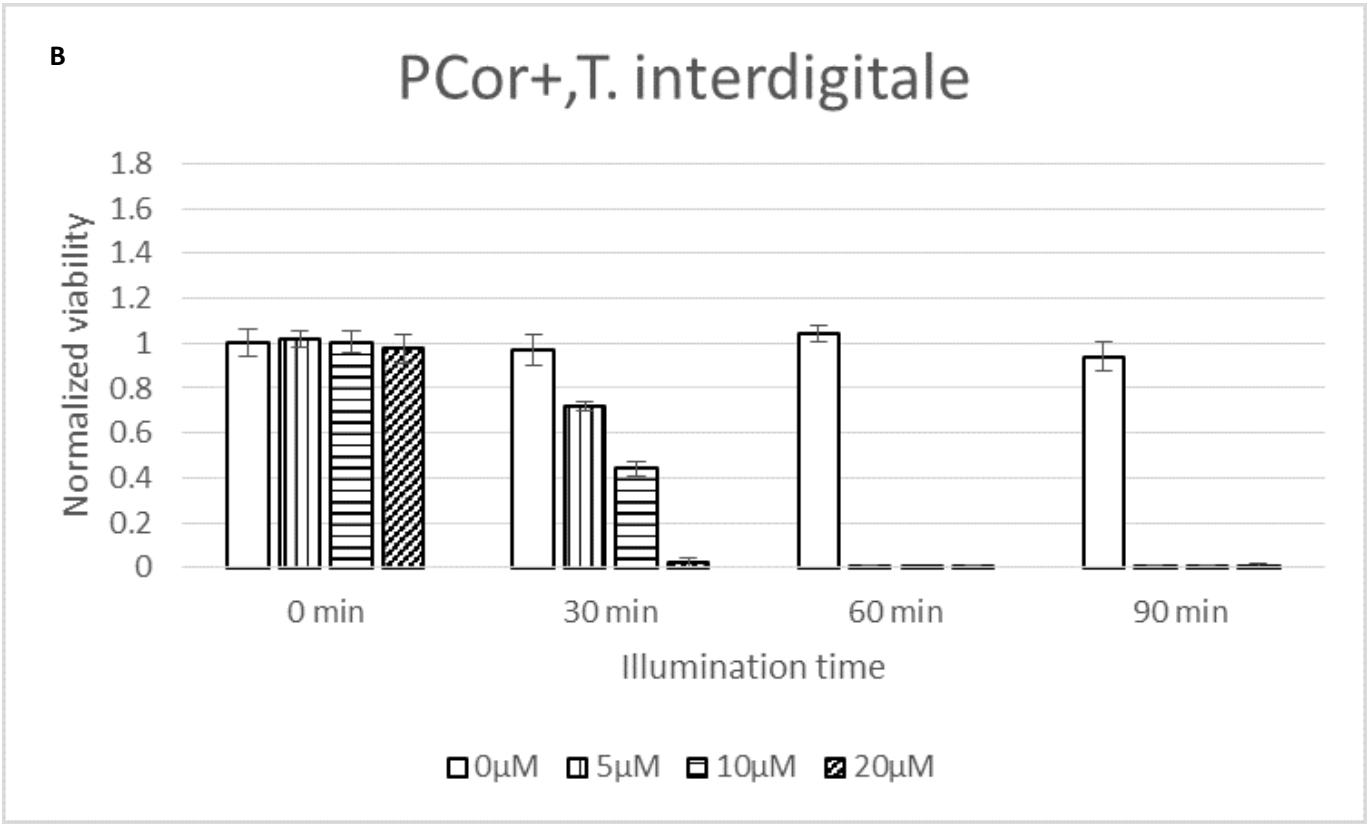

Figure 39b: The viablility of the suspension cultures of *T. interdigitale* after 24 h of phototoxicity test with PCor+. Error pars represent the standard deviation of 8 samples (n=8). For dark control, samples kept in darkness at room temperature. 0 µM represents reference samples.

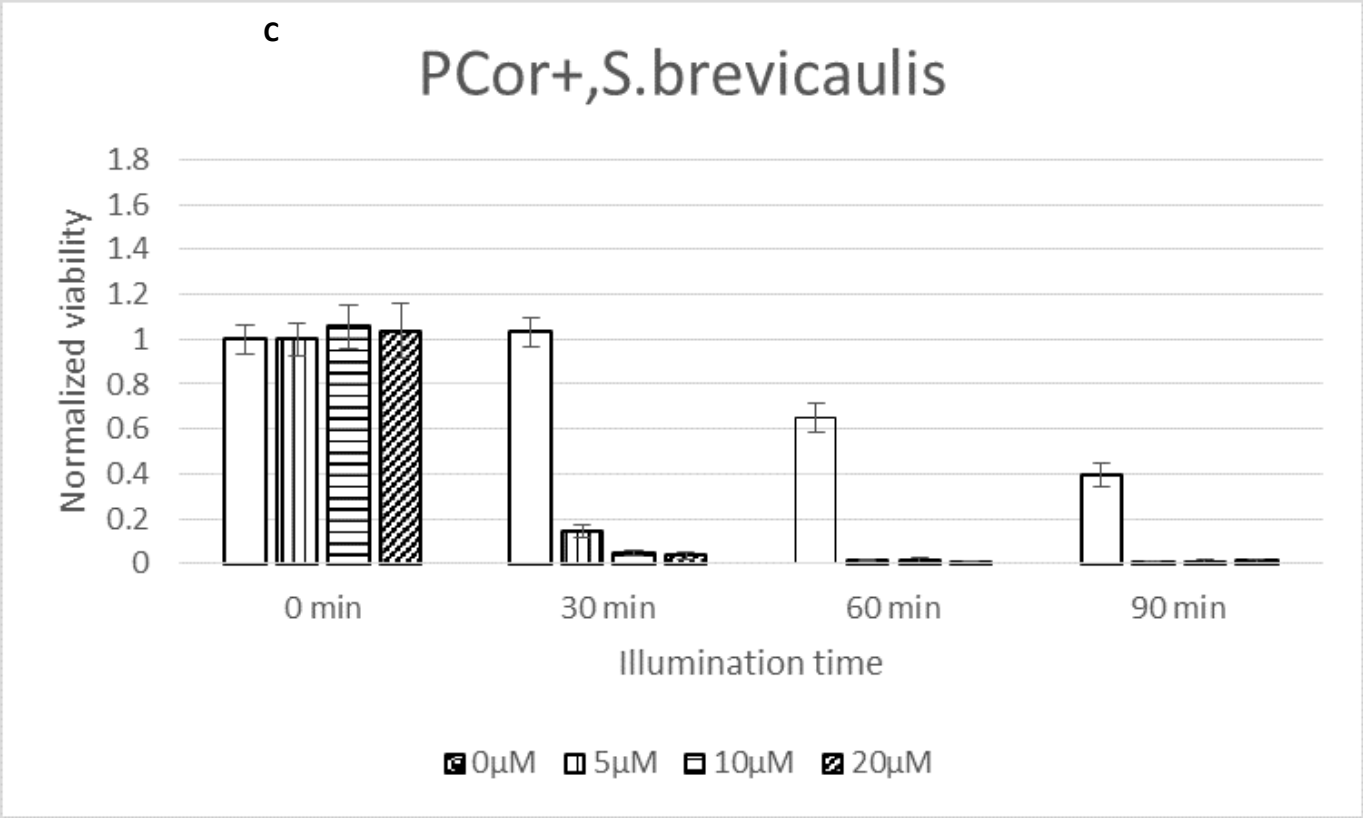

Figure 39c: The viablility of the suspension cultures of *S. breivecaulis* after 24 h of phototoxicity test with PCor+. Error pars represent the standard deviation of 8 samples (n=8). For dark control, samples kept in darkness at room temperature. 0 µM represents reference samples.

4.3 *In vitro* phototoxicity tests on cultures on surfaces

To imitate the living conditions of the microorganisms, the potential of the PSs to inactivate the growth of fungal spores on surfaces was investigated. The acquired results for PDI of suspension cultures encourage efforts to continue the PDI investigation on surfaces.

4.3.1 The phototoxic effect of PCor+

As already shown, the application of PCor+ mediated PDI leads to a complete eradication of spore suspension of the three fungi species. Figure 40 summarizes the results of PDI treatment using PCor+ as PS on *T. rubrum (*Figure 40*a)*, *T. interdigitale* (Figure 40b) and *S. brevicaulis* (Figure 40*c)*. The phototoxic effect of PCor+ resulted in full inhibition of the fungi spores. Up to two weeks after incubation at 28 ºC, no regrowth was observed. PCor+ has no dark toxicity.

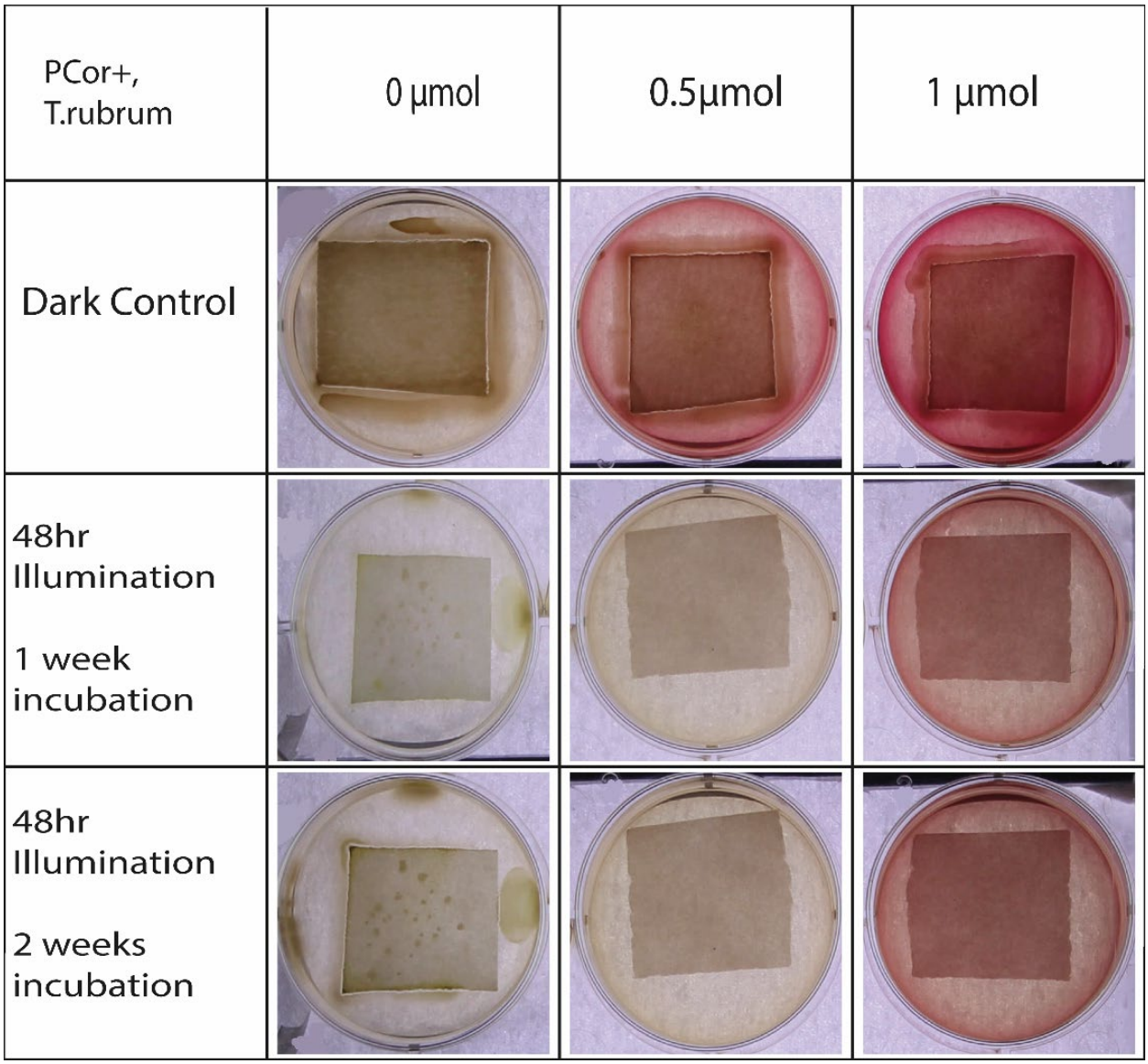

Figure 40a: Photographs illustrating phototdynamic activity of PCor+ on cultures of *T. rubrum* on surface. For dark control, samples kept in darkness at room temperature. 0 µM represents reference samples.

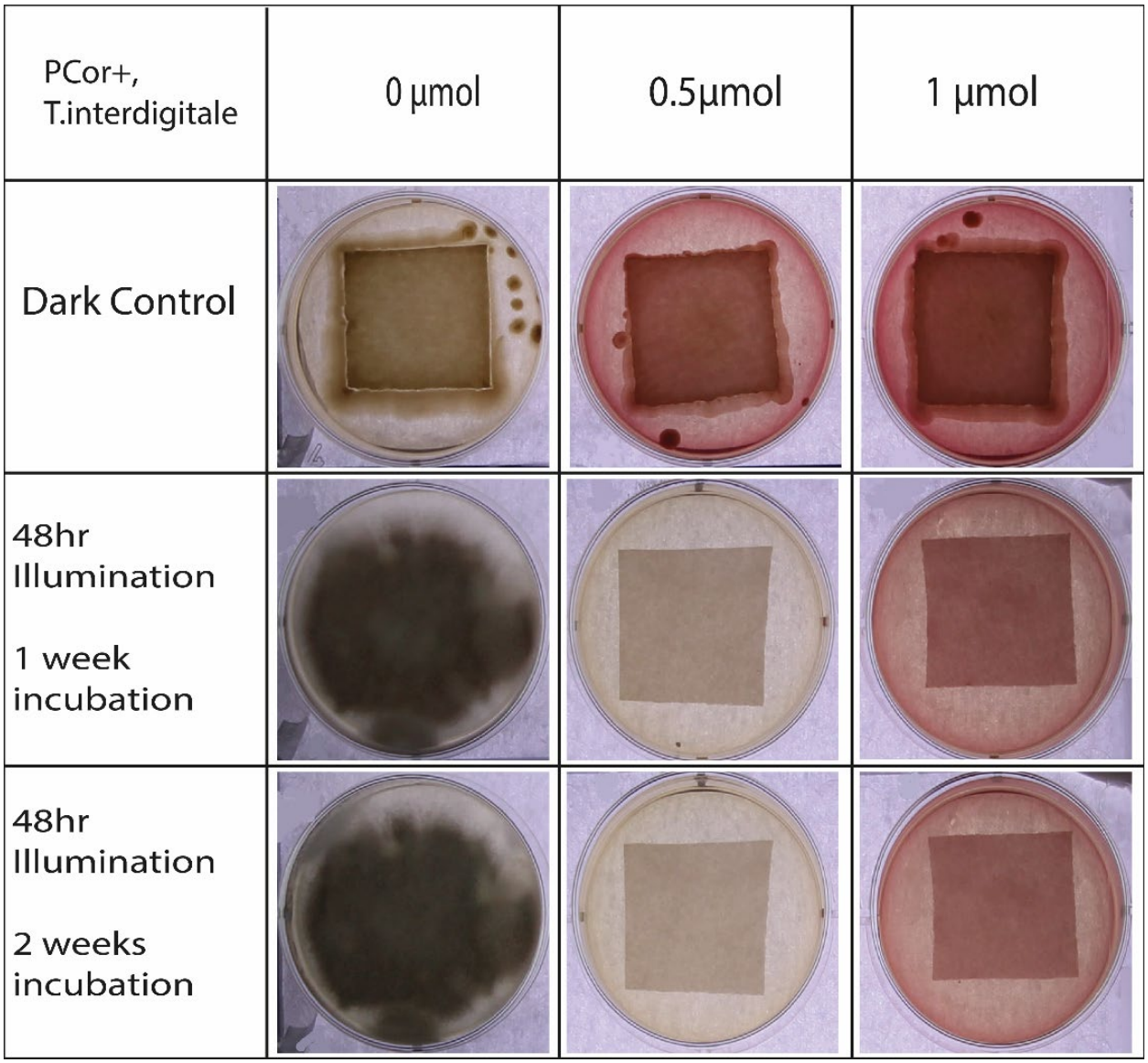

Figure 40b: Photographs illustrating phototdynamic activity of PCor+ on cultures of *T. interdigitale* on surface. For dark control, samples kept in darkness at room temperature. 0 µM represents reference samples.

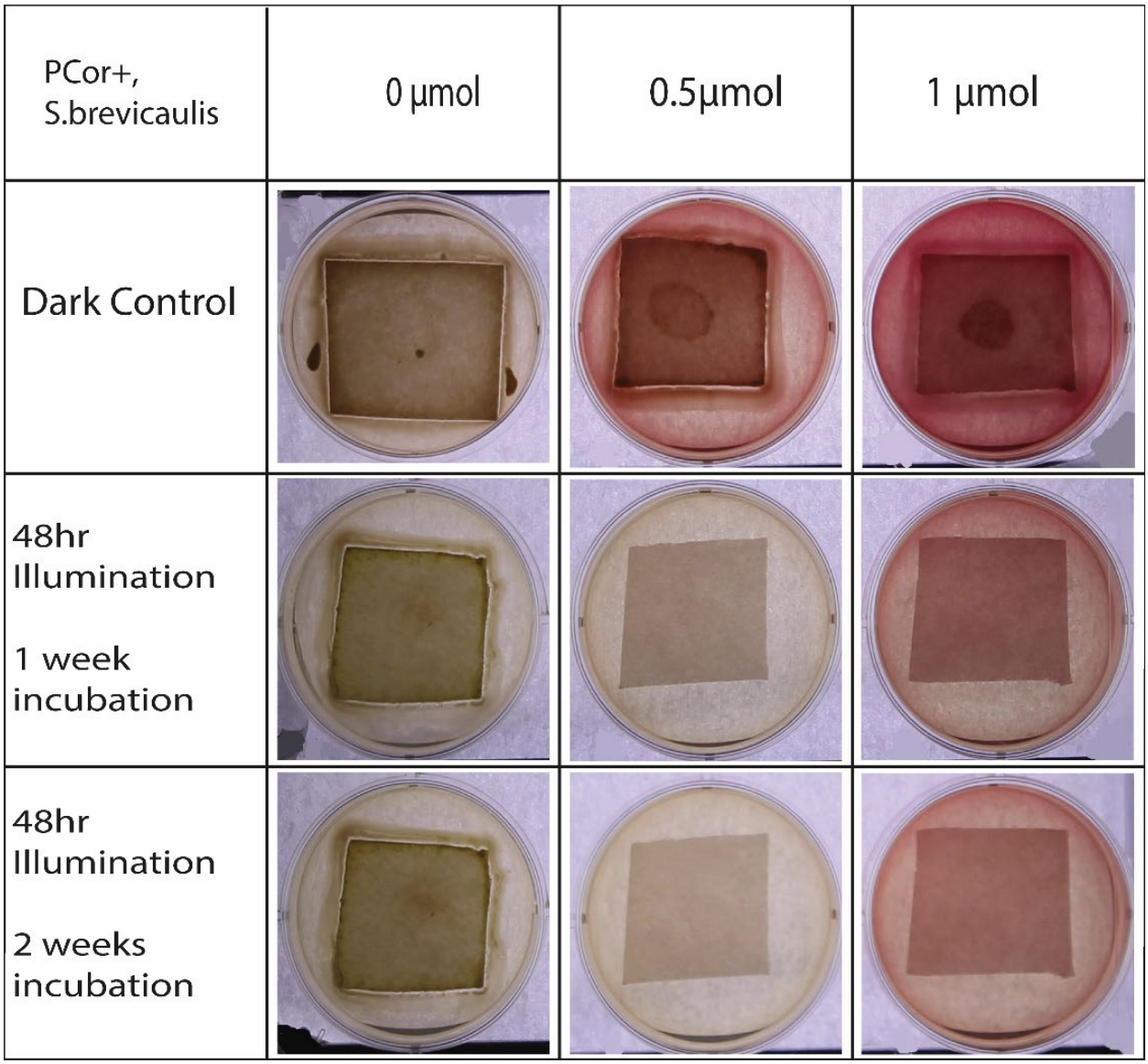

Figure 40c: Photographs illustrating phototdynamic activity of PCor+ on cultures of *S. brevicaulis* on surface. For dark control, samples kept in darkness at room temperature. 0 µM represents reference samples.

4.3.2 TMPyP phototoxic effect

Under the same conditions, phototoxicity tests with TMPyP were carried out on the three fungi species. As can be seen in figure 41 (a, b and c), an evident growth of the three fungi spores in the untreated control was detected. TMPyP leads to complete fungi growth eradication in the illuminated sample. To check the efficiency of TMPyP as PS, the samples were kept in the incubator at 28 ºC for two weeks after treatment. Growth continued only on the untreated control and dark control, where no recovery was observed for the illuminated samples. Due to the localization tendency of TMPyP that was shown in the previous section, halos formed around the filter paper.

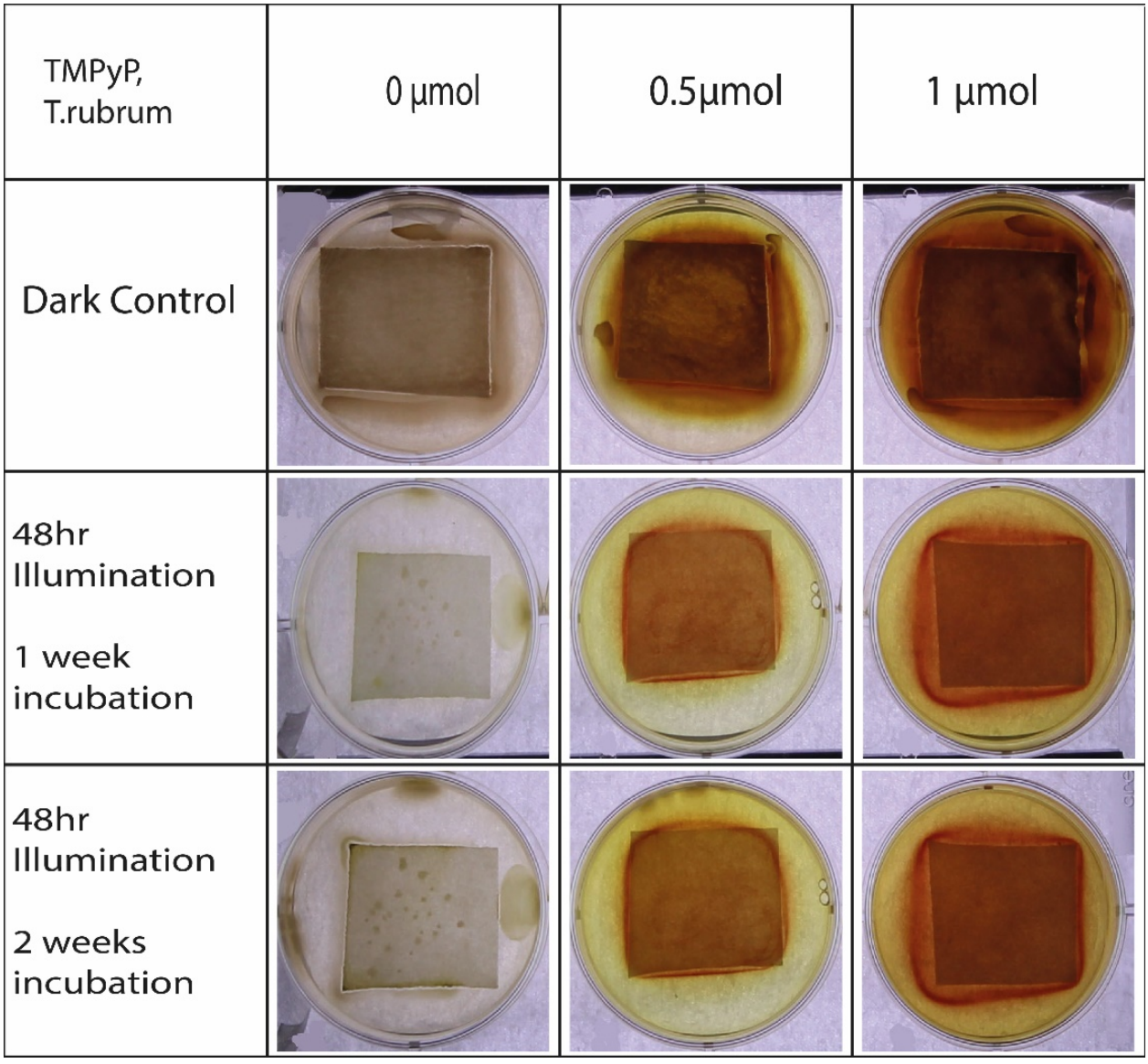

Figure 41a: Photographs illustrating phototdynamic activity of TMPyP on cultures of *T. rubrum* on surface. For dark control, samples kept in darkness at room temperature. 0 µM represents reference samples.

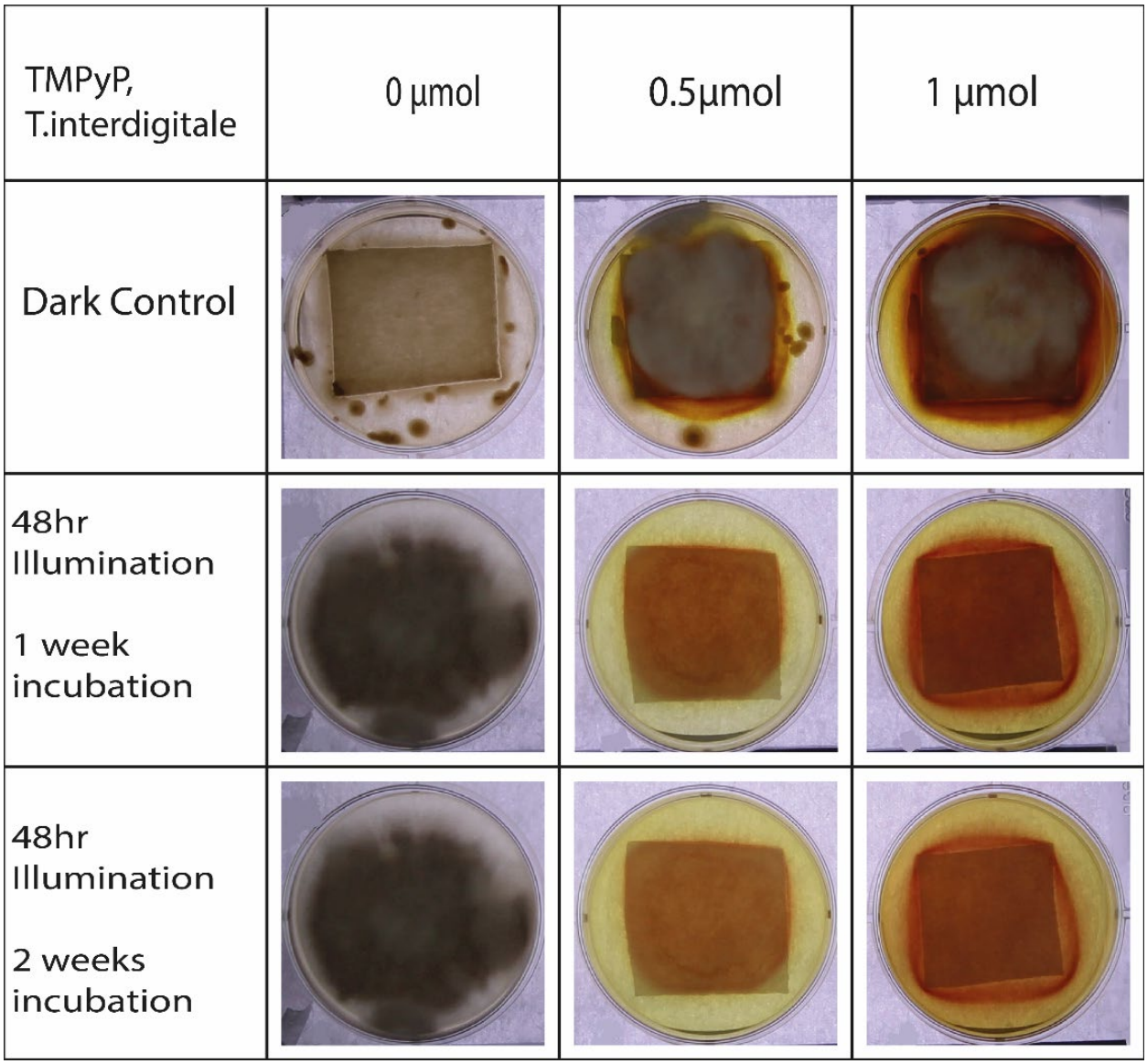

Figure 41b: Photographs illustrating phototdynamic activity of TMPyP on cultures of *T. interdigitale* on surface. For dark control, samples kept in darkness at room temperature. 0 µM represents reference samples.

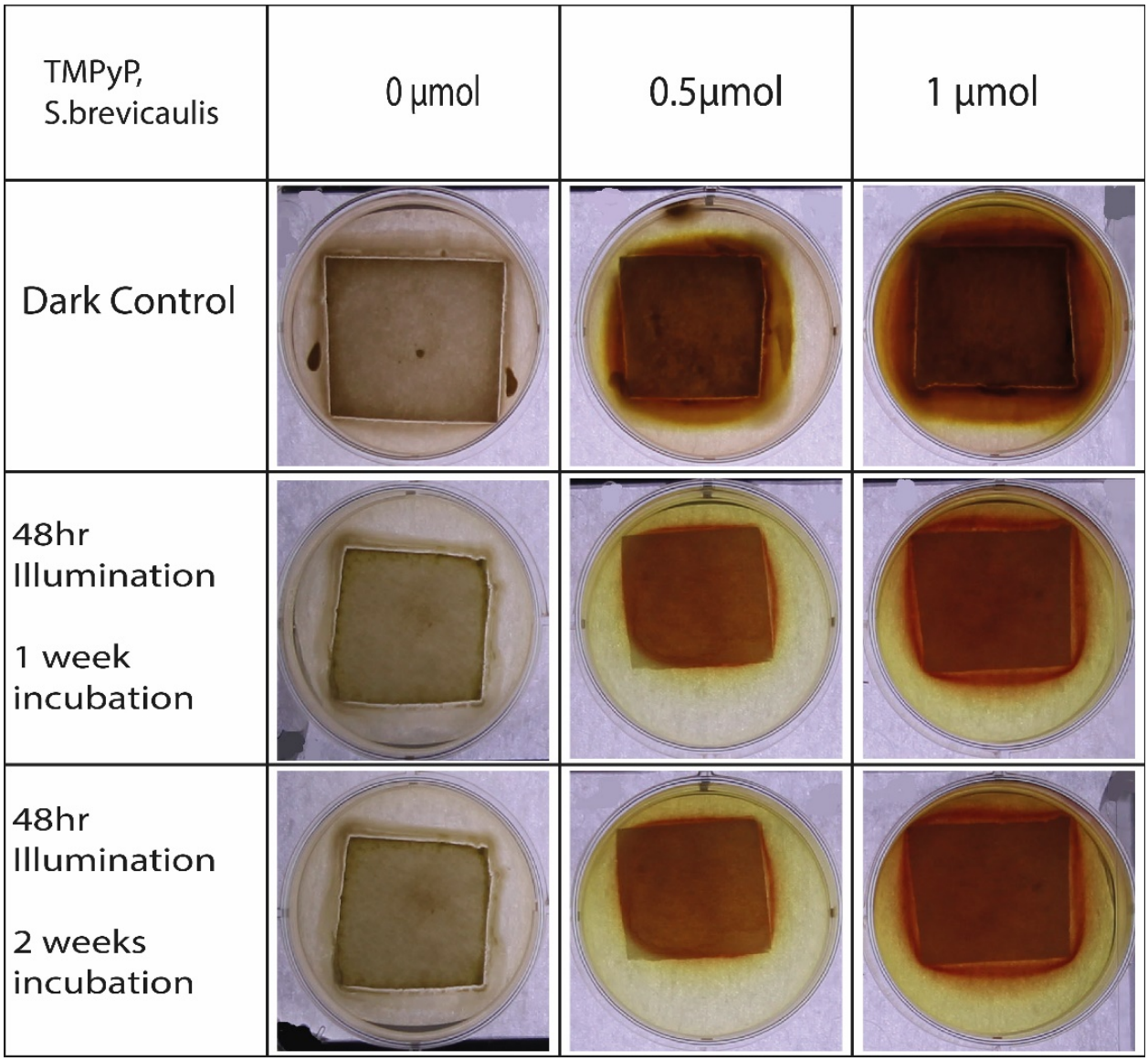

Figure 41c: Photographs illustrating phototdynamic activity of TMPyP on cultures of *S. brevicaulis* on surface. For dark control, samples kept in darkness at room temperature. 0 µM represents reference samples.

4.3.3 The phototoxic effect of eosin Y

Eosin Y is one of the very old photosensitizer that is used clinically. Due to its age it's clinically widely used for further applications e.g. in dentistry as a fluorescent marker. And since the project is related to a clinical issue, it was important to test its potential as PS in PDI of *T. rubrum, T. interdigitale* and *S. brevicaulis*. The phototoxicity of eosin Y was not tested on suspension cultures because of the interference between the absorbance spectrum of it and the spectrum of formazan. Formazan is the result of MTT reduction which was used to evaluate the viability of spore suspension samples after treatment (152). For that reason, the phototoxicity of eosin Y was tested only on agar surfaces. Efficient phototoxic effect of eosin Y was clearly observed for all three fungi species. Eosin Y prevents the growth of fungi spores in the treated samples. After an incubation period of two weeks, no recovery of the spores was observed. Untreated samples and the dark control show normal fungal growth (see figure 42 (a, b and c)). Despite the rapid photobleaching of eosin Y, a high phototoxicity was achieved.

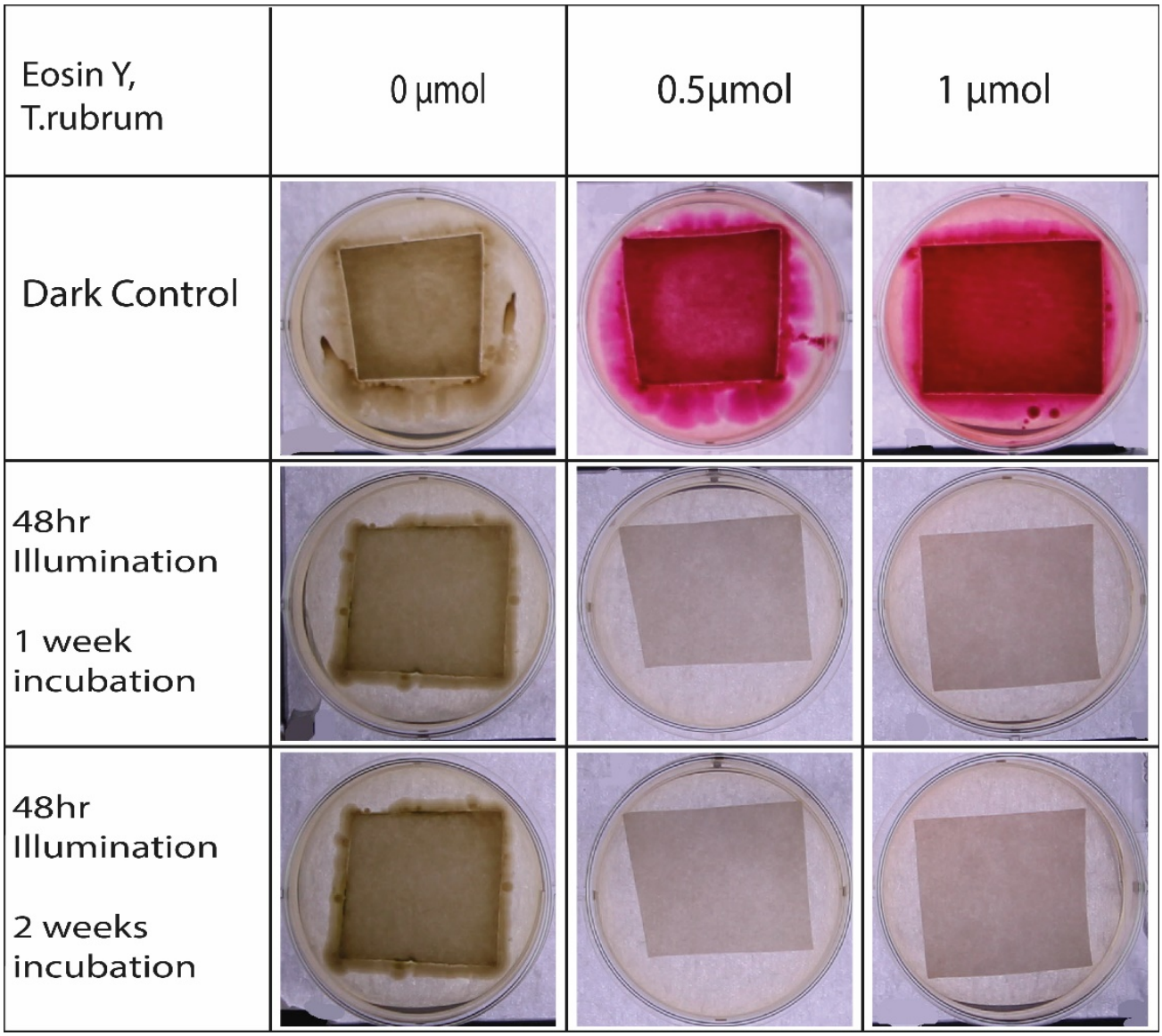

Figure 42a: Photographs illustrating phototdynamic activity of eosin Y on cultures of *T. rubrum* on surface. For dark control, samples kept in darkness at room temperature. 0 µM represents reference samples.

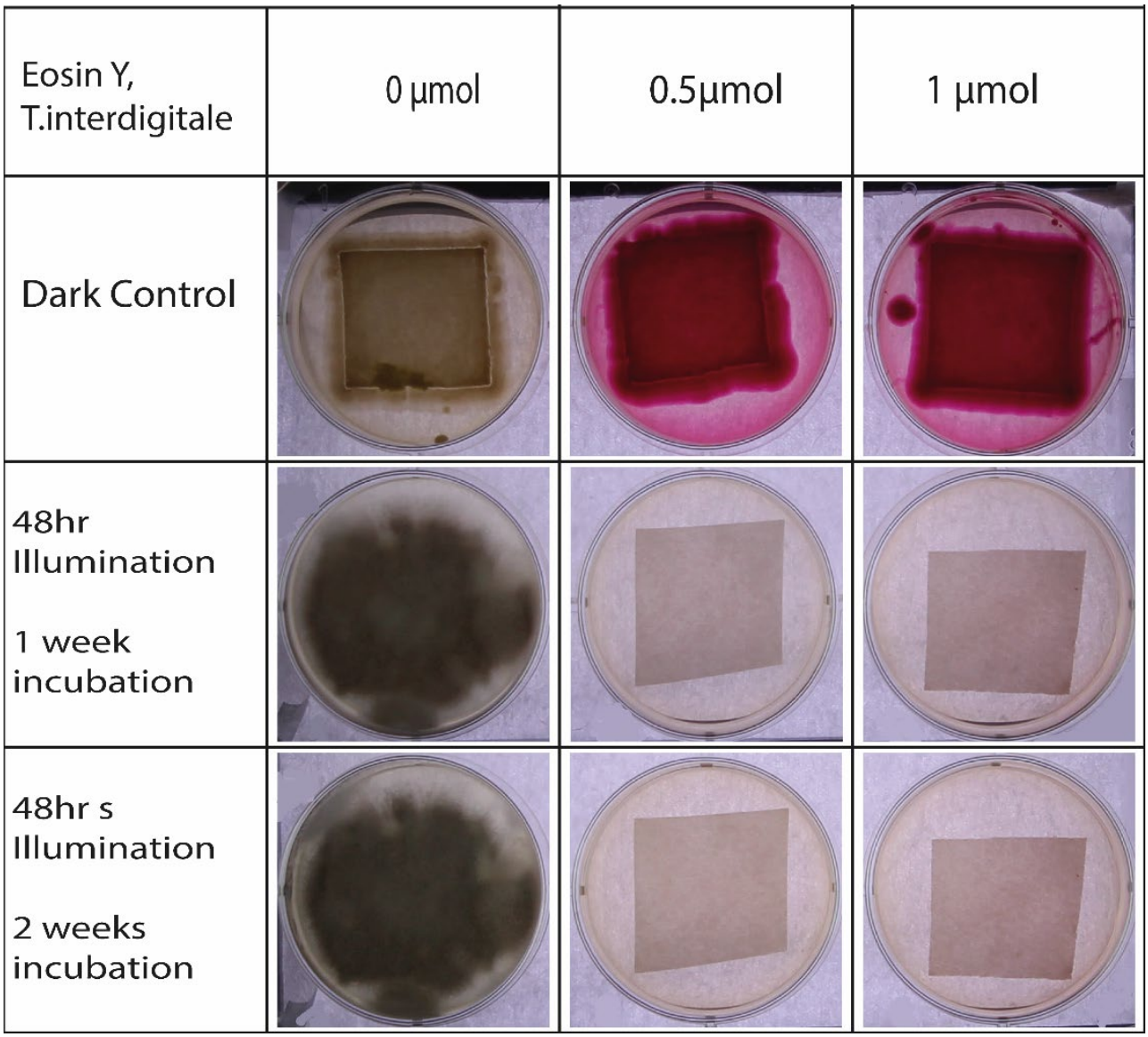

Figure 42b: Photographs illustrating phototdynamic activity of eosin Y on cultures of *T. interdigitale* on surface. For dark control, samples kept in darkness at room temperature. 0 µM represents reference samples.

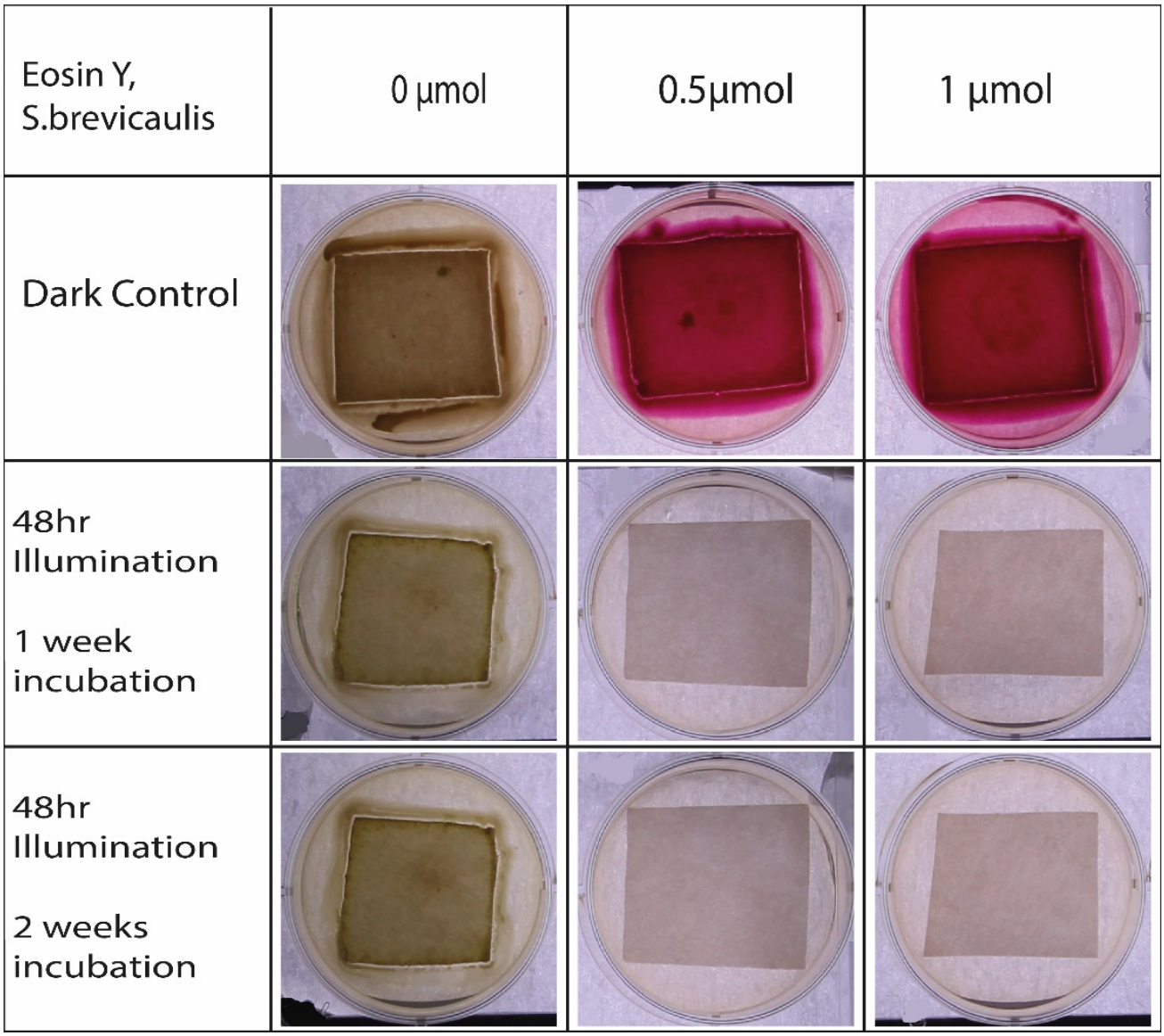

Figure 42c: Photographs illustrating phototdynamic activity of eosin Y on cultures of *S. brevicaulis* on surface. For dark control, samples kept in darkness at room temperature. 0 µM represents reference samples.

Discussion

2DTRSOL scans show a good singlet oxygen signal for up to one week of both TMPyP and PCor+ in the presence of the three fungi. The stability of the PSs and their singlet oxygen quantum yield shown by the scans indicate, that TMPyP and PCor+ would exhibit high phototoxicity on the involved fungi species. Based on this, phototoxicity tests of the PSs were conducted as second step of this investigation.

The potential of TMPyP and PCor+ was tested in both suspension and surfaces. Both PSs were able to photodynamically induce the death of the dermatophytes *T. rubrum* and *T. interdigitals* and the mold *S. brevicaulis*. The phototoxic effect of the PSs was achieved within short time using low concentrations of the PS.

Since the involved pathogens naturally rather grow on surfaces and not in suspension, it was important to test the effect of the PSs under conditions corresponding to natural growth conditions. Phototoxicity tests were carried out using filter papers applied to the surface of the SDA agar. Both PSs lead to the complete kill of the three fungi. Beside TMPyP and PCor+, the phototoxic effect of eosin Y was also tested on surfaces. Eosin Y is one of the oldest PSs and is currently in clinical use for medical purposes other than PDI. The use of a clinically approved PS in such medical-related project is very important as it facilitates any future application of eosin Y for the treatment of toe nail fungal infection. Eosin Y shows a very high phototoxic effect. No regrowth of any of the fungi was detected after two weeks of incubation after illumination. No dark toxicity of any of the PSs was observed.

Positively charged PSs are considered to be more efficiently in inhibiting microorganism, but in this study, eosin Y, despite its negative charge, shows a very high phototoxic effect.

According to aforementioned results, PDI may be a promising treatment modality of onychomycosis. The investigation was conducted to develop a treatment method aimed at avoiding the often-disappointing efficacy of the therapy of onychomycosis. Spores are the targeted part in this investigation. Killing the spores would end the life cycle of these pathogens and thus prevent the recurrences of the infection. The three PSs show high phototoxicity on the three fungi involved here. The most important fungi species is *T. rubrum*. It is considered as the main causative pathogen of onychomycosis and its resistance to a wide range of antifungals is the challenge. Killing *T. rubrum* by means of PDI is very important. For those PSs, being water soluble is advantageous. In the treatment of onychomycosis, aqueous treatments are preferred over alcohol-based treatment. Water is a natural hydration factor of the nails, which

helps to increase the permeability of the nails. Low permeability of the nails is one of the reasons that cause the failure of topical treatments.

The results of *in vitro* phototoxicity results meet the expectations of singlet oxygen luminescence scans. The great potential of the three PSs in *in vitro* encourages the efforts to continue the study and test the phototoxic effect of the PSs on an infected *ex vivo* model. The question is now, whether the PSs would have the same potential on an *ex vivo* model as in in-vitro tests.

4.4 *Ex vivo* phototoxicity tests on human nails

To continue the investigation and due to the great potential of the PSs on the three fungi species, *ex vivo* phototoxicity tests were carried out.

As shown in section 4.2.3, eosin Y has a high potential on the three kinds of fungi on agar surfaces. Moreover, eosin Y is clinically approved material, which would facilitate its future clinical application for the PDI treatment of Onychomycosis. For this reason, eosin Y was chosen for *ex vivo* tests.

As preliminary *ex vivo* tests, horse hooves were used as nail model. Figure 43 shows the first *ex vivo* phototoxicity tests. Horse hooves were infected with *T. rubrum*. The infected hooves were stored for four weeks before use. Two different concentrations (1 mM, and 2 mM) of eosin Y were used. For the two concentrations of eosin Y, no phototoxicity effect was detected. After two weeks of incubation after illumination, *T. rubrum* spores grow again in the same manner as reference where no PS was applied.

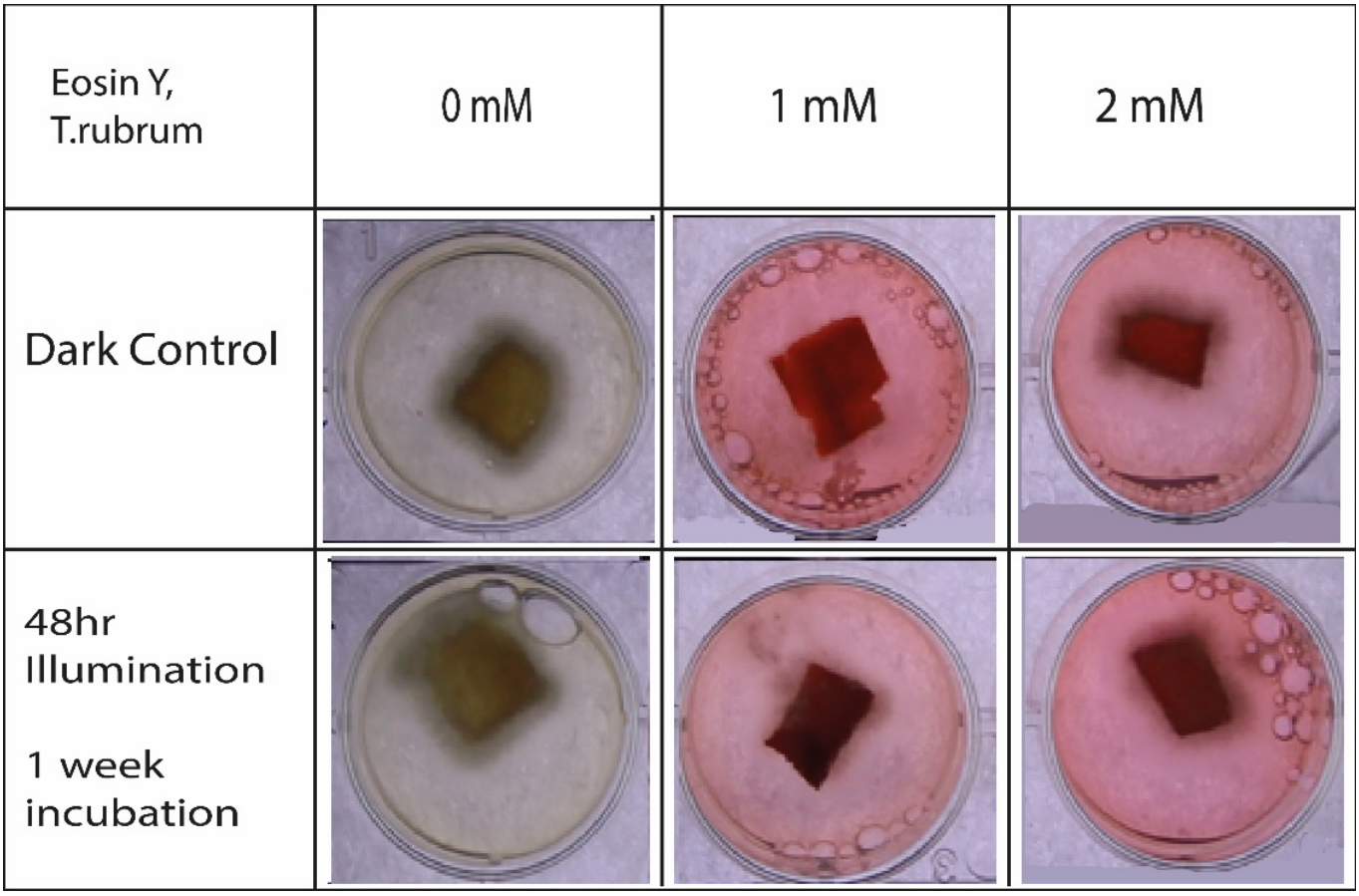

Figure 43: PDI of eosin Y on *T. rubrum* on infected hooves. For dark control, samples kept in darkness at room temperature. 0 mM represents reference samples.

As a follow-up to the experiments in this part, horse hooves were replaced by human nails. Here, a longer illumination was applied to see whether this would induce higher phototoxicity. Figure 44 shows the result of the phototoxicity tests of eosin Y on human nails under 48hr continuous illumination. The concentrations of eosin Y used here are 2 mM and 4 mM No phototoxic effect of eosin Y was observed even with longer illumination and higher concentration.

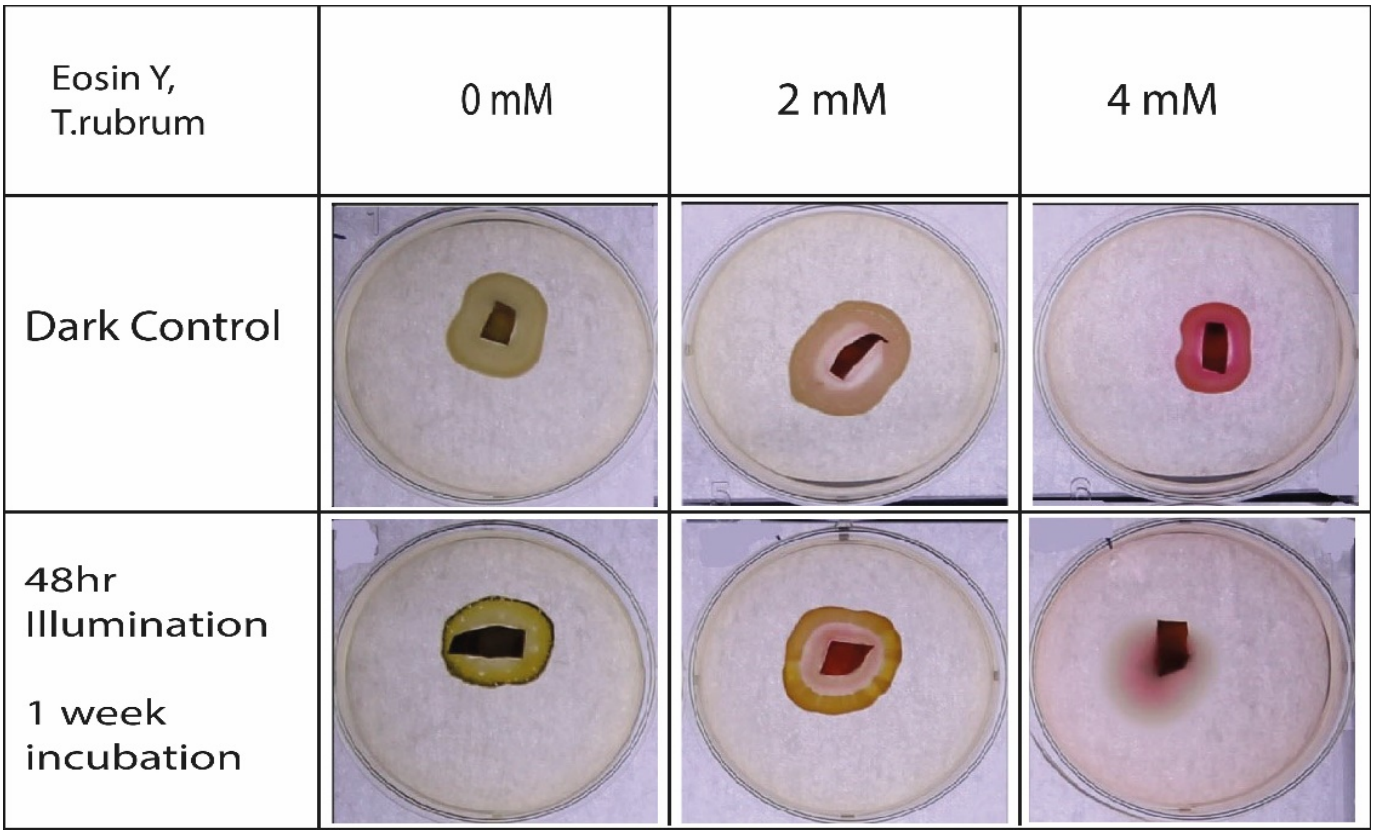

Figure 44: PDI of eosin Y on human nails infected by *T. rubrum.* For dark control, samples kept in darkness at room temperature. 0 mM represents reference samples.

To improve the illumination conditions, the white light illumination set-up used up to this point was replaced by a green light one. 20 green LEDs with a wavelength of 525 nm were used, which is suitable for the absorption spectrum of eosin Y with a total power 10 mW/cm^2. Figure 45 shows the results of the eosin Y phototoxicity test on infected human nails. No phototoxic effect was observed when using the green illumination and the pathogens grew naturally on the treated samples.

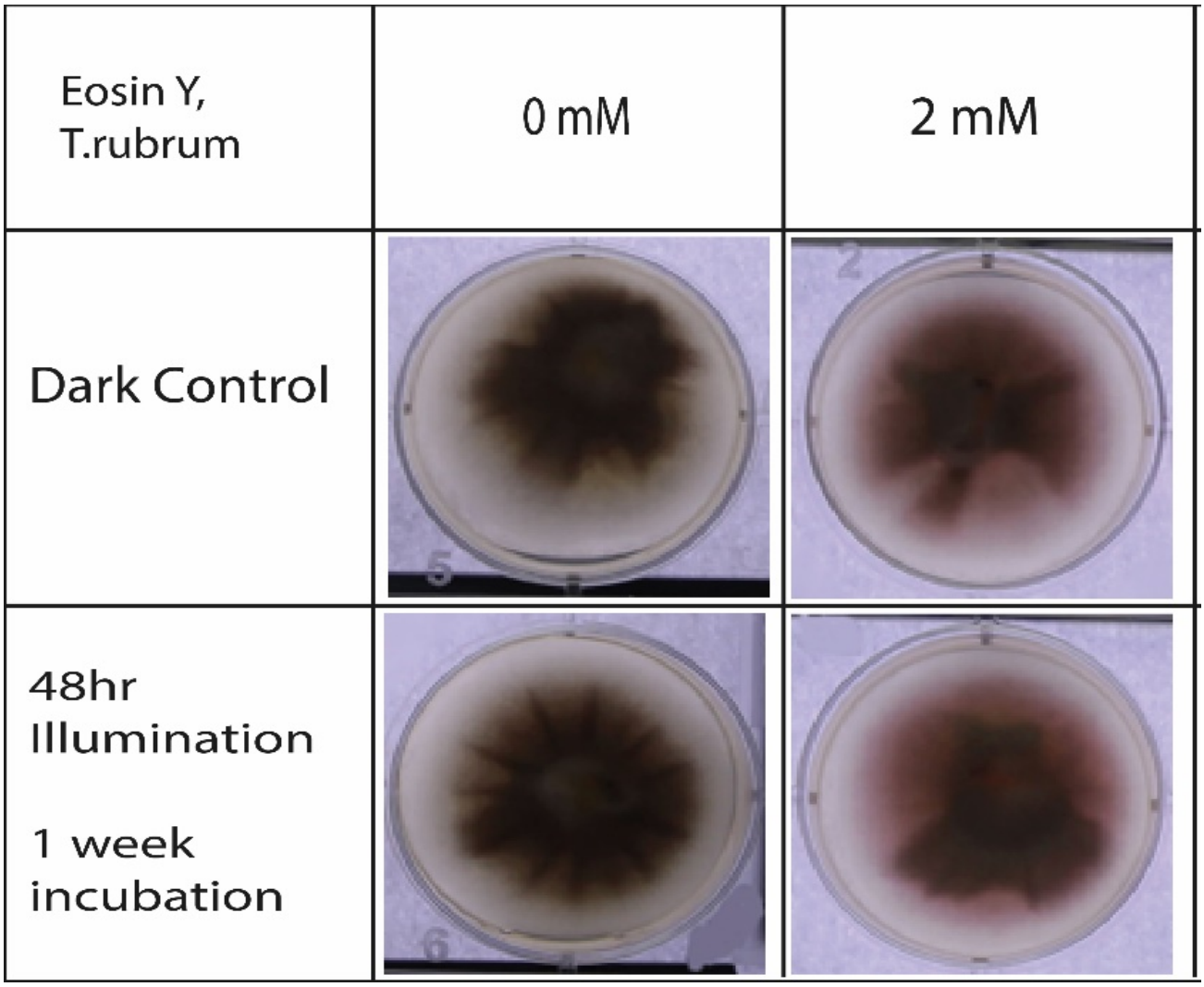

Figure 45: PDI by eosin Y of human nails infected by *T. rubrum*. For dark control, samples kept in darkness at room temperature. 0 µM represents reference samples.

After several trials and still negative results, the *ex vivo* investigation was stopped here. To figure out why there is no phototoxic effect of eosin Y on infected nails despite its great potential in *in vitro* investigations, singlet oxygen measurements were carried out on the surface of human nails.

4.5 Singlet oxygen luminescence scans on the surface of human nail

Ex vivo phototoxicity tests on human nails show no impact of eosin Y on infected human nails. To know the story behind the negative results, singlet oxygen detection measurements were conducted. Healthy nails were used to avoid any hazards associated with diseased nails. The analysis of singlet oxygen kinetics would provide information about the amount of singlet oxygen produced and its decay and diffusion.

During this part of the investigation, several factors had to be taken into account: the permeability of the nail plate and the concentration of oxygen in the internal microenvironment of the human nails. The lack of the permeability of the nail plate might be one of the reasons why no phototoxic effect was acquired. The low permeability of the nail plate is not the only problem in the treatment development, the oxygen concentration in the diseased nail and the chemical composition of the nail plate also have a significant impact.

All of the above mentioned factors have been considered in the luminescence detection of singlet oxygen. NAC was used as enhancer to overcome the permeability problem. During the experiment, molecular oxygen was blown on the surface of the nail samples.

Figure 46 shows normalized NIR signal integrated over time at 1270 nm, the figure shows a mixture of singlet oxygen counts and PS's phosphorescence counts. In both plots, the number of the total counts increases in an oxygenated atmosphere. The difference between the numbers of counts between aerated and oxygenated samples indicates that the generation of singlet oxygen is enhanced with additional oxygen. The Plots also show that there is a minor increment in the total counts when applying a permeability enhancer to the nails.

As we can see, the addition of NAC as an enhancer did not help so much. By comparing the upper and lower rows of figure 46, it can be seen, that in both cases there is no big difference (with and without enhancer) but the difference in the total counts with oxygenated atmosphere tells that there could be singlet oxygen and its generation is enhanced by adding additional molecular oxygen.

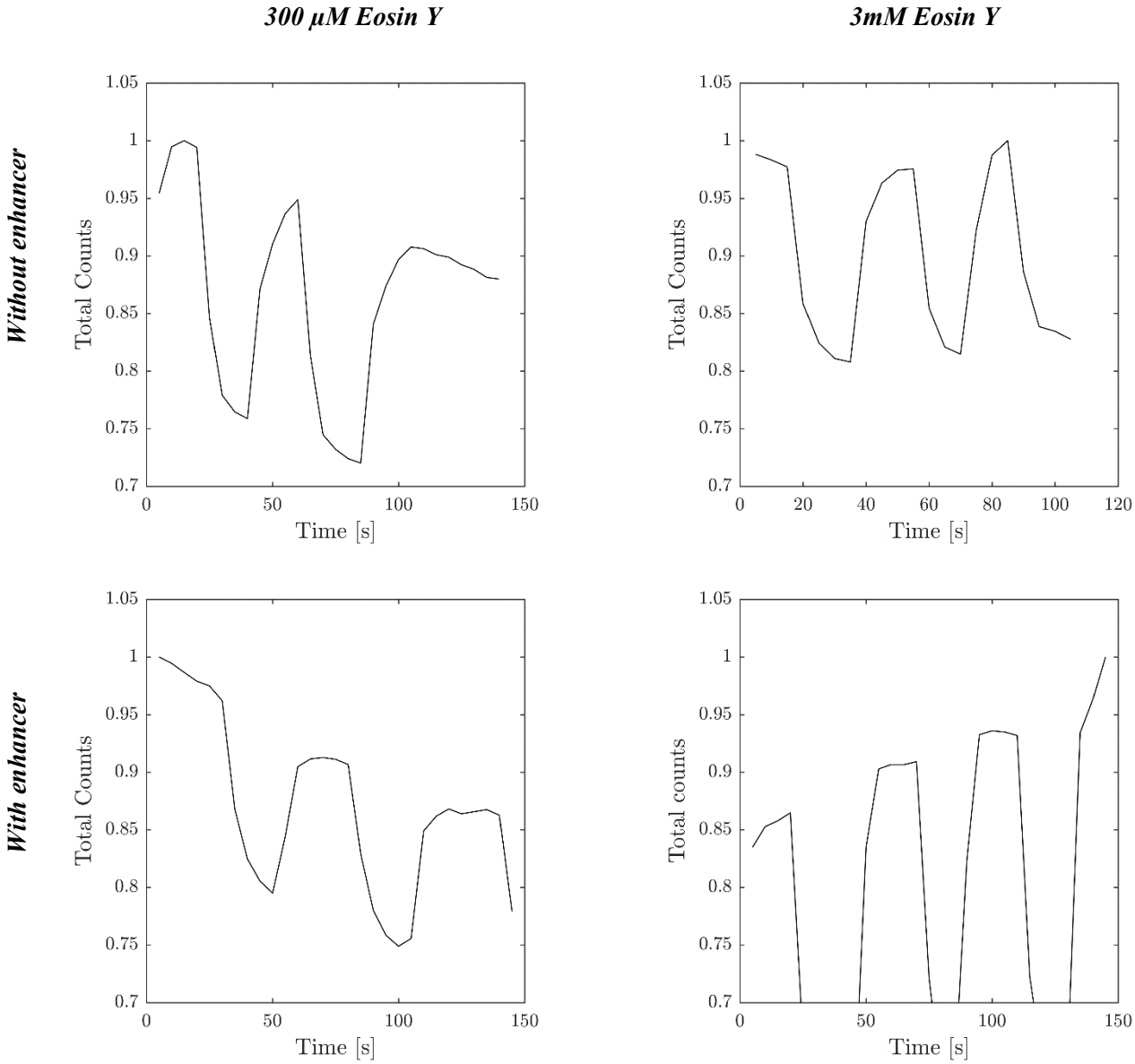

Figure 46: Normalized time integrated NIR signal at 1270nm without enhancer and with enhancer. Two concentrations of eosin Y were used 300 µM and 3 mM . On (Peak) and OFF (Valley) oxygen blowing regime was followed on the surfaces of the samples.

Figure 47 presents singlet oxygen kinetics of eosin Y in the nail microenvironment. No clear kinetics could be detected. The kinetics displayed is difficult to analyse. The kinetics shown here serve to find out, if any differences could be seen in the presence of additional oxygen. In figure 47, the kinetics correspond to two different concentrations of eosin Y, 300 µM and 3 mM. For each concentration, samples with and without enhancer were examined. The enhancer is NAC (3% vol. aqueous solution). No big difference was observed between different concentrations independent of presence of the chemical enhancer. The only difference is observed in the comparison of aerated and oxygenated atmospheres. The difference with

additional molecular oxygen indicates that there is a weak singlet oxygen generation, which can be enhanced by oxygenation.

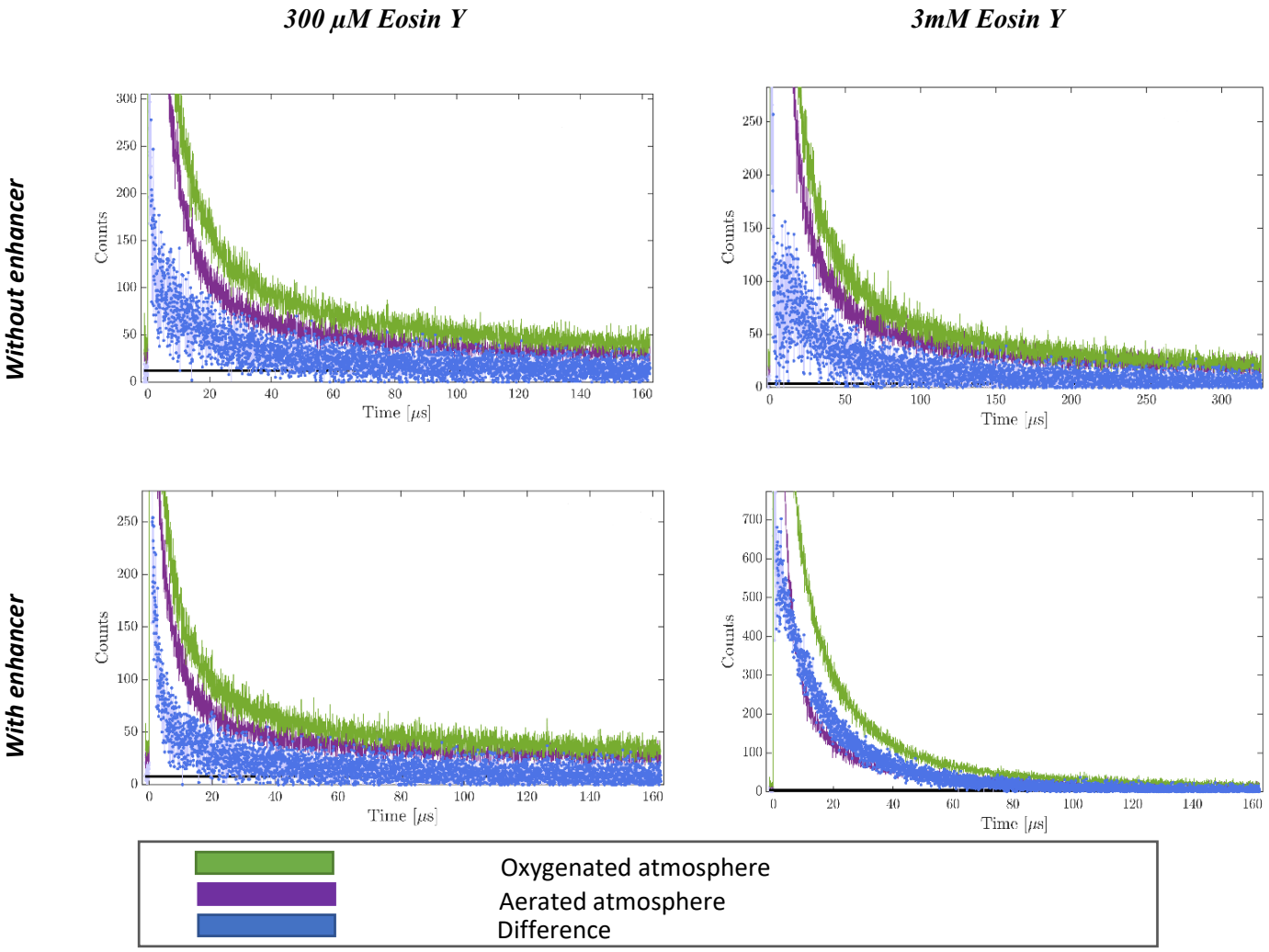

Figure 47: Singlet oxygen kinetics on the surface of healthy human nails without enhancer (upper row) and with enhancer (lower raw). Two concentrations of eosin Y were used 300 µM (left) and 3 mM (right). Altering On and OFF oxygen blowing regime was followed on the surfaces of the samples.

Discussion

Following the plan of this work and according to the successful results in the *in vitro* experiments, *ex vivo* phototoxicity tests were conducted using horse hooves and human nails. For *ex vivo* studies, eosin Y was chosen to study its impact.

Horse hooves have a similar chemical composition as human nails. For that reason, they were chosen as *ex vivo* model. The first hand experiment was conducted with horse hooves. The outcome of the experiment was contrary to expectations. *T. rubrum* grew normally on nails and no phototoxicity was observed. Hooves were chosen as they considered easy simple model of human nails. The negative results of phototoxicity tests on hooves was the reason to switch the original model, hence, human nails.

A second trial with human nails was conducted. The availability of human nails and the ease of collection and preparation of them were the reasons to use them as *ex vivo* model. No phototoxic effect of eosin Y was found on infected human nails as well. Several attempts were carried out and in each one, a different factor was modified: longer illumination time, higher illumination power, and higher concentration of eosin Y still, no difference was observed in the results.

To figure out the reason behind such results, singlet oxygen luminescence kinetics were measured on human nails. During the scans, additional molecular oxygen was blown on the surface of the nail samples.

The scans show a very low singlet oxygen signal, which was enhanced by additional oxygen. The nail barrier lowers the permeability of the PSs through nail plate. To overcome this problem, NAC was used as chemical permeation enhancer. Scans showed a slight difference in signal between nails with and without enhancer.

NAC was chosen as the chemical enhancer as it has a high effect as an enhancer. It is the most popular enhancer used for the application of topical antifungals. Cysteine, the main component of the enhancer is a chemical singlet oxygen quencher. Soaking nails in water after adding enhancer for two hours and washing them does not seem to be enough to get rid of all of the cysteine. Based on this, it would be better to use an enhancer with less singlet oxygen quenching effect.

The low singlet oxygen luminescence signal on the surface of nails can be related to the chemical composition of the nail plate. About eight amino acids that are considered chemical singlet oxygen quenchers contribute to the chemical structure of the nail plate. The most dominant amino acids are cysteine, serine, lucine and glutamic acid. It is known that the

chemical quenching is an irreversible process so a proper oxygenation might be the solution of this dilemma.

4.6 Phototoxicity on socks' textiles

After the unsuccessful phototoxicity tests on samples of human nails, a different approach was chosen to continue the investigation. Based on the fact, that socks and shoes play a major role in the recurrences of fungal infections, PDI tests were conducted on the typical material of socks.

Disinfection of footwear by means of PDI would be a good step towards killing any possibly attached fungi and thus preventing the recurrences of the infection.

Although the costs for individual socks are not high, they represent an enormous cost factor for patients with onychomycosis, as the socks have to be replaced after being worn once. If the PDI can be established as a disinfection method for socks, the wearing time of socks could easily be extended.

This idea was tested here on a pair of commercially available socks (80% cotton, 20% polyester) at affordable cost in the manner of a hand experiment.

Two different concentrations of eosin Y (3 mM and 10 mM) were used. A few drops of each prepared solution were applied on rectangular piece of the sock's textile infected with *T. rubrum*. The samples treated in this way were illuminated for 90 minutes. Figure 48 shows the results of the phototoxicity tests. As can be seen, eosin Y has had no phototoxic effect on the infected samples and *T. rubrum* grew in the treated and the untreated samples equally.

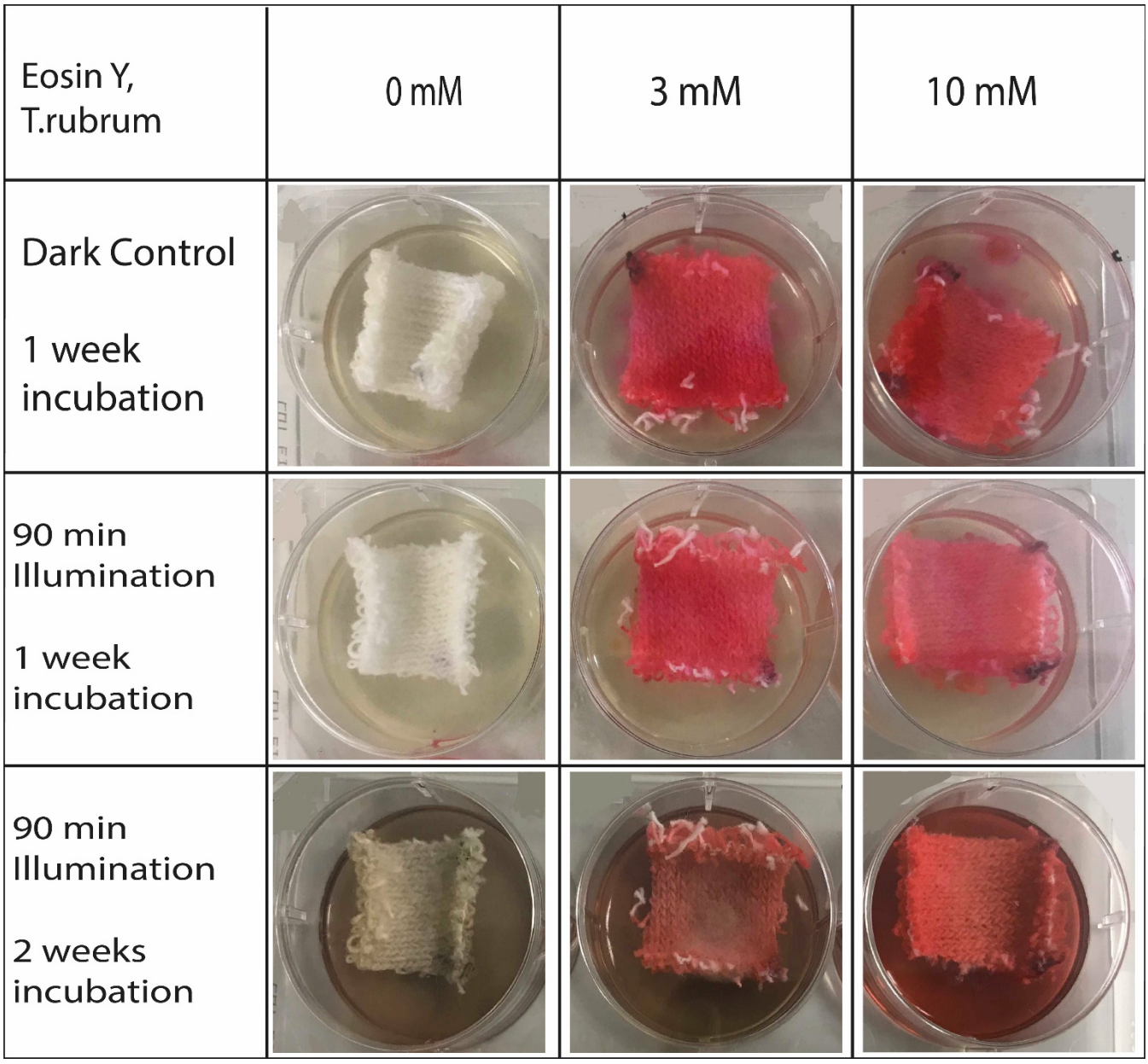

Figure 48: Photographs illustrating phototdynamic activity of eosin Y on cultures of *T. rubrum* on socks' textiles. For dark control, samples kept in darkness at room temperature. 0 µM represents reference samples.

Discussion

Self-disinfecting shoes and socks are very important for patients with onychomycosis. Wearing shoes and socks with the ability of inactivating adherent fungi would help prevent the recurrence of infections. Phototoxicity tests were carried out on sock textiles for this purpose. However, the results of the tests did not meet the expectations. Eosin Y shows no phototoxic effect on *T. rubrum* spores on sock textiles. Since this approach was only tested in a hand experiment, further attempts to determine the cause of the negative result are recommended. Sock textiles that are professionally equipped with effective PS could possibly lead to better phototoxicity. A higher illumination dose could also increase the potential for phototoxicity of PSs. It is also possible that the use of different textiles would influence the results of phototoxicity. The socks used here are very thick, thinner socks would reduce the distance of the PS to the adhering fungi and thus promote the effect of the PDI.

5. Summary and General Discussion

The study was carried out to develop PDI as non-invasive treatment of nail fungal infection. The project is divided into three consecutive steps. First, analysis of singlet oxygen kinetics on the presence of fungi on surfaces. Second, *in vitro* phototoxicity tests of the three PSs against fungi species. The third step was to test the phototoxicity of the PSs on infected *ex vivo* models.

The first two parts were achieved successfully, while some problems occurred when PDI was applied in an *ex vivo* model. Here I will show the possible explanation of the acquired results. Since the information about PSs in their microenvironments is very important to demonstrate the conditions for high phototoxic effect of the PSs, 2DTRSOL scans were performed in the presence of fungi at the beginning of this project.

The results show similar behaviour of the PSs regardless of the kind of fungi. Also, no big difference could be observed between singlet oxygen kinetics, which was validated by statistics and the first study. The difference of spore suspension concentrations has nearly no impact on the acquired fluorescence and singlet oxygen luminescence signals. A correlation between the growth phase of the fungi and the intensities of the fluorescence and singlet oxygen luminescence signals can be concluded. A clear signal of singlet oxygen luminescence was observed for up to seven days of the experiment. This indicates the stability of both PSs. The study also shows the diffusion of the PSs. TMPyP highly localizes relative to PCor+ as it diffuses very fast to the surrounding agar.

2DTRSOL detection helps to obtain information about singlet oxygen kinetics and the behaviour of the PSs in the presence of fungi. This information helps to better develop PDI as a suitable alternative to conventional antifungals.

The scans show a good singlet oxygen luminescence signal for up to one week. This indicates, that TMPyP and PCor+ would have a great potential on fungi. To test the phototoxicity of the PSs on the involved fungi species, *in vitro* phototoxicity investigations followed. The *in vitro* phototoxicity tests' results meet the expectation. TMPyP and PCor+ show a high phototoxic effect against *T. rubrum, T. interdigitale* and *S. brevicaulis*. The amount of surviving spores counts for less than 5% after 30 min illumination and further reduces with longer illumination.

It is known, that the involved pathogens grow on surfaces, not in suspension cultures, so *in vitro* studies on surfaces would be closer to reality. In order to mimic the natural growth behaviour of fungi, *in vitro* phototoxicity tests were carried out on surfaces. In addition to TMPyP and PCor+, the phototoxic effect of eosin Y was also tested on surfaces. Phototoxicity tests on

surfaces showed photo-induced death of the three fungi species with the three PSs. No re-growth of the spores was observed in samples stored two weeks after illumination, all three PSs exhibit no dark toxicity. Most of the studies in regard to PDI of onychomycosis are *in vitro* studies. The PSs used here also show very high phototoxic effect in both suspension and surfaces while only suspension cultures were investigated in other studies (17; 19; 24; 22; 132).

The great *in vitro* potential of the three PSs on the involved fungi was the reason to follow the investigation and apply the treatment on an *ex vivo* model. Human nails were collected from healthy volunteers for the application. *T. rurbum* was chosen to continue this part of the investigation as test microorganism as it is considered the most popular causing agent of onychomycosis and is also known for its high resistance. Several trials were carried out for *ex vivo* phototoxicity tests. During the different trials, different factors were changed. Old infection, fresh infection, water hydrated nails, different PS's concentrations and different illumination powers and times. Unfortunately, no phototoxic effect was achieved on the infected nails. Singlet oxygen luminescence kinetics scans were performed to explain the negative results of phototoxicity tests on human nails. The analysis of singlet oxygen kinetics is the direct method to determine the expected impact of a PS. In this part, NAC was used as chemical enhancer to overcome the low permeability of the nail barrier and allow eosin Y to diffuse through the nail plate. Additionally, molecular oxygen was blown on the surface of nail samples during scan in an on/off regime. No clear singlet oxygen kinetics was detected on the surface of human nails. Only a very small amount of singlet oxygen was produced, which was slightly increased with an oxygenated atmosphere. Two different concentrations of eosin Y (300 µM and 3 mM) were used. Scans show slight difference between the two concentrations. The difference in the total number of counts between the aerated and oxygenated atmospheres indicates that there is a generation of singlet oxygen, which is enhanced with additional molecular oxygen. The use of NAC was not the right choice. NAC is a very effective enhancer, which is widely used for drug delivery purposes (158). However, cysteine is one of the amino acids that is considered as a chemical quencher of singlet oxygen. So another enhancer with lower quenching effect should be used for PDI application. The chemical composition of the nail plate and its complexity is a challenge any treatment faces. For a PDI treatment modality, the high content of singlet oxygen quenching amino acids in the chemical structure of the nail is an additional challenge (137; 159). Based on the fact, that chemical quenching is an irreversible process, a proper oxygenation could be the solution. In 2015, Smiji et al (20) show a very interesting *ex vivo* study. They used an invasive multifunctional PS which acts as enhancer and PS at the same time. They used a porphyrin

sensitizer designed especially for their studies called 5,10,15-tris(4-N-methylpyridinium)-20-(4-(butyramido-methylcysteinyl)-hydroxyphenyl)-[21H,23H]-porphine trichloride (PORTHE). This multifunctional PS was able to exhibit complete cure of infected nail clippers as *ex vivo* model. They also mentioned that PORTHE's photodynamic action is a type I action, which is dominant in environments with low oxygen concentrations. This is somehow consistent with the results observed here. Singlet oxygen scans on the surface of human nails have shown, that the oxygen concentration in the nail microenvironment is very low. Based on the fact, that the PSs used here act through Type II action, adequate oxygenation is required to produce sufficient amount of singlet oxygen to lead to high toxicity on human nail infections. The use of Type I PSs in oxygen-depleted nail environments is another solution. Despite the great potential of PORTHE PS on infected human nails, no *in vivo* studies have yet been conducted by Smijis group. Some other studies use bovine hooves or nail powder instead of human nails. The complexity of the human nail plate cannot be expressed by bovine hooves or nail powder. Bovine hooves are found to be more porous than nails, and the alteration of their penetration is much easier than for human nails (160).

The final part of the plan of this study was the clinical trials with onychomycosis patients, which were not started due to the negative results of the *ex vivo* experiments. In order to continue the investigation from a different perspective, the possible photodynamic disinfection of footwear was investigated. The idea of using disinfected footwear has already been pursued. There are publications on the use of sterilized and disinfected insoles e.g. by ultraviolet LEDs (161–163). Although patents were filed several years ago, such soles are not yet in use. Therefore, it is important to further develop this idea for the disinfection of shoes and socks. The hand experiment carried out in the course of these investigations is neither sufficient to confirm the idea nor to reject it. Further experiments are therefore advisable.

6. Conclusions and Outlook

In this thesis, the efficacy of PDI was tested on onychomycosis causing pathogens. Three PSs, TMPyP, PCor+ and eosin Y were used. The behaviour under PDI treatment of the prevalence pathogenic dermatophytes, *T. rubrum, T. interdigitale*, and of the mold fungi *S. brevicaulis* was investigated. During the study, *in vitro* and *ex vivo* phototoxicity tests were carried out. As mentoring method, 2DTRSOL detection was applied to fungal surfaces and on healthy nail surfaces for the first time.

Singlet oxygen scans on human nails show a very low concentration of singlet oxygen. The signal of singlet oxygen on the nails was slightly improved in an oxygen-enriched atmosphere. For this reason, a proper oxygen supply is required for a better singlet oxygen production and thus a higher phototoxic effect. The oxygenation method should avoid a possible contamination with spores by diseased nails. Another approach to overcoming the problem of oxygen-depleted nail environments is to use the Type I PDI mechanism, as the Type I PDI mechanism dominates in environments with low oxygen concentrations.

PDI could be the desired alternative for conventional treatment modalities. Efficient treatment of toenail infections within short time and without recurrences of the infection could be achieved with PDI. With the suggested improvements, our PSs would possess a great potential for PDI of onychomycosis. PDI could also be used as disinfection method after treatment with antifungals to prevent the recurrences of the infection. It would be a great step to apply the PDI on antifungally treated nails on patients to see the potential of PDI to prevent the reinfection. Application on patients and outside of lab conditions deserve a trial.

Not only as a disinfection method for treated nails, but also for footwear. Sensitizing shoes and sock materials must be developed in such a way that they kill all adhering fungi and thus prevent the possibility of re-infection of the nails with used shoes and socks.

References

1. Aly, R. (1994) Ecology and epidemiology of dermatophyte infections. J Am Acad Dermatol 31, S21-S25.

2. Pirard, G. (2001) Onychomycosis and Other Superficial Fungal Infections of the Foot in the Elderly. Dermatology 202, 220–224.

3. Effendy, I., M. Lecha, M. Feuilhade de Chauvin, N. Di Chiacchio and R. Baran (2005) Epidemiology and clinical classification of onychomycosis. J Eur Acad Dermatol Venereol 19 Suppl 1, 8–12.

4. Hay, R.J. and R. Baran (2011) Onychomycosis: a proposed revision of the clinical classification. J Am Acad Dermatol 65, 1219–1227.

5. Kashyap, B., P. Bhalla and R. Kaur (2008) Onychomycosis - epidemiology, diagnosis and management. Indian J Med Microbiol 26, 108.

6. Welsh, O., L. Vera-Cabrera and E. Welsh (2010) Onychomycosis. Clin Dermatol 28, 151–159.

7. Poradzka A1, Jasik M, Karnafel W, Fiedor P. Clinical aspects of fungal infections in diabetes., Acta Pol Pharm. 2013 Jul-Aug;70(4):587-96.

8. Gupta, A.K., C. Drummond-Main, E.A. Cooper, W. Brintnell, B.M. Piraccini and A. Tosti (2012) Systematic review of nondermatophyte mold onychomycosis: diagnosis, clinical types, epidemiology, and treatment. J Am Acad Dermatol 66, 494–502.

9. Mugge, C., U.-F. Haustein and P. Nenoff (2006) Causative agents of onychomycosis--a retrospective study. J Dtsch Dermatol Ges 4, 218–228.

10. Cuenca-Estrella, M., A. Gomez-Lopez, E. Mellado, M.J. Buitrago, A. Monzon and J.L. Rodriguez-Tudela (2003) Scopulariopsis brevicaulis, a Fungal Pathogen Resistant to Broad-Spectrum Antifungal Agents. Antimicrobial Agents and Chemotherapy 47, 2339–2341.

11. Kushwaha, A., R.N. Murthy, S.N. Murthy, R. Elkeeb, X. Hui and H.I. Maibach (2015) Emerging therapies for the treatment of ungual onychomycosis. Drug Dev Ind Pharm 41, 1575–1581.

12. Preuss, A., L. Zeugner, S. Hackbarth, M.A.F. Faustino, M.G.P.M.S. Neves, J.A.S. Cavaleiro and B. Roeder (2013) Photoinactivation of Escherichia coli (SURE2) without intracellular uptake of the photosensitizer. J Appl Microbiol 114, 36–43.

13. Pohl, J., A. Preuß and B. Röder (2016) Chapter 41. Photodynamic Inactivation of Microorganisms. In Singlet Oxygen Vol. 2. (Edited by S. Nonell and C. Flors), pp. 305–318.

14. Pohl, J., I. Saltsman, A. Mahammed, Z. Gross and B. Roder (2015) Inhibition of green algae growth by corrole-based photosensitizers. J Appl Microbiol 118, 305–312.

15. Preuss, A., I. Saltsman, A. Mahammed, M. Pfitzner, I. Goldberg, Z. Gross and B. Roder (2014) Photodynamic inactivation of mold fungi spores by newly developed charged corroles. J Photochem Photobiol B 133, 39–46.

16. Hamblin, M.R. and T. Hasan (2004) Photodynamic therapy: a new antimicrobial approach to infectious disease? Photochem Photobiol Sci 3, 436–450.

17. Baltazar, L.d.M., B.M. Soares, H.C.S. Carneiro, T.V. Avila, L.F. Gouveia, D.G. Souza, M.V.L. Ferreira, M. Pinotti, D.d.A. Santos and P.S. Cisalpino (2013) Photodynamic inhibition of Trichophyton rubrum: in vitro activity and the role of oxidative and nitrosative bursts in fungal death. The Journal of antimicrobial chemotherapy 68, 354–361.

18. Calzavara-Pinton, P.G., M. Venturini and R. Sala (2005) A comprehensive overview of photodynamic therapy in the treatment of superficial fungal infections of the skin. J Photochem Photobiol B 78, 1–6.

19. Cronin, L., M. Moffitt, D. Mawad, O.C. Morton, A. Lauto and C. Stack (2014) An in vitro study of the photodynamic effect of rose bengal on Trichophyton rubrum. Journal of biophotonics 7, 410–417.

20. Hollander, C., J. Visser, E. de Haas, L. Incrocci and T. Smijs (2015) Effective Single Photodynamic Treatment of ex Vivo Onychomycosis Using a Multifunctional Porphyrin Photosensitizer and Green Light. JoF 1, 138–153.

21. Kamp, H., H.-J. Tietz, M. Lutz, H. Piazena, P. Sowyrda, J. Lademann and U. Blume-Peytavi (2005) Antifungal effect of 5-aminolevulinic acid PDT in Trichophyton rubrum. Mycoses 48, 101–107.

22. Smijs, T.G.M., R.N.S. van der Haas, J. Lugtenburg, Y. Liu, R.L.P. de Jong and H.J. Schuitmaker (2004) Photodynamic treatment of the dermatophyte Trichophyton rubrum and its microconidia with porphyrin photosensitizers. Photochemistry and Photobiology 80, 197–202.

23. Smijs, T.G.M. and S. Pavel (2011) The susceptibility of dermatophytes to photodynamic treatment with special focus on Trichophyton rubrum. Photochemistry and Photobiology 87, 2–13.

24. Smijs, T.G.M. and H.J. Schuitmaker (2003) Photodynamic Inactivation of the Dermatophyte Trichophyton rubrum. Photochem Photobiol 77, 556.

25. Li, M.Y., C.S. Cline, E.B. Koker, H.H. Carmichael, C.F. Chignell and P. Bilski (2001) Quenching of Singlet Molecular Oxygen (1O2) by Azide Anion in Solvent Mixtures. Photochem Photobiol 74, 760–764.

26. Matheson, I.B.C., R.D. Etheridge, N.R. Kratowich and J. Lee (1975) Quenching of singlet oxygen by Amino acids and proteins. Photochem Photobiol 21, 165–171.

27. Kohno, Y., Y. Egawa, S. Itoh, S.-i. Nagaoka, M. Takahashi and K. Mukai (1995) Kinetic study of quenching reaction of singlet oxygen and scavenging reaction of free radical by squalene in n-butanol. Biochimica et Biophysica Acta (BBA) - Lipids and Lipid Metabolism 1256, 52–56.

28. Tanielian, C. and C. Wolff (1988) Mechanism of physical quenching of singlet molecular oxygen by chlorophylls and related compounds of biological interest. Photochem Photobiol 48, 277–280.

29. Young, R.H., R.L. Martin, D. Feriozi, D. Brewer and R. Kayzer (1973) On the mechanism of quenching of singlet oxygen by Amines-III. Evidence for a charge-transfer-like complex. Photochem Photobiol 17, 233–244.

30. Martinez, L.A., C.G. Martínez, B.B. Klopotek, J. Lang, A. Neuner, A.M. Braun and E. Oliveros (2000) Nonradiative and radiative deactivation of singlet molecular oxygen (O2(a1Δg)) in micellar media and microemulsions. Journal of Photochemistry and Photobiology B: Biology 58, 94–107.

31. Paul B. Merkel and David R. Kearns (1972) Radiationless decay of singlet molecular oxygen in solution. Experimental and theoretical study of electronic-to-vibrational energy transfer. Journal of the American Chemical Society 94:21.

32. R. Schmidt and H. D. Brauer (1987) Radiationless deactivation of singlet oxygen ($^1\Delta$.g) by solvent molecules. J. Am. Chem. Soc. 109, 6976-6981.

33. Ogilby, P.R. (2010) Singlet oxygen: there is indeed something new under the sun. Chemical Society reviews 39, 3181–3209.

34. Ramel, F., S. Birtic, S. Cuiné, C. Triantaphylidès, J.-L. Ravanat and M. Havaux (2012) Chemical quenching of singlet oxygen by carotenoids in plants. Plant physiology 158, 1267–1278.

35. Pfitzner, S., J.C. Schlothauer, B. Röder and S. Hackbarth (2018) Time- and spectrally resolved singlet oxygen phosphorescence detection—discriminating disturbance signals. Laser Phys. 28, 85702.

36. Hackbarth, S., J. Schlothauer, A. Preuß, C. Ludwig and B. Röder (2012) Time resolved sub-cellular singlet oxygen detection – ensemble measurements versus single cell experiments. Laser Phys. Lett. 9, 474–480.

37. Hackbarth, S., S. Pfitzner, L. Guo, J. Ge, P. Wang and B. Röder (2018) Singlet Oxygen Kinetics in Polymeric Photosensitizers. J. Phys. Chem. C 122, 12071–12076.

38. Jarvi, M.T., M.J. Niedre, M.S. Patterson and B.C. Wilson (2006) Singlet oxygen luminescence dosimetry (SOLD) for photodynamic therapy: current status, challenges and future prospects. Photochemistry and Photobiology 82, 1198–1210.

39. Yamaguchi, S. and Y. Sasaki (2001) Spectroscopic determination of very low quantum yield of singlet oxygen formation photosensitized by industrial dyes. Journal of Photochemistry and Photobiology A: Chemistry 142, 47–50.

40. Boso, G., D. Ke, B. Korzh, J. Bouilloux, N. Lange and H. Zbinden (2016) Time-resolved singlet-oxygen luminescence detection with an efficient and practical semiconductor single-photon detector. Biomedical optics express 7, 211–224.

41. Bornhutter, T., J. Pohl, C. Fischer, I. Saltsman, A. Mahammed, Z. Gross and B. Roder (2016) Development of Singlet Oxygen Luminescence Kinetics during the Photodynamic Inactivation of Green Algae. Molecules (Basel, Switzerland) 21, 485.

42. Bornhütter, T., N. Shamali, I. Saltsman, A. Mahammed, Z. Gross, G. Däschlein and B. Röder (2017) Singlet oxygen luminescence kinetics under PDI relevant conditions of pathogenic dermatophytes and molds. Journal of Photochemistry and Photobiology B: Biology.

43. Egorov, S.Y., V.F. Kamalov, N.I. Koroteev, A.A. Krasnovsky, B.N. Toleutaev and S.V. Zinukov (1989) Rise and decay kinetics of photosensitized singlet oxygen luminescence in water. Measurements with nanosecond time-correlated single photon counting technique. Chemical Physics Letters 163, 421–424.

44. Grinvald, A. and I.Z. Steinberg (1974) On the analysis of fluorescence decay kinetics by the method of least-squares. Analytical biochemistry 59, 583–598.

45. Ehrenberg, B., J.L. Anderson and C.S. Foote (1998) Kinetics and Yield of Singlet Oxygen Photosensitized by Hypericin in Organic and Biological Media. Photochem Photobiol 68, 135–140.

46. Robert H. Young, David. Brewer and and Richard A. Keller Determination of rate constants of reaction and lifetimes of singlet oxygen in solution by a flash photolysis technique.

47. Time-resolved Singlet Oxygen Phosphorescence Measurements from Photosensitized Experiments in Single Cells: Effects of Oxygen Diffusion and Oxygen Concentration.

48. Han, P. and D.M. Bartels (1996) Temperature Dependence of Oxygen Diffusion inH2O and D2O†. J. Phys. Chem. 100, 5597–5602.

49. Skovsen, E., J.W. Snyder, J.D.C. Lambert and P.R. Ogilby (2005) Lifetime and diffusion of singlet oxygen in a cell. The journal of physical chemistry. B 109, 8570–8573.

50. Hackbarth, S. and B. Röder (2015) Singlet oxygen luminescence kinetics in a heterogeneous environment - identification of the photosensitizer localization in small unilamellar vesicles. Photochem Photobiol Sci 14, 329–334.

51. Ormond, A. and H. Freeman (2013) Dye Sensitizers for Photodynamic Therapy. Materials 6, 817–840.

52. Plaetzer, K., B. Krammer, J. Berlanda, F. Berr and T. Kiesslich (2009) Photophysics and photochemistry of photodynamic therapy: fundamental aspects. Lasers in medical science 24, 259–268.

53. Macdonald, I.J.A.N. and T.J. Dougherty (2001) Basic principles of photodynamic therapy. J. Porphyrins Phthalocyanines 05, 105–129.

54. Ackroyd, R., C. Kelty, N. Brown and M. Reed (2001) The History of Photodetection and Photodynamic Therapy¶. Photochem Photobiol 74, 656.

55. Pass, H.I. (1993) Photodynamic Therapy in Oncology. JNCI Journal of the National Cancer Institute 85, 443–456.

56. Triesscheijn, M., P. Baas, J.H.M. Schellens and F.A. Stewart (2006) Photodynamic therapy in oncology. The oncologist 11, 1034–1044.

57. Huang, Z. (2005) A review of progress in clinical photodynamic therapy. Technology in cancer research & treatment 4, 283–293.

58. Nyst, H.J., I.B. Tan, F.A. Stewart and A.J.M. Balm (2009) Is photodynamic therapy a good alternative to surgery and radiotherapy in the treatment of head and neck cancer. Photodiagnosis and photodynamic therapy 6, 3–11.

59. Juarranz, Á., P. Jaén, F. Sanz-Rodríguez, J. Cuevas and S. González (2008) Photodynamic therapy of cancer. Basic principles and applications. Clin Transl Oncol 10, 148–154.

60. Moghissi, K. and K. Dixon (2003) Photodynamic therapy (PDT) in esophageal cancer. Technology in cancer research & treatment 2, 319–326.

61. Kelly, J.F. and M.E. Snell (1976) Hematoporphyrin Derivative. The Journal of Urology 115, 150–151.

62. Peng, Q., T. Warloe, K. Berg, J. Moan, M. Kongshaug, K.-E. Giercksky and J.M. Nesland (1997) 5-Aminolevulinic acid-based photodynamic therapy. Cancer 79, 2282–2308.

63. Wiegell, S.R. and H.C. Wulf (2006) Photodynamic therapy of acne vulgaris using 5-aminolevulinic acid versus methyl aminolevulinate. J Am Acad Dermatol 54, 647–651.

64. (2012) Global action plan to control the spread and impact of antimicrobial resistance in Neisseria gonorrhoeae. World Health Organization, Geneva, Switzerland.

65. (2014) Antimicrobial resistance. Global report on surveillance. World Health Organization, Geneva Switzerland.

66. Maisch, T. (2007) Anti-microbial photodynamic therapy. Lasers in medical science 22, 83–91.

67. Jori, G., C. Fabris, M. Soncin, S. Ferro, O. Coppellotti, D. Dei, L. Fantetti, G. Chiti and G. Roncucci (2006) Photodynamic therapy in the treatment of microbial infections. Lasers in surgery and medicine 38, 468–481.

68. Almeida, J., J.P.C. Tomé, M.G.P.M.S. Neves, A.C. Tomé, J.A.S. Cavaleiro, Â. Cunha, L. Costa, M.A.F. Faustino and A. Almeida (2014) Photodynamic inactivation of multidrug-resistant bacteria in hospital wastewaters. Photochem Photobiol Sci 13, 626–633.

69. Tavares, A., C.M.B. Carvalho, M.A. Faustino, M.G.P.M.S. Neves, J.P.C. Tomé, A.C. Tomé, J.A.S. Cavaleiro, A. Cunha, N.C.M. Gomes, E. Alves and A. Almeida (2010) Antimicrobial photodynamic therapy. Marine drugs 8, 91–105.

70. Nitzan, Y., M. Gutterman, Z. Malik and B. Ehrenberg (1992) Interaction of Gram - negative bacteria by photosensitized porphyrins. Photochem Photobiol 55, 89–96.

71. Adams, D.J. (2004) Fungal cell wall chitinases and glucanases. Microbiology-SGM 150, 2029–2035.

72. Gaynes, R. and J.R. Edwards (2005) Overview of nosocomial infections caused by gram-negative bacilli. Clinical infectious diseases : an official publication of the Infectious Diseases Society of America 41, 848–854.

73. Hall-Stoodley, L., J.W. Costerton and P. Stoodley (2004) Bacterial biofilms. Nature Reviews Microbiology 2, 95 EP -.

74. Spellberg, B., R. Guidos, D. Gilbert, J. Bradley, H.W. Boucher, W.M. Scheld, J.G. Bartlett and J. Edwards (2008) The epidemic of antibiotic-resistant infections. Clinical infectious diseases : an official publication of the Infectious Diseases Society of America 46, 155–164.

75. Madhi, S.A., K. Petersen, A. Madhi, M. Khoosal and K.P. Klugman (2000) Increased disease burden and antibiotic resistance of bacteria causing severe community-acquired lower respiratory tract infections in human immunodeficiency virus type 1-infected children. Clinical infectious diseases : an official publication of the Infectious Diseases Society of America 31, 170–176.

76. Li, J., R.L. Nation, J.D. Turnidge, R.W. Milne, K. Coulthard, C.R. Rayner and D.L. Paterson (2006) Colistin. The Lancet Infectious Diseases 6, 589–601.

77. Pankey, G.A. and L.D. Sabath (2004) Clinical relevance of bacteriostatic versus bactericidal mechanisms of action in the treatment of Gram-positive bacterial infections. Clinical infectious diseases : an official publication of the Infectious Diseases Society of America 38, 864–870.

78. Ball, P. (2002) Antibiotic therapy of community respiratory tract infections. Journal of antimicrobial chemotherapy 49, 31–40.

79. Hamblin, M.R. (2016) Antimicrobial photodynamic inactivation: a bright new technique to kill resistant microbes. Current opinion in microbiology 33, 67–73.

80. Maisch, T., S. Hackbarth, J. Regensburger, A. Felgentrager, W. Baumler, M. Landthaler and B. Roder (2011) Photodynamic inactivation of multi-resistant bacteria (PIB) - a new approach to treat superficial infections in the 21st century. J Dtsch Dermatol Ges 9, 360–366.

81. Tim, M. (2015) Strategies to optimize photosensitizers for photodynamic inactivation of bacteria. J Photochem Photobiol B 150, 2–10.

82. Maisch, T. (2015) Resistance in antimicrobial photodynamic inactivation of bacteria. Photochem Photobiol Sci 14, 1518–1526.

83. Hamblin, M.R. (2002) Polycationic photosensitizer conjugates. Journal of chemotherapy 49, 941–951.

84. Durantini, E. (2006) Photodynamic Inactivation of Bacteria. CBC 2, 127–142.

85. Bornstein, E., W. Hermans, S. Gridley and J. Manni (2009) Near-infrared photoinactivation of bacteria and fungi at physiologic temperatures. Photochemistry and Photobiology 85, 1364–1374.

86. Kalus, A. (2017) Fungal Skin Infections. In The Travel and Tropical Medicine Manual, pp. 488–500.

87. Alferd M. Allen Robert D. king (1978) Occlusion, Carbon dioxide, and fungal skin interactions. The Lancet, 360–362.

88. Prieto-Granada, C.N., A.Z.C. Lobo and M.C. Mihm (2010) Skin Infections. In Diagnostic Pathology of Infectious Disease, pp. 519–616.

89. Raugi, G. and T.U. Nguyen (2012) Superficial Dermatophyte Infections of the Skin. In Netter's Infectious Diseases, pp. 102–109.

90. Weedon, D. (2010) Mycoses and algal infections. In Weedon's Skin Pathology, 581-606.e24.

91. Maura A. Fitzgerald et.al. Ringworm, 435–436.

92. Martinez-Rossi, N.M., N.T.A. Peres and A. Rossi (2008) Antifungal resistance mechanisms in dermatophytes. Mycopathologia 166, 369–383.

93. Campoy, S. and J.L. Adrio (2017) Antifungals. Biochemical pharmacology 133, 86–96.

94. Martinez-Rossi, N.M., G.F. Persinoti, N.T.A. Peres and A. Rossi (2012) Role of pH in the pathogenesis of dermatophytoses. Mycoses 55, 381–387.

95. Cuenca-Estrella, M.; Gomez-Lopez, A.; Mellado, E.; Buitrago, M. J.; Monzon, A.; Rodriguez-Tudela, J. L. (2003) Scopulariopsis brevicaulis, a Fungal Pathogen Resistant to Broad-Spectrum Antifungal Agents. Antimicrobial Agents and Chemotherapy 47, 2339–2341.

96. Nafsika H Georgopapadakou (1998) Antifungals: mechanism of action and resistance, established and novel drugs. Current opinion in microbiology, 1:547-557.

97. Weitzman, I. and R.C. Summerbell (1995) The dermatophytes. Clinical microbiology reviews 8, 240–259.

98. Dahl, M.V. (1994) Dermatophytosis and the immune response. J Am Acad Dermatol 31, S34-S41.

99. Vermout, S., J. Tabart, A. Baldo, A. Mathy, B. Losson and B. Mignon (2008) Pathogenesis of dermatophytosis. Mycopathologia 166, 267–275.

100. Achterman, R.R. and T.C. White (2012) Dermatophyte virulence factors: identifying and analyzing genes that may contribute to chronic or acute skin infections. International journal of microbiology 2012, 358305.

101. Smith, M.B. and M.R. McGinnis (2011) Dermatophytosis. In Tropical Infectious Diseases: Principles, Pathogens and Practice, pp. 559–564.

102. Anaissie, E.J., M.R. McGinnis and M.A. Pfaller, eds. (2009) Clinical mycology. Churchill Livingstone, Edinburgh.

103. Woodfolk, J.A. (2005) Allergy and dermatophytes. Clinical microbiology reviews 18, 30–43.

104. Mukherjee, P.K., S.D. Leidich, N. Isham, I. Leitner, N.S. Ryder and M.A. Ghannoum (2003) Clinical Trichophyton rubrum Strain Exhibiting Primary Resistance to Terbinafine. Antimicrobial Agents and Chemotherapy 47, 82–86.

105. (2010) Weedon's Skin Pathology. Elsevier.

106. Jayatilake, J.A.M.S., W.M. Tilakaratne and G.J. Panagoda (2009) Candidal onychomycosis: a mini-review. Mycopathologia 168, 165–173.

107. A.K.GUPTA, J.E.R.A.A.M.J. (2004) Cumulative meta-analysis of systemic antifungal agents for the treatment of onychomycosis. British Journal of Dermatology, 537–544.

108. Faergemann, J. and R. Baran (2003) Epidemiology, clinical presentation and diagnosis of onychomycosis. Br J Dermatol 149, 1–4.

109. Das, N.K., P. Ghosh, S. Das, S. Bhattacharya, R.N. Dutta and S.R. Sengupta (2008) A study on the etiological agent and clinico-mycological correlation of fingernail onychomycosis in eastern India. Indian journal of dermatology 53, 75–79.

110. Ghannoum, M.A., R.A. Hajjeh, R. Scher, N. Konnikov, A.K. Gupta, R. Summerbell, S. Sullivan, R. Daniel, P. Krusinski, P. Fleckman, P. Rich, R. Odom, R. Aly, D. Pariser, M. Zaiac, G. Rebell, J. Lesher, B. Gerlach, G.F. Ponce-De-Leon, A. Ghannoum, J. Warner, N. Isham and B. Elewski (2000) A large-scale North American study of fungal isolates from nails. J Am Acad Dermatol 43, 641–648.

111. Gérald Piérard (2001) Onychomycosis and Other Superficial Fungal Infections of the Foot in the Elderly: A Pan-European Survey. Dermatology, 220–224.

112. B Sigurgeirsson, Ó.S. (2004) Risk factors associated with onychomycosis. Journal of the European Academy of Dermatology and Venereology : JEADV, 48–51.

113. Drake et al (1999) The impact of onychomycosis on quality of life: Development of an international onychomycosis-specific questionnaire to measure patient quality of life. J Am Acad Dermatol, 189–196.

114. Drake et al (1998) Effect of onychomycosis on quality of life. Journal of the American Academy of Dermatology, 702-704.

115. Lubeck, D.P., D.L. Patrick, P. McNulty, S.K. Fifer and J. Birnbaum (1993) Quality of life of persons with onychomycosis. Qual Life Res 2, 341–348.

116. Lubeck, D.P. (1998) Measuring health-related quality of life in onychomycosis. Journal of the American Academy of Dermatology 38, S64-S68.

117. SCHER, R.K. (1994) Onychomycosis is more than a cosmetic problem. Br J Dermatol 130, 15.

118. Vejnovic, I., L. Simmler and G. Betz (2010) Investigation of different formulations for drug delivery through the nail plate. International Journal of Pharmaceutics 386, 185–194.

119. Murdan, S. (2002) Drug delivery to the nail following topical application. International Journal of Pharmaceutics 236, 1–26.

120. Kathiravan, M.K., A.B. Salake, A.S. Chothe, P.B. Dudhe, R.P. Watode, M.S. Mukta and S. Gadhwe (2012) The biology and chemistry of antifungal agents: a review. Bioorganic & medicinal chemistry 20, 5678–5698.

121. Katz, H.I. and A.K. Gupta (1997) Oral antifungal drug interactions. Dermatologic Clinics 15, 535–544.

122. Ledon, J.A., J. Savas, K. Franca, A. Chacon and K. Nouri (2014) Laser and light therapy for onychomycosis: a systematic review. Lasers in medical science 29, 823–829.

123. Galvan Garcia, H.R. (2014) Onychomycosis. Journal of cosmetic dermatology 13, 232–235.

124. Jasmina Kozarev (ol. 2010,) Novel Laser Therapy in Treatment of Onychomycosis. Journal of the Laser and Health Academy, 1–8.

125. Lim, E.-H., H.-r. Kim, Y.-O. Park, Y. Lee, Y.-J. Seo, C.-D. Kim, J.-H. Lee and M. Im (2014) Toenail onychomycosis treated with a fractional carbon-dioxide laser and topical antifungal cream. Journal of the American Academy of Dermatology 70, 918–923.

126. Hees, H., C. Raulin and W. Bäumler (2012) Laser treatment of onychomycosis: an in vitro pilot study. Journal der Deutschen Dermatologischen Gesellschaft = Journal of the German Society of Dermatology : JDDG 10, 913–918.

127. Bhatta, A.K., X. Huang, U. Keyal and J.J. Zhao (2014) Laser treatment for onychomycosis: a review. Mycoses 57, 734–740.

128. Hochman, L.G. (2011) Laser treatment of onychomycosis using a novel 0.65-millisecond pulsed Nd:YAG 1064-nm laser. Journal of Cosmetic and Laser Therapy 13, 2–5.

129. Baltazar, L.M., A. Ray, D.A. Santos, P.S. Cisalpino, A.J. Friedman and J.D. Nosanchuk (2015) Antimicrobial photodynamic therapy. Frontiers in microbiology 6, 202.

130. Baltazar, L.M., A.E. Krausz, A.C.O. Souza, B.L. Adler, A. Landriscina, T. Musaev, J.D. Nosanchuk and A.J. Friedman (2015) Trichophyton rubrum is inhibited by free and nanoparticle encapsulated curcumin by induction of nitrosative stress after photodynamic activation. PloS one 10, e0120179.

131. Bhatta, A.K., U. Keyal and X.L. Wang (2016) Photodynamic therapy for onychomycosis. Photodiagnosis and photodynamic therapy 15, 228–235.

132. Mehra, T., M. Schaller, B. Walker, C. Braunsdorf, D. Mailänder-Sanchez, F. Schynowski, R. Hahn, M. Röcken, M. Köberle and C. Borelli (2015) Efficacy of antifungal PACT in an in vitro model of onychomycosis. Journal of the European Academy of Dermatology and Venereology : JEADV 29, 86–90.

133. Watanabe, D., C. Kawamura, Y. Masuda, Y. Akita, Y. Tamada and Y. Matsumoto (2008) Successful treatment of toenail onychomycosis with photodynamic therapy. Archives of dermatology 144, 19–21.

134. Silva, A.P.d., C. Kurachi, V.S. Bagnato and N.M. Inada (2013) Fast elimination of onychomycosis by hematoporphyrin derivative-photodynamic therapy. Photodiagnosis and photodynamic therapy 10, 328–330.

135. Nail (anatomy).

136. Berker, D. de (2013) Nail anatomy. Clinics in dermatology 31, 509–515.

137. Baswan, S., G.B. Kasting, S.K. Li, R. Wickett, B. Adams, S. Eurich and R. Schamper (2017) Understanding the formidable nail barrier: A review of the nail microstructure, composition and diseases. Mycoses 60, 284–295.

138. Technical Brief (2009) Skin and Nail: Barrier Function, Structure, and Anatomy Considerations for Drug Delivery. Particle Sceinces 3.

139. Wang, B., W. Yang, J. McKittrick and M.A. Meyers (2016) Keratin. Progress in Materials Science 76, 229–318.

140. Baden, H.P. (1970) The Physical Properties of Nail**From the Department of Dermatology. Massachusetts General Hospital and Harvard Medical School, Boston, Massanchusetts 02114. Journal of Investigative Dermatology 55, 115–122.

141. Baden, H.P., L.A. Goldsmith and B. Fleming (1973) A comparative study of the physicochemical properties of human keratinized tissues. Biochimica et Biophysica Acta (BBA) - Protein Structure 322, 269–278.

142. Grayson, S. and P.M. Elias (1982) Isolation and Lipid Biochemical Characterization of Stratum Corneum Membrane Complexes. Journal of Investigative Dermatology 78, 128–135.

143. Trommer, H. and R.H.H. Neubert (2006) Overcoming the stratum corneum. Skin pharmacology and physiology 19, 106–121.

144. Chouhan, P. and T.R. Saini (2012) Hydration of nail plate: a novel screening model for transungual drug permeation enhancers. International Journal of Pharmaceutics 436, 179–182.

145. Murdan, S. (2008) Enhancing the nail permeability of topically applied drugs. Expert opinion on drug delivery 5, 1267–1282.

146. Walters, K.A. and G.L. Flynn (1983) Permeability characteristics of the human nail plate. International journal of cosmetic science 5, 231–246.

147. Malhotra, G.G. and J.L. Zatz (2002) Investigation of nail permeation enhancement by chemical modification using water as a probe. Journal of Pharmaceutical Sciences 91, 312–323.

148. Yanbin Zhang, Cong Ye, Shijie Li, Aishun Ding, Guangxin Gu and Hao Guo (2017) Eosin Y-catalyzed photooxidation of triarylphosphines under visible light irradiation and aerobic conditions. RSC Advances 7, 13240–13243.

149. Gold, M.E., ed. (2018) An Introduction to Labor Law. Cornell University Press, Ithaca, NY.

150. Zurita, J. and R.J. Hay (1987) Adherence of Dermatophyte Microconidia and Arthroconidia to Human Keratinocytes In Vitro. Journal of Investigative Dermatology 89, 529–534.

151. Stentelaire, C., N. Antoine, C. Cabrol, G. Feron and A. Durand (2001) Development of a rapid and highly sensitive biochemical method for the measurement of fungal spore viability. An alternative to the CFU method. Enzyme and Microbial Technology 29, 560–566.

152. Levitz, S.M. and R.D. Diamond (1985) A Rapid Colorimetric Assay of Fungal Viability with the Tetrazolium Salt MTT. Journal of Infectious Diseases 152, 938–945.

153. swolfford 2511 M9 Minimal Agar/Broth.

154. himedialabs Sabouraud Dextrose Agar.

155. Schlothauer, J., B. Röder, S. Hackbarth and J. Lademann (2010) In vivo detection of time-resolved singlet oxygen luminescence under PDT relevant conditions. In BiOS. (Edited by D.H. Kessel), 755106-755106-9.

156. Berberan-Santos, M.N., E.N. Bodunov and B. Valeur (2005) Mathematical functions for the analysis of luminescence decays with underlying distributions 1. Kohlrausch decay function (stretched exponential). Chemical Physics 315, 171–182.

157. Meier, P. (1953) Variance of a Weighted Mean. Biometrics 9, 59.

158. Bseiso, E.A., M. Nasr, O.A. Sammour and N.A. Abd El Gawad (2016) Novel nail penetration enhancer containing vesicles "nPEVs" for treatment of onychomycosis. Drug delivery 23, 2813–2819.

159. Davies, M.J. (2004) Reactive species formed on proteins exposed to singlet oxygen. Photochemical & photobiological sciences : Official journal of the European Photochemistry Association and the European Society for Photobiology 3, 17–25.

160. Nogueiras-Nieto, L., J.L. Gómez-Amoza, M.B. Delgado-Charro and F.J. Otero-Espinar (2011) Hydration and N-acetyl-l-cysteine alter the microstructure of human nail and bovine hoof: implications for drug delivery. Journal of controlled release : official journal of the Controlled Release Society 156, 337–344.

161. David I. Reuben (Aug. 30, 2006) Antifungal shoe insole with built-in ultraviolet LED.

162. David Isidore Reuben (Aug. 26, 2008) Shoe with ultraviolet LED irradiated photocatalyst coated surfaces.

163. Jacob Fraden, La Jolla, CA (US) (Dec. 28, 2000) Shoe disinfectant and deodorizer.

Figures

Tables

Publications

Bornhütter T, Shamali N, Saltsman I, et al. Singlet oxygen luminescence kinetics under PDI relevant conditions of pathogenic dermatophytes and molds. J Photochem Photobiol B*: Biology*. 2017

Shamali N, Preuß A, Saltsman I, et al. In vitro photodynamic inactivation (PDI) of pathogenic germs inducing onychomycosis. *Photodiagnosis and photodynamic therapy*. 2018.

Conferences

2nd Sino-German Symposium on Singlet molecular Oxygen and Photodynamic Effects, Berlin, Germany N. Shamali,T. Bornhütter, A. Preß, B.Röder "**Towards photodynamic treatment of *onychomycosis*: photodynamic inactivation of dermatophytes"**

10th International Conference on Porphyrins and Phthalocyanines (ICPP), Munich, Germany. N. Shamali, A. Preß, B. Röder "**In vitro photodynamic inactivation of pathogenic dermatophytes and molds"**

Acknowledgement

My work in this project gives me the chance to acquire more knowledge about the biophysics field and the microbiology laboratory techniques. I would like to express my significant gratitude and great thanks to all intelligent people I met along my PhD journey whom I am greatly appreciative for their guidance and endless efforts in helping me in every way possible throughout the work in this thesis to be ready in your hands. My gratitude is beyond words. The prior thanks is to the God for the good health. Thanks is also due to Yousef Jameel scholarship for their financial support that I otherwise would not have been able to do my PhD.

The most special thanks goes to Prof. Dr. Beate Röder, she gave me this golden opportunity to do my PhD in her group. She supported me the whole time and she was always there whenever I needed any consultation or inquiry in both scientific and social levels. Her extraordinary power and her great experience and knowledge inspire and motivate me in every occasion.

I would also thank Dr. Anngret Preuß and her family for their support in my very first days in Germany. The special thanks goes to her mother Anne Preuß who was like my mother and who learned me my first German words.

I would like to thank Dr. Anngret Preuß, Jakob Pohl for their efficient help and practicing in microbiology laboratory.

I would like to thank Tobias Bornhütter, Michael Pfitzner and Dr. Steffen Hackbarth for their cooperation and help throughout singlet oxygen measurements.

Special thanks goes to Jakob Pohl, Dr. Anngret Preuß and Dr. Steffen Hackbarth who have proofread my thesis and did not hesitate to give me all support and motivation throughout writing process.

I would like to thanks all members of Photobiophysics group for the friendly atmosphere they provided.

I would also like to thank department of dermatology, university hospital in Greifswald, Germany and the head of the department Prof. Dr. Geaorg Däschlein for providing me with the required fungi strains needed for the research and for their medical consultation.

Last but not least, I would like to thank my family: my parents, my brother and sisters , my husband Osama Arafat and my friends for supporting me spiritually throughout my research and my whole life.

Erklärung

Hiermit erkläre ich, die Dissertation selbstständig und nur unter Verwendung der angegebenen Hilfen und Hilfsmittel angefertigt zu haben. Ich habe mich nicht anderwärts um einen Doktorgrad in dem Promotionsfach beworben und besitze keinen entsprechenden Doktorgrad. Die Promotionsordnung der Mathematisch-Naturwissenschaftlichen Fakultät, veröffentlicht im Amtlichen Mitteilungsblatt der Humboldt-Universität zu Berlin Nr. 42 am11. Juli 2018, habe ich zur Kenntnis genommen.

Declaration

I declare that I have completed the thesis independently using only the aids and tools specified. I have not applied for a doctor's degree in the doctoral subject elsewhere and do not hold a corresponding doctor's degree. I have taken due note of the Faculty of Mathematics and Natural Sciences PhD Regulations, published in the Official Gazette of Humboldt-Universität zu Berlin no. 42 on July 11 2018.